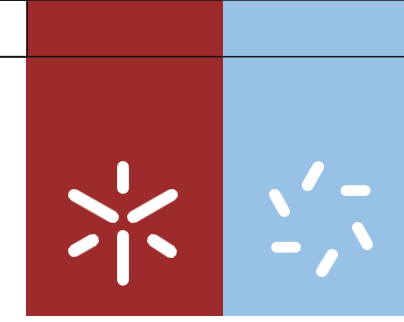




Validation of a microfluidic device for the isolation and enumeration of circulating tumour cells and cancer progression monitoring in metastatic breast cancer

Ana Cláudia da Silva Lopes

UMinho|2019



Universidade do Minho
Escola de Ciências

Ana Cláudia da Silva Lopes

Validation of a microfluidic device for the isolation and enumeration of circulating tumour cells and cancer progression monitoring in metastatic breast cancer

October 2019



Universidade do Minho
Escola de Ciências

Ana Cláudia da Silva Lopes

**Validation of a microfluidic device for the
isolation and enumeration of circulating
tumour cells and cancer progression
monitoring in metastatic breast cancer**

Master Thesis
Master in Biophysics and Bionanosystems

Work developed under the supervision of
Doctor Lorena Diéguez Moure
and
**Professora Doutora Elisabete Maria dos
Santos Castanheira Coutinho**

October 2019

Declaration

Name: Ana Cláudia da Silva Lopes

Email: claudia_lopes96@outlook.com Phone: 918456063

ID nº: 15077072

Thesis title: Validation of a microfluidic device for the isolation and enumeration of circulating tumor cells and cancer progression monitoring in metastatic breast cancer

Supervisors:

Doutora Lorena Diéguez Moure

Professora Doutora Elisabete Maria dos Santos Castanheira Coutinho

Conclusion year: 2019

Master course: Master in Biophysics and Bionanosystems

IN ACCORDANCE WITH CURRENT LEGISLATION, THE REPRODUCTION OF ANY PART OF THIS THESIS/WORK IS NOT PERMITTED

University of Minho, October of 2019

Signature: Ana Cláudia da Silva Lopes

Acknowledgments

Esta dissertação representa uma das maiores e melhores experiências que vivenciei, sendo também a realização de um sonho e a melhor forma de homenagear a memória de uma pessoa muito especial. A sua realização só foi possível com o apoio de um número de pessoas, a quem quero prestar o meu profundo agradecimento.

À minha orientadora, Professora Doutora Elisabete Maria dos Santos Castanheira Coutinho, quero expressar o meu agradecimento pela constante disponibilidade, enorme prestabilidade, partilha de conhecimentos e gentileza para comigo, sempre que necessitei.

To my supervisor, Dr. Lorena Diéguez, who gave me the unique opportunity and trusted me on the develop of this amazing project at INL. For always being available when I needed, supportive and encouraging at every moment. I wouldn't trade this past year or this project for any other one. For everything, thank you!

I would also like to thank everyone with whom I had the pleasure to work at INL. To the entire microfluidic group, for all the help, motivation and knowledge sharing. A special thanks to Pedro, Alexandra and Raquel, for all the good moments, all the laughs and talks, more than colleagues, you became good friends. It was a pleasure working with you all this past year!

Aos meus colegas de mestrado e amigos, por toda a partilha de conhecimento e companheirismo durante estes dois anos.

À Paulina, por todos os ensinamentos e partilha de conhecimento, por toda a paciência e horas passadas no laboratório. Tive a sorte de aprender com a melhor pessoa possível. Obrigada por, muito além de toda a orientação dada ao longo deste ano, todo o apoio, ânimo, boa disposição. A tua ajuda e presença tornou tudo muito mais fácil!

A todas as pacientes que voluntariamente entraram neste estudo, por se mostrarem disponíveis a doar as suas amostras. A vossa coragem nos piores momentos é um exemplo para todos. Obrigada!

Aos meus amigos de sempre e para sempre, que estiveram presentes, nas gargalhadas e nas lágrimas. Obrigada por todas as conversas, por toda a entrega, por todas as horas e momentos em que me fizeram sorrir. Ao Rui, por todas as séries que partilhamos, ao Ricardo, por todos os pseudo-roubos que me arrancaram gargalhadas, à Sara, por ser uma das melhores ouvintes e apoiar cada decisão, à Cátia, que apesar de recente, tenho o prazer de chamar de amiga, por todo o apoio oferecido e todos os bons e genuínos momentos passados, à Guida, por ser uma irmã do coração, por ter estado presente em todos os momentos, sem exceção, por me disponibilizar sempre um ombro amigo e partilhar comigo

as melhores memórias. Levo-vos a todos no coração. A vossa presença na minha vida é fundamental, por tudo, obrigada!

Ao Kevin, por me fazer acreditar na genuinidade e bondade das pessoas, sendo o melhor exemplo disso. Por toda a ajuda e apoio incansável e tão fundamental, por acreditar em mim e me fazer sentir o mesmo, por me acalmar nos piores momentos e fazer acreditar que no final tudo iria correr bem. A ti, agradeço as tantas horas que gastaste a ouvir-me lamuriar, oferecendo-me o teu ombro sempre que necessitei, e todos os sorrisos que foste capaz de me arrancar. To infinity and beyond!

À minha família, em especial aos meus pais, por me deixarem voar, com a promessa de que estariam sempre de braços abertos para me amparar em todos os momentos. Por todo o amor e afeto que me deram, por todo o apoio, pelos melhores conselhos. Obrigada por serem os pilares que sustentam todas as minhas decisões, e por toda a educação que me foram dando. A vós, devo tudo, e por isso, o meu mais sincero e sentido obrigada!

Ao meu irmão, por ser A pessoa. Se almas gémeas existem, és com certeza a minha. Obrigada por todas as gargalhadas, pela partilha das melhores músicas, por todos os momentos parvos. Obrigada por seres a melhor pessoa do mundo, a mais verdadeira. Obrigada pelos melhores abraços do mundo, e por todo o orgulho que tens em mim, acredita que é mútuo. Obrigada por existires!

Dedico esta dissertação à minha Avó Rosa,

“Aqueles que passam por nós, não vão sós, não nos deixam sós.

Deixam um pouco de si, levam um pouco de nós.”
(Antoine de Stain-Exupéry)

STATEMENT OF INTEGRITY

I hereby declare having conducted this academic work with integrity. I confirm that I have not used plagiarism or any form of falsification of results in the process of the thesis elaboration.

I further declare that I have fully acknowledged the Code of Ethical Conduct of the University of Minho.

Validação de um dispositivo de microfluídica para o isolamento e enumeração de células tumorais circulantes para monitorização da progressão do cancro em cancro da mama metastático.

Resumo

O cancro é uma das causas líderes de morbimortalidade mundialmente, estimando-se um aumento no número de diagnósticos a cada ano. O cancro da mama é o segundo tipo de cancro com maior incidência, e uma das principais causas de mortalidade em mulheres. A causa subjacente a esta morbimortalidade são as metástases. De modo a aprimorar a precisão da biomedicina para melhores diagnósticos clínicos e decisões terapêuticas, é necessário desenvolver novas estratégias baseadas na deteção de biomarcadores tumorais. As células tumorais circulantes (CTCs) foram observadas pela primeira vez no século XIX, surgindo depois a hipótese de que estas seriam responsáveis pela formação de metástases, pois escapam do tumor primário disseminando-se pela corrente sanguínea, potencialmente invadindo outros órgãos. Consequentemente, o estudo das CTCs contidas nos fluidos corporais ganhou importância na investigação oncológica, já que estas fornecem informação importante para a gestão do tratamento clínico de doentes oncológicos, representando, em tempo real, o estado do tumor (CTCs estão em circulação de 1 a 2 horas). Adicionalmente, permite a obtenção de amostras de pacientes de forma fácil e pouco invasiva, a biopsia líquida.

O objetivo deste projeto foi desenvolver e validar um dispositivo de microfluídica projetado para processar e analisar amostras de fluidos corporais recorrendo à biopsia líquida, ou seja, providenciar dispositivos de microfluídica, eficientes e pouco dispendiosos, capazes de isolar e caracterizar células tumorais circulantes, relevantes para a deteção precoce do cancro, prognósticos precisos e tratamento personalizado. A validação do dispositivo foi feita através da caracterização fenotípica de CTCs isoladas e posterior comparação com o único dispositivo de referência que atualmente dispõe de aprovação pela FDA, CellSearch®. É esperado que os resultados desta investigação assistam na monitorização de doenças metastáticas, estratificação dos pacientes e prognóstico preciso, contribuindo para uma terapia personalizada e precisa. Foram usadas técnicas relacionadas com diferentes áreas científicas, incluindo microfabricação, cultura celular, imunocitoquímica e microscopia de fluorescência. O trabalho foi desenvolvido nas instalações de última geração do INL e em colaboração com o Hospital de Santa Maria, Lisboa, no qual foram obtidas amostras de pacientes de cancro da mama metastático.

Palavras-chave: Cancro; Cancro da mama; Células Tumorais Circulantes; Dispositivo de Microfluídica; Biopsia Líquida.

Validation of a microfluidic device for the isolation and enumeration of circulating tumor cells and cancer progression monitoring in metastatic breast cancer.

Abstract

Cancer is a leading cause of morbidity and mortality worldwide, and it is estimated that the number of diagnoses will grow every year. Breast cancer is the second most common cancer in the world and one of the leading causes of cancer-related mortality in women. The underlying cause of morbidity and cancer-related mortality is cancer metastasis.

In order to foster biomedicine accuracy for better clinical diagnostic and therapeutic decisions, it is necessary to develop new strategies for biomarker detection.

Circulating tumour cells (CTCs) were first observed in the 19th century, later followed by the hypothesis that these cells could be responsible for the formation of metastasis. Indeed, CTCs are shed from the primary and metastatic tumours and disseminate through the bloodstream, potentially invading other organs. Thus, the study of CTCs in peripheral blood gained great importance in cancer research, since they might provide valuable information for the clinical management of cancer patients, representing a real-time snapshot of the tumour burden (CTCs half-life in circulation is 1 to 2 hours). Additionally, the study of CTCs offers unique opportunities for low invasive sampling in cancer patients, constituting the so-called liquid biopsy.

The aim of this project was to demonstrate the validity of a microfluidic system designed for the preparation of a body fluid sample towards liquid biopsy analysis, that is, to isolate and characterize circulating tumor cells, overall relevant for early cancer detection at the point-of-care, accurate prognosis and personalized treatment. The system validation was executed by phenotypical characterization of isolated CTCs and comparison of the system performance against the gold standard and FDA-approved system CellSearch®.

We expected that the results of this research would assist in the monitoring of metastatic disease, patient stratification and accurate prognosis, as well as contribute to oriented therapeutic selection.

Techniques related to different scientific fields from biochemistry to microengineering were used, including microfabrication, cell culture, and immunocytochemistry and fluorescence microscopy. In addition, the work was developed using state-of-the-art facilities at INL and in close collaboration with Hospital de Santa Maria, in Lisbon, where samples from metastatic breast cancer patients were obtained.

Keywords: Cancer; Breast cancer; Circulating Tumor Cells; Microfluidic Device; Liquid Biopsy;

Table of Content

Acknowledgments.....	iii
Resumo.....	vi
Abstract.....	vii
Table of Content	viii
List of Abbreviations and Acronyms.....	x
List of Figures.....	xii
List of Tables.....	xv
CHAPTER 1: General Introduction	1
1. General Introduction	2
1.1. Cancer and Breast Cancer.....	2
1.1.1. Different types of primary breast cancer	2
1.1.2. HER2 mutation.....	4
1.1.3. Metastatic breast cancer	6
1.2. Liquid biopsy.....	8
1.2.1. Circulating tumour cells (CTCs).....	8
1.3. Technologies for CTC isolation.....	9
1.3.1. CellSearch®	10
1.3.1.1. CellSearch® limitations.....	11
1.3.2. Biomarkers in Cancer research	12
1.3.3. Microfluidic separation of CTCs from blood	14
1.4. Breast cancer CTCs in the clinic	16
1.4.1. Metastatic Breast Cancer CTCs in the clinic.....	16
1.4.1.1. Studies and significant findings to date	17
1.4.2. Early Breast Cancer CTCs in the clinic	18
1.4.2.1. Studies and significant findings to date	18
1.4.3. HER2 in CTCs.....	19
1.4.4. Potential	20
CHAPTER 2: Objectives	23
2. Objectives.....	24
CHAPTER 3: Techniques.....	25
3. Techniques.....	26
3.1. Micro and Nanofabrication techniques.....	26
3.1.1. Photolithography.....	26
3.1.2. Soft lithography	28
3.2. Fluorescence microscopy	30
3.3. Immunohistochemistry (IHC) / Immunocytochemistry (ICC)	32
3.4. Cell Culture	32
CHAPTER 4: Materials and Methods	35
4. Materials and methods	36
4.1. Microfluidic device design and fabrication.....	36
4.2. Cell Culture	38

4.3.	Optimization studies	39
4.3.1.	Spiking experiments.....	39
4.3.2.	Immunofluorescence studies	41
4.3.2.1.	Immunocytochemistry performed in well plate (ICC-in-well).....	42
4.3.2.2.	Immunocytochemistry performed in device (ICC-in-device)	44
4.3.2.3.	Immunocytochemistry in healthy donors' blood.....	45
4.4.	Immunofluorescence and CTC enumeration in the RUBYchip™	46
4.5.	Patient sample collection and analysis	47
4.6.	Statistical method.....	48
CHAPTER 5: Results and Discussion		49
.....		49
5.	Results and Discussion.....	50
5.1.	RUBYchip™ performance in spiking experiments	50
5.2.	Cell staining and analysis	52
5.2.1.	Optimisation of cell labelling and analysis.....	52
5.2.2.	Cell staining and analysis on chip	57
5.2.3.	Controls in samples from healthy donors.....	59
5.2.4.	Patient sample staining and analysis	59
5.3.	Patient clinical characteristics	60
5.4.	Comparative analysis: Isolation of CTCs by the RUBYchip™ versus CellSearch®	63
5.5.	Tissue biopsy versus Liquid Biopsy: HER2 status	66
5.6.	Correlation of clinicopathological information with CTC enumeration	71
CHAPTER 6: Conclusion and Future Perspectives		73
CHAPTER 7: References		75
CHAPTER 8: Annexes		89

List of Abbreviations and Acronyms

<i>AKT</i>	Oncogenic serine kinase 1
<i>ALDH1</i>	Aldehyde dehydrogenase-1
<i>BSA</i>	Bovine serum albumin
ctDNA	Circulating tumor DNA
CEA	Carcinoembryonic antigen
CTC	Circulating tumor cell
CT	Computerized tomography scans
CK	Cytokeratin
C4F8	Octafluorocyclobutane
DEP	Dielectrophoresis
DMEM	Dulbecco's Modified Eagle's Medium
DNA	Deoxyribonucleic acid
DWL	Direct Write Laser
ECD	Extracellular kinase domain
<i>EGFR</i>	Epidermal growth factor receptor
EMA	Epithelial membrane antigen
<i>EMT</i>	Epithelial to mesenchymal transition
<i>EpCAM</i>	Epithelial cell adhesion molecule
<i>ER</i>	Estrogen receptor
<i>ESPR1</i>	Epithelial splicing regulator 1
<i>EVA</i>	Ethyl vinyl acetate microtube
<i>FBS</i>	Fetal bovine serum
<i>FFPE</i>	Formalin-fixed paraffin-embed
<i>GD 2, 3, 1a</i>	Gangliosides 2, 3, 1a
<i>HDMS</i>	Hexamethyldisilazane
<i>HER2</i>	Human epithelial growth factor 2
<i>HIV</i>	Human immunodeficiency virus
<i>ICC</i>	Immunocytochemistry
<i>IF</i>	Immunofluorescence

<i>IHC</i>	Immunohistochemistry
<i>IPA</i>	Isopropyl Alcohol
<i>MBC</i>	Metastatic breast cancer
<i>MET</i>	Mesenchymal-epithelial transition
<i>MFGM</i>	Milk fat globule membrane antigen
<i>MUC-1</i>	Mucin 1
<i>MRI</i>	Magnetic resonance imaging
<i>OPM</i>	Optical Profilometer
<i>PBMCs</i>	Peripheral blood mononuclear cells
<i>PBS</i>	Phosphate buffer saline
<i>PDMS</i>	Poly(dimethylsiloxane)
<i>PFA</i>	Paraformaldehyde
<i>PI3K</i>	Phosphatidylinositol 3-kinase
<i>PR</i>	Progesterone receptor
<i>PTEN</i>	Phosphatase and tensin homolog
<i>TKD</i>	Tyrosine kinase domain
<i>TMD</i>	Transmembrane kinase domain
<i>RBC</i>	Red Blood Cells
<i>REM</i>	Replica moulding
<i>RIE</i>	Reactive ion etching
<i>RT</i>	Room Temperature
<i>RS</i>	Recurrence score
<i>SAMIM</i>	Solvent-assisted micromolding
<i>SF6</i>	Sulfur Hexafluoride
<i>SPTS</i>	Silicon Deep Reactive Ion Etching
<i>WBC</i>	White Blood Cells
<i>ZEB1</i>	Zinc finger E-Box binding homebox 1
<i>ZO</i>	Zonula occludens
μ CP	Microcontact printing
μ TM	Microtransfer moulding

List of Figures

- Figure 1: Schematic image showing the immunohistochemistry profile of the four-molecule subtype of breast cancer based on the three most important markers. (ER- estrogen receptor; PR- progesterone receptor; HER2- human epithelial growth factor receptor 2). 4
- Figure 2: Schematic image showing the input of CTCs into the bloodstream and posterior formation of metastasis in other organs. (A) shows the location of the primary tumour. (B) Schematizes the tumour cells, and (C) their dissemination into the blood vessels, so that a possible metastasis formation (D) in distant organs occurs. 9
- Figure 3: Representative images showing the CellSearch® workflow overview. (A) The sample collection is made in specific tubes, CellSave Preservative Tubes, with a cell preservative that is able to store cells for up to 96 hours at room temperature, allowing, for example, shipment to distant locations. (B) The sample preparation is made with the CELLTRACKS®AUTOPREP® system, allowing an automated and standardized sample processing using immunomagnetic cell capture, enrichment and fluorescence staining. (C) Sample analysis is made with the CELLTRACKS ANALYZER II®, a semiautomated system based on fluorescence optics, and the events are later validated by a trained technician. (Based on the CellSearch® protocol). 11
- Figure 4: Schematic image of the photolithography process. (A) Resist coating; (B) Mask alignment and UV-light exposure; (C) Development: behavior of the positive and negative resists; (D) Etching; (E) Resist strip. 28
- Figure 5: Schematic image of the soft lithography process, namely replica molding. (A) The elastomer Poly(dimethylsiloxane (PDMS) is poured over the master. (B) The replica is carefully peeled off, containing the exact same pattern of the master. 29
- Figure 6: Schematic image representing the behavior of an electron during photon excitation and emission. The electron is excited by a laser light, transiting from S0 level to a superior one S1, and after relaxation to lower energy levels, emits a photon with less energy..... 31
- Figure 7: Schematic image of the Stokes shift. The light with short wavelength has more energy than the light with longer wavelength, this means that in a fluorescence event the light emitted has a longer wavelength and less energy than the excitation light. 31
- Figure 8: Schematic representation of part of the devices design in AutoCAD. (A) Represents one of the RUBYchip™ modules. (B) Represents an amplified area, corresponding to 25 fields, when acquiring the images in a microscope..... 37
- Figure 9: Workflow representation of the fabrication of a PDMS microfluidic device. (A) PDMS polymer is prepared by adding PDMS elastomer and crosslinker in a 10:1 ratio and vigorously mixed, afterwards the aerated mixture is degasses using vacuum, in the desiccator. Once degassed the PDMS is poured over the master. (B) The master is also put under vacuum to further degass the PDMS. (C) the master is brought to the oven, at 65°C for 2h to cure the PDMS. (D) once the PDMS is cured, the replica is peeled off from the master, and inlet and outlet holes are punched. (E) Previously cleaned and inspected replica and glass slide are put under oxygen plasma treatment, to allow irreversible linkage between them. (F) EVA tubing is placed both in the inlets and outlets. (G) The device is connected to a syringe pump to proceed with device functionalization..... 38
- Figure 10: Representation of the benchtop setup for the spiking experiment. (A) Cultured cells are spiked in 7.5 ml of whole blood from healthy volunteers. (B) The blood containing the cells is transferred to a syringe. The syringe is properly placed in a syringe pump and the blood is pumped

into the devices at a predetermined flow rate. (C) RUBYchip™ picture, once the blood is in the device, device design features become evident..... 41

Figure 11: Representative images of the antibody panel used in the study. DAPI is used to stain the nucleus, CK used to target epithelial cells, HER2 used to target cells with the HER2 overexpression and CD45 used to target blood cells, used as CTC exclusion criteria..... 42

Figure 12: Representative image of the experimental design used to perform immunocytochemistry in well plate (ICC-in-well). Three different cell lines (MCF-7, MDA-MB-435 and SKBR3) and PBMCs from healthy volunteers were used separately and mixed. Cell lines were seeded on sterile glass coverslips, treated with Poly-Lysine to facilitate the cell attachment, and placed in a 24-well plate at ideal densities to grow for 24 h. PBMCs were isolated by density gradient centrifugation using Histopaque®, since PBMCs are suspension cells, they are not able to adhere to solid surfaces, so these cells were maintained in eppendorf tubes. For the mix, that is, all the cells present in a cover slip, a single drop of a solution containing the PBMCs was added to the mounting medium when mounting the glass slides, after the entire process including the antibody incubation. The antibodies (Cytokeratin (CK), HER2, and CD45) to be used in this study were tested, as well as DAPI, individually. A cocktail with all the antibodies was also tested (ALL in the well plate scheme). 43

Figure 13: PBMCs isolation by density gradient centrifugation. (A) Centrifuged tube showing cells distributed in the solution in layers based in the differences in their density/size, buffy coat is the fraction enriched with PBMCs (Peripheral blood mononuclear cells). (B) Representative image of the PBMCs isolation. The blood from a healthy volunteer is gently poured over Histopaque® and centrifuged according to manufacture’s instructions. Afterwards, the different blood components are separated, and PBMCs can be isolated. 44

Figure 14: Representative image of the different cell lines trapped inside the RUBYchip™ after the spiking assay, in the micropillars that work as the filtering area, namely, MCF-7, MDA-MB-435 and SKBR3 with diameter 56.59 μm, 21.02 μm and 33.44 μm respectively. This image was visualised and acquired using Nikon-TI-E microscope, and posterior measurements were done using NIS® Software. The images were acquired and observed with a 20x objective. The scale bars corresponds to 50 μm. 50

Figure 15 : Graphical representation of the isolation efficiency of the RUBYchip™ at four different flow rates, with three different cell lines, MCF-7, MDA-MB-435 and SKBR3. The highest results were achieved at 120 μl/min, for all the cell lines, with an isolation of 53%, 59% and 56% for MCF-7, MDA-MB-435 and SKBR3 breast cancer cells, respectively, showing consistency of the results. 51

Figure 16: Histograms representing the frequency of pixels of an intensity value, for each colour channel. The left bar, with the black triangle on top, allows the regulation of the contrast, adjusted in the peak. The right bar, with the white triangle in top, allows the regulation of the brightness..... 52

Figure 17: Immunocytochemistry in well of MCF-7 cells. (A) CK expression; (B) HER2 expression, at 2 μg/ml; (C) HER2 expression, at 6 μg/ml; (D) DAPI expression; (E) CD45 expression; (F) Cocktail of antibodies expression. DAPI is shown in all the images, staining the nucleus. 53

Figure 18: Immunocytochemistry in well of MDA-MB-435 cells. (A) CK expression; (B) HER2 expression, at 2 μg/ml; (C) HER2 expression, at 6 μg/ml; (D) DAPI expression; (E) CD45 expression; (F) Cocktail of antibodies expression. DAPI is shown in all the images, staining the nucleus. 54

Figure 19: Immunocytochemistry in well of SKBR3 cells. (A) CK expression; (B) HER2 expression, at 2 µg/ml; (C) HER2 expression, at 6 µg/ml; (D) DAPI expression; (E) CD45 expression; (F) Cocktail of antibodies expression. DAPI is shown in all the images, staining the nucleus. 54

Figure 20: Immunocytochemistry in well of PBMCs- (A) CK expression; (B) HER2 expression, at 2 µg/ml; (C) HER2 expression, at 6 µg/ml; (D) DAPI expression; (E) CD45 expression; (F) Cocktail of antibodies expression. DAPI is shown in all the images, staining the nucleus. 55

Figure 21: Immunocytochemistry in well of all the cells previously demonstrated, MCF-7, MDA-MB-435, SKBR3 and PBMCs. (A) CK expression; (B) HER2 expression, at 2 µg/ml; (C) HER2 expression, at 6 µg/ml; (D) DAPI expression; (E) CD45 expression; (F) Cocktail of antibodies expression..... 56

Figure 22: Histograms representing the frequency of pixels of an intensity value, for each colour channel. The left bar, with the black triangle on top, allows the regulation of the contrast, adjusted in the peak. The right bar, with the white triangle in top, allows the regulation of the brightness..... 57

Figure 23: Images obtained from the immunocytochemistry in device assays (ICC 1, ICC 2 and ICC 3). Each ICC was made in separate devices with different antibodies dilutions, using all the cells previously demonstrated, MCF-7, MDA-MB-435, SKBR3 and PBMCs. It is possible to observe the cells trapped inside the device in the filtering area, and all the antibodies have expression in cells with distinct morphology, namely MCF-7 are CK+/DAPI+, MDA-MB-435 are DAPI+, SKBR3 are CK+/DAPI+/HER2+ and PBMCs are CD45+/DAPI+..... 58

Figure 24: Images obtained from the immunocytochemistry assays using healthy donors blood. The assay was made in triplicate, (1), (2) and (3) represent images of the devices with PBMCs from the three different volunteers. As expected, only DAPI and CD45 staining is observed. No CTCs were detected in the blood of the healthy donors. 59

Figure 25: Comparative bar chart demonstrating the enumeration of CTCs using the RUBYchip™, in green *versus* the CellSearch® system, in grey, for all the 14 patient’s samples analysed in both time points. Baseline results are shown on the left side of the graphic, and follow-up results on the right..... 64

Figure 26: Representative images obtained with the different technologies, CellSearch® on the top, and RUBYchip™ at the bottom. With the RUBYchip™ is possible to obtain high resolution images, when compared to those obtained with the CellSearch®. In this particular case, it is possible to observe CTCs (DAPI+/CK+/CD45-). The RUBYchip™ images show 3 CTCs, both in a merged image (bright field and fluorescence) and fluorescence only..... 65

Figure 27 : Bar chart demonstrating the number of CTCs isolated by the RUBYchip™ in 14 metastatic breast cancer patients, in both moments of collection, baseline (before starting systemic therapy, in yellow bars)and follow-up (after 12 weeks of systemic treatment, in grey bars). It is also possible to observe the presence of HER2+ cell, represented by striped bars..... 69

Figure 28: Representative images obtained with the different technologies, CellSearch® on the top, and RUBYchip™ at the bottom. RUBYchip™ technology image quality is considerably higher than those obtained with the CellSearch®. In this particular case, it is possible to observe HER2+ CTCs (DAPI+/CK+/HER2+/CD45-). The RUBYchip™ images show 1 CTC with HER2 presence, both in a merged image (bright field and fluorescence) and fluorescence only..... 70

List of Tables

Table 1: Microfluidics technologies used for CTC isolation. Adapted from [149]	16
Table 2: Working dilutions tested for each of the selected antibodies and DAPI in this immunocytochemistry experiment in well, using adherent cells cultured on coverslips. (AB: antibodies).....	44
Table 3: Working dilutions tested for each of the selected antibodies and DAPI in this immunocytochemistry experiment performed in device (ICC 1), using adherent cells cultured on coverslips.....	45
Table 4: Working dilutions tested for each of the selected antibodies and DAPI in this immunocytochemistry experiment in device (ICC 2). Compared to the previous assay, ICC 1, CK and CD45 dilutions were increased.....	45
Table 5: Working dilutions tested for each of the selected antibodies and DAPI in this immunocytochemistry experiment in device (ICC 3). The dilutions used for CK and CD45 are twice as high as ICC1.	45
Table 6: Working dilutions tested for each of the selected antibodies and DAPI in this immunocytochemistry experiment as a negative control test.	46
Table 7: Immunofluorescent staining characteristics for identifying CTCs. Cells isolated by the RUBYchip™ were classified according to immunostaining against CK, CD45, DAPI and HER2. Events DAPI+/CK+/CD45- OR DAPI+/CK+/HER2+/CD45- were defined as CTCs.....	47
Table 8: Antibody dilution selected to be used in patient samples.....	47
Table 9: Isolation efficiency of the RUBYchip™ for four different flow rates tested.....	51
Table 10 : Clinicopathological characteristics of patients enrolled in this study.....	62
Table 11: Technology comparison, RUBYchip™ <i>versus</i> CellSearch®, results for both baseline and follow-up collection times. Results showing the enumeration of CTCs by each technology are presented, as well as the number of samples above the threshold established for breast cancer (≥ 5 CTCs).....	63
Table 12: Evaluation of the HER2 status in the patients' tumours and CTCs. The presence (✓) or absence (✗) of this biomarker were assessed in tissue biopsy and liquid biopsy, based on patient clinical reports and results obtained with the RUBYchip™ and the CellSearch®. Presented data refers to pool of patients that exhibited HER2 positivity in at least one of the assessments or time points. (0 stands for the samples with no CTCs isolated)	67

CHAPTER 1: General Introduction

1. General Introduction

1.1. Cancer and Breast Cancer

Cancer is one of the main causes of death worldwide, and despite all efforts, statistics showed that it caused 9.55 million deaths, in 2018, and this number is expected to increase to 13 million in less than 20 years [1]–[3].

Cancer is a broad term that designates a disease that can occur in many parts of the body when cellular changes happen, causing abnormal and rapid cell division and growth.

There are many causes of cancer, among them genetics ones, when cells present mutations in their genome that result in a protein with an oncogenic function that ignites the abovementioned abnormal growth, resulting in the formation of tumours [4], [5].

The disease can also be caused by environmental and/or behavioural influences (that can be avoided) such as obesity, tobacco, physical inactivity or even alcohol, already proven to be related with cancer formation. Some infections have also been proven to have a role in cancer appearance, such as *Helicobacter pylori*, hepatitis and human immunodeficiency virus (HIV) [6], [7].

The tumours can be very heterogeneous, comprising tumour cells with different genetic and phenotypic characteristics, representing an essential cause of the clonal evolution of the tumour [8].

Breast cancer is the second most common cancer in the world and one of the leading causes of cancer-related mortality in women, with incidence mainly in women between 35 and 75 years of age [8], [9]. In most of the cases, the disease appears sporadically, however, in a small percentage of about 5% of the cases the disease is hereditary with a mutation in coding DNA, leading to a high risk of developing cancer during life [9]–[12].

Fortunately, clinical management and technological advancements occur every day, and so, most primary breast cancers can be treated, either by surgery alone, or surgery and complementary therapy, achieving an overall 5-year survival rate is of 90%, currently [13].

1.1.1. Different types of primary breast cancer

The high mortality still caused by breast cancer is mainly related to late detection, disease recurrence and drug resistance. Good biomarkers are still lacking to continuously predict response to

therapy and disease progression. A panoply of attempts in this direction have been unsuccessful, mainly because of the heterogeneity and dynamics of the disease [9], [14].

Research efforts are currently focused on identifying the molecular heterogeneity of breast cancer and in classifying patients into meaningful groups. Classification into subtypes allows to stratify patients according to prognosis and to define the best therapeutic approach for each group [9].

Histologically, breast cancer can be divided into *in situ* and invasive carcinoma, according to the tumour location, and subclassified into ductal and lobular carcinomas, based on their architectural patterns and immunohistochemically profiles [9], [16], [17].

Additionally, it is possible to identify four distinct groups of breast cancer, based on the gene expression patterns, luminal A, luminal B, human epithelial growth factor receptor 2 (HER2) overexpression, and basal-like [9], [16], [17], depending on the presence or absence of the most important molecular markers (Figure 1).

The luminal group, correlated with the presence of hormonal receptors (estrogen receptor and/or progesterone, ER+ and/or PR+), can be subclassified into two different ones, luminal A and B, associated with different clinical outcomes. Luminal A tumours have high levels of expression of hormone-activated genes and low levels of proliferation, also they have low histological grade (1-2) and good outcome, also with no expression of HER2; on the other hand, luminal B tumours have higher histological grade (2-3), higher proliferation rates and overexpression of HER2, consequently, with a significantly worse prognosis [16]–[19].

The other subtypes, HER2 and basal-like, are related to the lack of hormonal receptors (ER- and PR-) [17] and associated with an aggressive tumour, with complicated clinical behaviour [9], [17].

Basal-like tumours have this name because of their cells express genes normally found in basal/myoepithelial cells of the breast, and are also known as the triple-negative breast cancer, since these tumours lacks in the expression of estrogen, progesterone, and HER2 receptors, representing 15-20% of the cancers and usually having unfavourable diagnosis and outcome, with high histological grade (3), high proliferative index and higher risk of metastases [19]–[25].

HER2 tumours display an overexpression of the HER2 protein and associated genes. HER2 tumours show a rapid growth, high histological grade (2-3) and poor behaviour in the therapy [26], [27].

It is known that the mutations and their accumulation are responsible for the process of mammary carcinogenesis and its progression, and so, several markers have been identified and studied, being related to the appearance and evolution of breast cancer.

As discussed above, the study of PR, ER, and HER2 receptors in the tissue predicts disease evolution and provides prognostic information for the patients, but other biomarkers, such as cytokeratins, mucin-1 (MUC-1), B-cell lymphoma 2, phosphatase and tensin homolog (PTEN), phosphatidylinositol 3-kinase (PI3K), BRCA mutation and the carcinoembryonic antigen family (CEA), have also an important role in carcinogenesis [9], [28]–[31].



Figure 1: Schematic image showing the immunohistochemistry profile of the four-molecule subtype of breast cancer based on the three most important markers. (ER- estrogen receptor; PR- progesterone receptor; HER2- human epithelial growth factor receptor 2).

1.1.2. HER2 mutation

HER2 is a member of the epidermal growth factor receptor (EGFR) family of homologous transmembrane receptor tyrosine kinases [32]–[35].

The amplification and overexpression of this proto-oncogene occurs in 20%-30% of breast cancers and has an important role in the progression of the disease, associated with an aggressive disease course and poor survival [32], [33], [36].

When a ligand binds to EGFR it induces a conformational change in proteins that facilitates receptor dimerization, and so, both tyrosine kinase domains get together in an asymmetrical manner, subsequently, exposing docking sites for downstream proteins to be recruited, these signalling molecules can affect multiple cellular processes, such as proliferation and differentiation [34], [37], [38].

HER2 is a major proliferative stimulator that activates downstream signalling through the phosphoinositide 3-kinase/AKT and MEK-ERK pathways, and although there is no known ligand for HER2, it can be activated by heterodimerization with other members of the EGFR family, affecting the downstream signalling of these receptors [33], [34], [39], [40].

HER2 mutations consist of in-frame insertions in exon 20, and can be found across all exons of the HER2 gene, affecting the extracellular, transmembrane and tyrosine kinase domains (ECD, TMD and TKD respectively) of the HER2 protein, which leads to an activation of the receptor and downstream AKT and MEK pathways, even in the presence of a normal HER2 gene copy [36], [41], [42].

The HER2 mutations were first identified in the tyrosine kinase domain of this gene in HER2-positive breast cancer patients, however, recently they were also identified in HER2-negative breast cancer, suggesting that, even with a low mutation rate (<2%), these mutations can activate the HER2 signalling pathways in HER2-negative cells, being an alternative mechanism for the activation of the gene in HER2-negative breast cancers [42]–[53].

Once the role of HER2 in breast cancer was under covered, it arose the need to develop drugs such as Trastuzumab, a monoclonal antibody against HER2, which is used as an alternative or adjuvant therapy in breast cancers with the occurrence of the proto-oncogene, and in the treatment of metastatic breast cancer, lowering the risk of recurrence of the disease by 50% [32], [35], [54].

Since this biomarker has an important role in the evolution of breast cancer, along with others referred above, their analysis in the clinic is routine practice, in order to make a prognosis and establish therapeutic options such as chemotherapy, hormone therapy or anti-HER2 therapy [55].

Nowadays, immunohistochemistry (IHC) is the protocol that is used in the clinic to evaluate those markers since it can characterize cellular proteins in tumour tissues. IHC, along with the fluorescence *in situ* hybridization (FISH), are used to evaluate the presence or absence of HER2, hormone receptors and other biomarkers (i.e. Ki-67, p53) in the cancer cells [56], [57]. Thus IHC and FISH allow for the characterization of the tumour subtypes, the distinction of the tissue of origin, metastatic from the primary tumour and provides information that has an important role in diagnostic and treatment planning [57].

Tests for HER2 consists of a score of 0 to +3, measuring the amount of HER2 receptors on the cell surface of a breast cancer tumour. If the score is 0 to +1, the tumour is considered HER2 negative, a score of +2 is weakly positive and a score of +3 is considered HER2 positive [56]. Thus, a HER2 positive result indicates an intense membrane staining of >30% of tumour cells [58], [59]. Still, HER2 tests can be inaccurate, probably because of the laboratories' different conditions and rules. Each laboratory can stipulate the HER2 values that will determine the status of a patient, and also have different standardization aspects such as pre-analytical sample tissue handling, type of fixation, interpretation, and reporting [59], [60].

Thus, although IHC has become an important and integral part of the clinic protocol, it is not enough for a good and correct diagnosis, prognosis and therapy appliance. It lacks in specificity and is not very sensitive since there are not established values and each laboratory can have different rules for the classification of the tumour, so the results can be widely depending on factors like the choice of fixative or antibody. Also, the tissue biopsy currently made in the clinics at the time of diagnosis, and used

for continuous monitoring has limitations, being a very invasive technique. Despite this, IHC is a cost-effective test, so it can be performed along with other tests [57].

1.1.3. Metastatic breast cancer

Metastatic disease is the dissemination of the tumour cells throughout the body, and although breast cancer starts as a local disease, cancer spreading is accountable for the majority of cancer related deaths. Cancer spreading, or metastasis, occurs when an early diagnosis is missed or when treatment of the primary tumour is unsuccessful. In the case of breast cancer, metastasis is one of the greatest causes of death among women, such that the 5-year survival rate for metastatic breast cancer (MBC) remains at 26%, [1], [3], [61].

MBC occurs when tumour cells shed from the primary tumour, entering the circulation and migrating to other organs, contaminating them and forming secondary tumours [62], [63]. Thus, metastases formation can occur at almost any site, however, the most common sites are the lymph nodes, bone marrow, lung, and liver, such that the site of metastases is associated with prognosis and survival. Brain metastases are the most aggressive, being correlated with a worst outcome [64].

A correlation between the BC subtype and the site of metastases formation has also been made. Luminal and HER2 subtype tumours are correlated with the formation of metastases in brain, liver, bone and lung, and basal tumours correlate with brain, lung, bone and distant nodal metastases sites [65].

When diagnosed and localized, the majority of breast cancers can be cured by surgery, however, once metastasis has occurred, surgery is not curative [66]. In adult women, cancer can take up to 20 to 30 years to evolve into late-stage disease, and even when metastasis has already initiated but is not yet disseminated, MBC can be cured in up to 50% of cases with traditional therapy such as immunotherapy and cytotoxic drugs. But once disseminated on a large scale, metastatic tumours are rarely cured, thus there is an urgent need for better tools towards cancer prevention, early cancer diagnostics, accurate prognosis and personalised medicine, before cancer metastasizes to distant sites [67]–[69].

The main problem is that metastasis can be formed years after the first diagnosis and the patients remain asymptomatic, this phenomenon can be called “tumour dormancy”, which means cancer cells can disseminate and colonize distant sites but stay dormant until enough genetic mutations occur or appropriate environmental conditions take place, allowing their awakening and proliferation. This process can happen by two different ways, either tumour cells can leave the primary tumour and colonize different

sites only if they have the competence to generate metastasis, or normal cells leave the preneoplastic lesions and evolve to tumour cells simultaneously with the primary tumour [9].

Currently, in the clinic, the protocol to follow up patients both before and after surgery uses tissue biopsy or re-biopsy and imaging technologies such as magnetic resonance imaging (MRI) and computerized tomography scans (CT). MRI is a technology that uses radio waves in order to produce detailed images of the body, and CT is a technology that used X-ray waves that produced 2D slices with information on the internal body [9], [58]. However these methods have several cons, since biopsy is a very invasive and painful procedure, limited to certain tumour locations and not always possible for the patients, and the imaging technologies do not provide enough information on the tumour evolution over time, since they do not have enough sensitivity to detect micrometastasis, and do not provide information on tumour heterogeneity [7].

After several studies, it is currently thought that the spread of breast cancer is a complex process which depends on environmental factors, such as diet and tobacco, and internal stimuli, such as mutations and hormones, thus the growth of metastasis at different sites depends on many clinical features such as tumour size and age at diagnosis, but mostly on interactions between tumour cells and the host, since those cells are capable of acquiring several alterations that make them competent to establish metastatic lesions in various specific organs [61].

Also, many genes are known to play a role in metastasis formation since their increased expression is correlated with the metastatic process. However, how the different genes can cooperate to create tissue-specific metastasis and how the expression of these genes relates to the evolution of the primary tumour remains unknown. Some researchers have shown that some tumour cells, with these group of genes, enhance their metastatic activity when in contact with TGF β , a ubiquitous cytokine that inhibits growth of epithelial and early-stage tumour but on the other hand increases the invasion and metastasis of aggressive tumours, also, many of these genes encode secretory and cell surface proteins, influencing the tumour environment in favour of the formation of metastasis [70].

Nowadays, traditional prognostic factors cannot identify breast cancer patients that can eventually develop metastasis, making it impossible to apply a timely treatment [71]. However, recurring to recent methods such as liquid biopsy and the identification of the risk biomarkers, it may be possible to predict tumour progression [72].

1.2. Liquid biopsy

Since cancer development is a dynamic process in constant clonal evolution, tumour biopsy may not reflect the real state of the patient during disease progression [73]. Still, tumour cells are constantly shed from the primary and/or secondary tumour into the bloodstream, and since they have a short half-life, their continuous analysis can provide a more accurate status of the disease in real-time, allowing a more accurate prognosis [4], [5]. Also, once the haematogenous dissemination of tumour cells is the principal mechanism for metastatic formation, the analysis of blood from cancer patients with breast cancer may be the ideal approach to timely detect tumour cells spreading and the possible formation of metastasis [71], [74]. This analysis of tumour material in peripheral blood and other body fluids is called liquid biopsy [75].

Liquid biopsy is a minimally invasive and painless method that provides continuous, reliable and real-time information on the tumour progression, overcoming the limitations of the clinical procedures [76]. Through the analysis of circulating biomarkers, like CTCs (circulating tumour cells) and ctDNA (circulating DNA), liquid biopsy has the potential to access genetic and phenotypic information about the primary and secondary tumours, allowing early diagnosis, accurate prognosis and personalized therapeutics [14], [73], [77], [78].

Due to this advantages, the liquid biopsy field has grown in the last decade and can be a better solution for the study of breast cancer and an attractive concept in oncology in general to investigate tumour heterogeneity, dynamics and progression along time [79]–[81].

1.2.1. Circulating tumour cells (CTCs)

CTCs are cells shed from the primary or secondary tumour into the peripheral blood, that have molecular characteristics specific of the local where they were formed, and with the ability to invade other organs causing metastasis [82], [83]. (Figure 2)

Just as the tumours, CTCs are heterogeneous and can be classified in different subtypes, according to different phenotypic and functional characteristics such as the expression of specific proteins and genes [84].

Researchers have shown that CTCs can be found in patients at early stages of tumour growth or even before the detection of cancer by the traditional methods [85], [86], still CTCs are rare, with an estimated ratio of 1:10⁷ (one CTC per billion of normal blood cells), and consequently, their technical isolation and their applicability in the clinic is challenging [14], [87].

Nevertheless, the study of CTCs in cancer patients, can provide real-time information on the tumour progression and holds a great promise for early detection and prognosis of metastatic breast cancer [14]. Thus in the past years, many technologies have been developed for this purpose such as microfluidic devices for the isolation of CTCs [88].

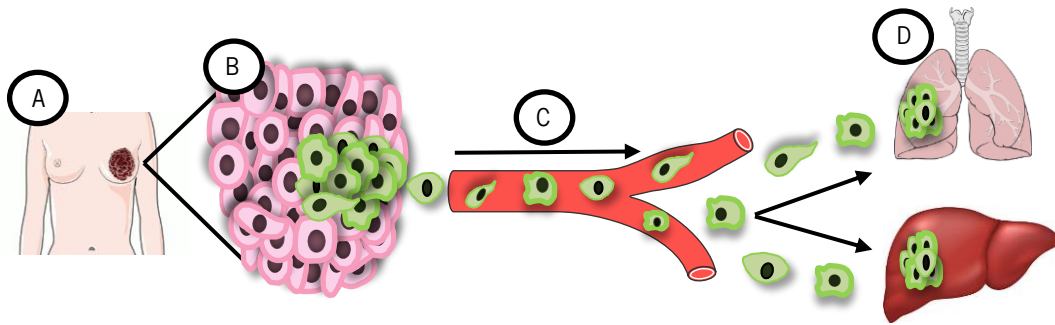


Figure 2: Schematic image showing the input of CTCs into the bloodstream and posterior formation of metastasis in other organs. (A) shows the location of the primary tumour. (B) Schematizes the tumour cells, and (C) their dissemination into the blood vessels, so that a possible metastasis formation (D) in distant organs occurs.

1.3. Technologies for CTC isolation

The detection and isolation of CTCs remains a challenge mainly because of two major factors, CTCs are rare events in the bloodstream of cancer patients, and it is hard to distinguish them from normal blood cells. When the term detection is mentioned, it refers to the identification of CTCs in a sample, and isolation means the efficient separation of CTCs from other cells in a sample, thus, in order to study CTCs completely, the ultimate goal is to efficiently detect and isolate these cells from the whole blood sample [3], [31].

Before the detection of CTCs, due to their low frequency, it may be necessary to make an initial enrichment/isolation step, and there are currently some methods for this purpose based on the different properties of CTCs that distinguish them from the other blood cells [3], [73]. There are some parameters that should be considered when validating a system for this purpose, such as recovery rate (the ratio of isolated CTCs *versus* the total number of CTCs in sample); purity rate (the ratio of detected CTCs *versus* the total number of isolated cells); enrichment rate (the ratio of CTCs to blood cells before and after isolation); throughput (the speed by which the blood sample is analysed) and viability (the percentage of viable CTCs to all CTCs detected and isolated) [3].

To date, many technologies have been developed to enrich and/or isolate CTCs, based on their physical properties, such as size, density, electric charges or/and deformability [89], [90], and biological properties, such as antigen expression or/and viability [73], [91], [92].

When analysing their physical properties, the advantage is that they allow CTC separation without labelling, and the methods for this purpose include density gradient centrifugation, filtration recurring to special filters, a biochip that exploits the differences in size and deformability of cancer cells compared to blood cells, a photoacoustic flow cytometer, a microfluidics device that matched multi-orifice flow fractionation and the dielectrophoresis (DEP) technique [93], [94].

Regarding the biological properties, immunobead assays can be made, these assays use immunologic procedures with antibodies against tumour-associated antigens (positive selection) or against the common white blood cells antigen CD45 (negative selection). Also microdevices can be used, such as microfluidic devices that can handle very small blood volumes, with the objective of capture CTCs recurring to the use of a cocktail of antibodies against epithelial cell surface antigens (for example: HER2, MUC1, EGFR) and mesenchymal or stem cell antigens (for example: c-MET, CD318, VIM) [93], [95].

After the enrichment process, the sample usually contains a considerable number of normal blood cells and the CTCs need to be identified so that their analysis is possible [73].

Despite all the methods and technologies available, the CellSearch® system is the only platform for detection and enumeration of CTCs in clinical settings, approved by the Food and Drug Administration (FDA) to date [96]–[98].

1.3.1. CellSearch®

CellSearch® system was first introduced in 2004 [97], and since then it has been employed in numerous clinical studies, validated as a diagnostic tool for prognostic evaluation and monitoring in patients with metastatic breast, colorectal and prostate cancer, such that it has a major role in the data on clinical utility of CTCs [99]–[102]. The system was designed for the immunomagnetic enrichment, fluorescent labelling, and detection of rare cell populations, such as CTCs [97] (Figure 3).

It uses ferrofluids coupled with an anti-EpCAM antibody (magnetic beads covalently conjugated with EpCAM antibodies) to recognize and capture only epithelial tumour cells expressing EpCAM, discriminating the other cells [97], [103].

The anti-EpCAM antibodies are added to 7.5 ml of peripheral whole blood for magnetic cell sorting, and isolated cell are posteriorly stained with a cocktail of antibodies against CKs (CK8, CK18, CK19) as

positive markers, the common leukocyte antigen CD45 as negative marker to exclude contaminating by this type of cells, and a nuclear dye DAPI (4',6-diamidino-2-phenylindole). Thus, CTCs are defined as EpCAM+/CK+/CD45-/DAPI+ [97], [104].

More in detail, after sample collection, multiple pre-processing steps are performed (including aspiration of plasma, followed by addition of anti-EpCAM ferrofluids and buffer; magnetic incubation; aspiration of unlabelled cells; magnetic removal of the cells re-suspended in buffer; cell labelling with antibodies and transfer to an appropriate holder), followed by the sample analysis, that is done using immunomagnetic and fluorescence imaging technology. CTCs can be counted and validated by a trained technician, and the results can be correlated with the disease status of the patients. They can be divided into different subgroups depending on the number of CTCs present in their sample of blood, with 0 CTC, 1-4 CTC, 5-24 CTC, and >24 CTC, thus it is possible to correlate the survival with the number of CTCs, wherein the higher the number of CTCs the worse the prognosis will be [97].

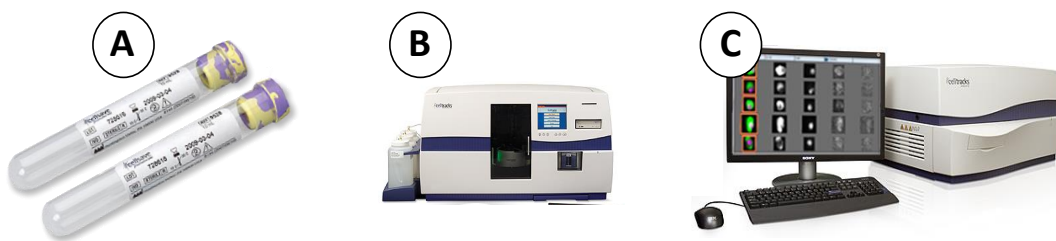


Figure 3: Representative images showing the CellSearch® workflow overview. (A) The sample collection is made in specific tubes, CellSave Preservative Tubes, with a cell preservative that is able to store cells for up to 96 hours at room temperature, allowing, for example, shipment to distant locations. (B) The sample preparation is made with the CELLTRACKS®AUTOPREP® system, allowing an automated and standardized sample processing using immunomagnetic cell capture, enrichment and fluorescence staining. (C) Sample analysis is made with the CELLTRACKS ANALYZER II®, a semiautomated system based on fluorescence optics, and the events are later validated by a trained technician. (Based on the CellSearch® protocol).

1.3.1.1. CellSearch® limitations

When the term “cell-plasticity” is referred, it means that the cells, in this case, CTCs, have the ability to change their characteristics. Epithelial-mesenchymal transition (EMT) is a complex process by which epithelial cells have the capacity to lose their cell polarity and adhesion, changing their phenotype, and gaining migratory and invasive properties, that is, differentiating into mesenchymal cells [73]. Although EMT is a normal process during wound healing and organogenesis, during metastasis formation in cancer, EMT occurs to increase the invasion capability of cancer cells and has been proposed to be related with cancer aggressiveness and metastasis formation [105]–[107]. The reverse process can also

occur, named mesenchymal-epithelial transition (MET), and is responsible for the formation of metastasis after the CTCs settled down in distant organs [73].

Despite the demonstrated clinical validity of CellSearch® to evaluate disease prognosis and resistance to therapy, its enrichment methods causes some cell loss which affects the sensitivity of the system, and only selects CTCs expressing EpCAM, not capturing the other CTC phenotypes, such as mesenchymal and stem cell-like tumour cells that have low levels or lack EpCAM expression [98], [108], [109]. Consequently, using the CellSearch® system, only 50-70% of CTCs are captured [110]–[114].

1.3.2. Biomarkers in Cancer research

Among the biomarkers that can be present in CTCs, the most studied markers are related to the epithelial, mesenchymal and stemness markers [84]. That said, it is very important to be aware of the variety of those biomarkers and make a correct decision when it comes to choosing the right one for sample analysis.

The most important epithelial markers are:

EpCAM, a cell surface glycoprotein expressed at high levels in epithelial cancer cells and at a low level in normal epithelial cells. It is very important in the detection and enumeration of CTCs and is the major marker in the CellSearch® system, yet, the expression of this protein depends on EMT stage, and when downregulated it can be expressed with N-cadherin and vimentin, disappearing with E-cadherin. This means that patients with undetected CTCs by EpCAM based technology do not always have a favourable prognosis [114], [115].

E-cadherin, a component of adherens junctions with functions that collaborate with the actin cytoskeleton and enable resistance to forces, causing cell detachment, that meaning, it is one of the proteins that support epithelial tissue architecture. This protein has an important role in the EMT progression, such that when a cell is going through EMT, its levels decrease [116].

Cytokeratins, the most diverse class of intermediate filaments that are cytoskeleton components, can be used as a diagnostic tool to detect different CTCs, since epithelial cancer cells express CK8, CK18, and CK19, and can be used along with EpCAM for the enumeration of CTCs [117].

Zonula occludens (ZO), proteins of tight junctions involved, along with E-cadherin, in epithelial tissue architectural maintenance. When a lack of these proteins occurs, the cells won't be able to form tight junctions. Its downregulation is one of the first signs of EMT induction [118], [119].

Epithelial splicing regulator1 (ESPR1), a gene, that is a mark of epithelial phenotype when in high levels, and is downregulated when EMT occurs, in fact, ESPRs are very important genes in the process of the phenotypic cellular switch in EMT [120]–[122].

When CTCs are analysed and, at least, two of this markers are detected, at the single cell level, this CTCs can be characterized as a differentiated epithelial cancer cell, as long as mesenchymal and stem markers are not observed [84].

Regarding mesenchymal-like CTCs, when a cancer cell is transformed into the mesenchymal state during the EMT process, the most important markers to considerate are:

N-cadherin, a protein with functions related to the adherens junctions that is expressed especially in mesenchymal cells, and therefore used as an EMT marker. It is related to E-cadherin since when E-cadherin is downregulated, N-cadherin is switched on, thus, the abnormal expressing of N-cadherin occurs, associated with a decrease of E-cadherin is a hallmark of the mesenchymal character of CTCs [123], [124].

Vimentin, a protein expressed in mesenchymal cells that induce the shape of the cells and increases their mobility [125].

Twist 1, a basic helix-loop-helix transcription factor, involved in embryogenesis and reactivated in cancers, leading to EMT. Its role in the dissemination of CTCs and metastasis is a complex process related to oncogenic and anti-oncogenic proteins. It was used to determine the presence of mesenchymal CTCs for the first time, along with Akt2 and Pi3K [126], [127].

Akt and Pi3K, are correlated, since the oncogenic serine kinase Akt is a downstream effector of the phosphatidylinositol 3' kinase (Pi3K), and are described as a transcriptions repressor of E-cadherin gene [127].

Zeb1 (zinc finger E-box binding homebox 1), is a DNA binding transcription factor that represses E-cadherin, thus, is an activator of EMT [127].

Since mesenchymal CTCs are rare and difficult to demonstrate and study, these markers help to follow EMT occurrence. When two of the markers above referred, are associated with epithelial or stem markers, we can classify the cell as having a mesenchymal character [84].

Stem cells are known to be the only cancer cell subpopulation with the capacity to relapse or metastasize since they can migrate from the primary tumour into the blood, undergoing EMT. So, the study of their markers are also important and are:

Aldehyde dehydrogenase-1 (ALDH1), an enzymatic protein responsible for the oxidation of retinol to retinoic acid that can be considered as a prognostic and predictive breast cancer marker [127].

CD44, a cell surface glycoprotein related to cell migration and metastasis that is able to give rise to various isoforms some of them can be specific markers of CTC stemness. In breast cancer, CD44⁺/CD24^{low} cells are known to be tumorigenic [127].

Gangliosides (GD2, GD3, GD1a), glycosphingolipid involved in cell growth and motility that can be used as CTC stemness markers [128], [129].

ABC proteins that are expressed in high levels in CTCs phenotype, thus a potential candidate as a marker of stemness [128], [129].

Due to the heterogeneity of CTCs, it is important to develop new techniques that do not focus only on the epithelial marker expression. These include, as previously referred, physical properties including selection based on size, density and electrical charge based separation and negative enrichment [98][130].

1.3.3. Microfluidic separation of CTCs from blood

Microfluidics, as the name implies, is the technology capable to manipulate a small amount of fluids at the micrometre scale, generally using micrometre sized channels. This technology is now being used in many research fields, such as engineering, physics, biophysics, nanotechnology, lab-on-chip concepts and, of course, cancer research.

These microfluidic devices have many advantages since they are low cost and easy to fabricate, reducing, as well, the volumes of reagents to use, and the time of each experiment [74], [131], [132].

Microfluidic-based separation methods are an attractive alternative to traditional cell isolation technologies, due to added numerous advantages such as the use of small sample and reagent volumes with a reduced cost, low contaminating issues and no sample-processing steps, such that cell loss is also reduced, resulting in systems with superior sensitivity and enhanced cell recovery [133]–[136]. All these properties and advantages make microfluidics ideal for clinical practice, enabling high throughput, portability, and automation [137], [138]. These devices have been used for microfluidic flow cytometry, size-based separation and chromatographic separation [136].

Several microfluidic devices have been developed for CTCs isolation, with high efficiency, a necessary characteristic since CTCs abundance in the blood is low. Microfluidic enrichment can be done through physical/size based filtration or immune selection, positive or negative [136], [139],[140] (Table 1).

Microfluidic isolation of CTCs can also be made by immobilizing specific capture molecules on magnetic beads, microstructures or array channels [74], [136], [141], [142]. These methods, as referred

above, depend on specific antigen expression and knowledge of CTC biomarkers, yet they provide better separation purity. Currently, various positive selection microfluidic devices, with diverse geometries and architectures, have demonstrated high efficiency, but only after following various pre-processing and optimization steps [92], [143]. Microfluidic devices have also been shown excellent performance for negative enrichment of CTCs [144]. Negative enrichment relies on the removal of cells that are not of interest. In this case, normal blood cells are depleted from the sample, hence enriching the CTCs. This method is usually achieved using magnetic beads immune-conjugated to target a specific antigen on the cell membrane of the non-target cells. The main goal is to remove white blood cells (WBC), for CTC isolation, which is targeted using CD45 [145] [60]. Some microfluidic approaches have introduced a nanoroughness on PDMS devices in order to enhance the binding of WBCs to the anti-CD45-coated surface. These structures have shown great efficiency, increasing binding yields of CTCs. Then, combining this device with imaging flow cytometry is possible to know the phenotype changes associated with CTCs, and improve patient prognosis [98][60].

Since CTCs are physically distinct from blood cells, in deformability, electrical properties, but especially in size (CTCs: $\approx 20 \mu\text{m}$; Red blood cells (RBC): $6\text{-}8 \mu\text{m}$; White blood cells (WBC): $10\text{-}20 \mu\text{m}$), size-based microfluidic chips are made using structures of different geometries in order to capture and isolate CTCs. These approaches offer fast processing, and recently technology advancement has been made to separate different cell population by size, such as hydrodynamic forces, inertial focusing and acoustic waves [92], [146]–[148]. This kind of microfluidic devices vary in the pore size and gap used, usually around 5 to $10 \mu\text{m}$, and some of them present very high efficiency to isolate CTCs, however, this method needs to be complemented with other such as immunofluorescence, since other cells with bigger size, like WBC, can also be trapped and need to be excluded [92], [146]–[148].

Table 1: Microfluidics technologies used for CTC isolation. Adapted from [149]

Assay	Developer	Methods
OncoCEE	Biocept	Biotin-tagged antibodies that bind selectively to CTCs
ClearCell FX System	Clearbridge	High-throughput microfluidics sheath low isolation technology by ferrofluids with cell staining plus downstream DNA analysis via NGS or qPCR
Isoflux	Fluxion Biosystems	Microfluidic chip based on immunomagnetic capture
CTCChip	Daniel Haber and Mehmet Toner, Dana-Farber and MGH	Microfluidic filter with anti-EpCAM antibodies
Herringbone-Chip	Daniel Haber and Mehmet Toner, Dana-Farber and MGH	Microvortices are used to significantly increase the number of interactions between target CTCs and the antibody-coated chip surface

1.4. Breast cancer CTCs in the clinic

Many years have passed since the first evidence of CTCs in breast cancer and their clinical validity, and CTCs have proven to have a crucial role in metastasis and in resistance to drug administration, thus it is fundamental to study and understand their clinical role during the different stages of the disease [150]–[152].

The CTCs value in clinic depends on the BC stage since their detection value differs between metastatic BC and early BC. Therefore, studies have been made in the clinic to evaluate the potential of CTCs detection in BC, diverging from early BC to metastatic BC, and evaluating the prognostic relevance, monitoring therapy and CTC-driven therapy choice [152], [153].

CTC analysis can be used along with traditional methods for monitoring metastatic BC, and for disease prognosis in early BC [154], [155].

1.4.1. Metastatic Breast Cancer CTCs in the clinic

Even when an early diagnosis is made and initial treatment applied, BC still has a recurrence of 20-30%, and metastatic BC remains incurable so that the actual goal of clinical treatment at this stage is to maximize the quality of life and improve survival of the patient by slowing the tumour progression, and minimizing the side effects of therapy.

Therefore, the need urges for the development of treatments able to reduce tumour by targeting metastasis, however, the bigger problem is that the therapeutic steps in metastatic BC are based on the

primary tumour and the first biopsy made, and as already described, cancer is a dynamic and heterogeneous disease, thus CTCs and consequently metastasis, can have different phenotypes and genotypes from the primary tumour [156]–[159].

Since CTCs are present in the blood of metastatic BC and are associated with the progression-free survival as well as with the overall survival, they can be considered a non-invasive tool to characterize the metastasis progression and have a considerable clinical value [160], [161].

1.4.1.1. Studies and significant findings to date

The first trial regarding the prognostic value of CTCs in breast cancer was done in 2004, by Cristofanilli et al., and showed clinical validity of CTC count in MBC using the CellSearch® system. In this study, the blood of 177 patients was analysed, and CTCs were counted at baseline and after a few weeks of treatment. It was established a threshold to distinguish patients with short or long progressing free survival, set up at ≥ 5 CTC/7.5 ml of blood. It was shown that detection of 5 CTC or more per 7.5 ml of blood was correlated to shorter progression-free survival and overall survival [96].

Continuing with this study, and using the same samples and data, Hayes et al. (2006), analysed CTC levels, high or low, at two different times, baseline, as in the previous study, and after an entire cycle of treatment (20 weeks), obtaining 4 different profiles of progression-free survival, and, as expected, when the number of CTCs was high at both time points, the prognosis was worse, however, when the number of CTCs decreased from the first time point to the second, the prognosis was better, as well as with patients with low levels of CTCs at both time points [160].

These studies together with analytic data allowed the FDA approval of the CellSearch® system as a technique for the monitoring of patients with metastatic BC, and several reports were published after that, with more limited size and some discordant results [149], [152], [153]

A more recent study, by Bidard et al. (2014), involved 1944 patients from 17 centres in Europe, confirmed with undisputable results the independent prognostic of CTCs in metastatic BC, and, in addition, also showed the superiority of CTC count over some tumour markers (such as carcinoembryonic antigen and cancer antigen 15-3) since these did not improve prognostication in this large number of patients[162].

Regarding their clinical utility and therapy monitoring, CTCs have shown to be an alternative tool to the usual methods to decide therapy, since their levels reflect treatment effects and can be used for therapy monitoring.

The first study to demonstrate the clinical utility of CTCs was conducted by the SouthWest Oncology Group, named “SWOG S0500”. In this trial, the treatment was changed after 3 weeks on first-line chemotherapy on persistently high CTC levels, however, it did not improve overall survival compared to treatment change when there’s actual clinical evidence of disease progression. Also, the patients who remained with high levels of CTCs after the 3 weeks did not improve overall survival compared to the patients with low CTCs occurrence or those with CTCs decreased after treatment, indicating that CTCs persistence may identify the patients that do not respond to traditional therapy [163].

Two other studies with this purpose are ongoing, the “CirCe01” trial (NCT01349842), based on early changes of CTC count, and “STIC CTC” trial (NCT01710605) based on the clinical utility of the prognostic value of baseline CTC count [164].

As already mentioned, numerous CTC detection techniques have been developed, however, only CellSearch® has reached the clinical market [152],[165].

1.4.2. Early Breast Cancer CTCs in the clinic

A big number of patients with early BC, adequately treated, suffered a relapse, so, for these patients, the development of different techniques and diagnostic tools have been made for the analysis of CTCs, based on epithelial cell staining and cytological visual screening, since their number is related with clinical outcome in metastatic BC.

Unlike metastatic BC, the studies for CTCs isolation in early BC are not abundant, with only a few reports published and heterogeneous techniques, such as molecular detection methods [152].

The detection of CTCs as a prognostic biomarker in early BC was considered and reported for the first time in patients treated with neoadjuvant chemotherapy, that is, before surgery, using CellSearch®. The studies demonstrated a homogeneity of detection rates [152].

1.4.2.1. Studies and significant findings to date

An international meta-analysis study of CTCs detection in neoadjuvant treated patients called the “IMENEO” was performed, which aimed to prove the clinical validity of CTCs count as an independent prognostic factor [152], [153].

Pachmann et al. (2008) carried out a study with 91 early BC patients using Maintrack® cytology-based CTC detection system, that proved to have extraordinary capture rates, with a high concentration

of CTCs (up to 100 CTC per mm³) and showed that CTCs are influenced by neoadjuvant and adjuvant therapy, such that an increase in the number of CTCs is a predictor of relapse and pathological responses [166].

The largest study was conducted by the German SUCCESS study group, with more than 2000 patients with early average-to-high BC and 1500 patients after chemotherapy. It was shown that CTCs were present in 21.5% of the blood from patient before chemotherapy, correlated with the nodal status (19.6% in node-negative and 22.4% in node-positive tumors), indicating a shorter disease-free and overall survival, and confirming that CTC positivity before chemotherapy is an independent prognostic marker for disease-free survival. Also, various cut-off values for prognostic relevance were considered [(0 x >1);(0-1 x >2);(0-4 x >5 CTCs in 30 ml of blood)], and for all the cut-off values it was confirmed a statistically significant impact on clinical outcome, the patient with >5 CTCs had a higher risk for relapse and lower overall survival [152], [167], [168].

Thus, although there are not many studies in the field of early breast cancer CTCs in clinic and large studies are still needed to validate the clinical relevance of CTCs, the ones that took place showed that CTCs detection and their study in early and metastatic BC are of extreme importance, having potential in early diagnosis, patient screening, patient prognosis and therapy resistance [169].

1.4.3. HER2 in CTCs

Breast cancer and its expression profile can change over time, such that the phenotype and genotype of the primary tumour, CTCs and metastasis may differ. Thus, the phenotype of the primary tumour may not reflect the metastasis status, especially when it comes to the HER2 status.

Therefore, HER2 is one of the biggest targets in current studies, with crescent evidence that its status in distant metastasis and CTCs is different from the primary tumour in more than 30% of the cases [170].

The HER2 status in BC could be determined recurring to CTCs, using different methods such as real-time polymerase chain reaction after magnetic enrichment of the sample, immunofluorescence or FISH [171].

Studies showed that some patients have HER2-positive CTCs, even when the primary tumour is HER2-negative, leading to new trials in order to investigate if these patients can benefit from an anti-HER2 therapy [172], [173]. However, it is not well understood if changes in HER2 status are due to the imprecise

HER2 status assessment of the primary tumour or to the metastatic growth of HER2-positive cells, initially camouflaged by the larger number of HER2-negative cells [152].

Rack et al. (2012) demonstrated that using trastuzumab as secondary adjuvant treatment, HER2-positive CTCs were eliminated, in patients with the HER2-negative primary tumour. However, this study is still under evaluation in the TREAT CTC trial, in which patients with HER2-negative primary tumour and high levels of CTCs even after neoadjuvant chemotherapy, will receive trastuzumab therapy for 18 weeks, and the response to this treatment will be studied by CTCs measurement [154], [157], [173], [174].

Other study, the German DETECTIII study, with patients whom had, at least, one CTC with strong HER2 overexpression by immunocytochemistry, compared the lapatinib (a strong inhibitor of the ErbB1) and chemotherapy combination with chemotherapy alone, and stated that approximately 19% of HER2-negative metastatic BC patients have at least 1 CTC with strong HER2 fluorescence signal [152], [175].

Thus, the study of the presence or absence of HER2 in CTCs can help in providing a more accurate prognosis on the disease evolution, and therefore assist in improving the treatment strategies that may be more effective in lowering CTC burden, reducing the possibility of metastasis formation.

1.4.4. Potential

The analysis and evaluation of CTCs in the blood of both metastatic and early breast cancer patients holds great promise and has the potential to revolutionize our understanding of breast cancer, and are the pillars of liquid biopsy, and many clinical trials are currently ongoing [31], [152], [153].

Liquid biopsy diagnostics holds great promise to help on the current cancer screening on patients with higher risk, and this method would help to reduce side effects and costs, however, the present studies and results on early detection of BC have problems regarding sensitivity and specificity and needs improvements [14].

Yet, monitoring CTCs during traditional treatment may be easier to achieve and is closer to the introduction to the clinics. CTCs, due to their characteristics and role in the metastatic process and its corresponding clinical prognostic impact, is a major clinical tool in BC patients, contributing to the better understanding of the metastasis formation, and although their role is still limited to prognosis, the interest for new techniques able to make their molecular characterization increases [14], [153].

Studies on potential therapeutic targets on CTCs open new perspectives on the individual and personalized therapy field. The first clinical trials with therapy choice based on CTCs presence took place already, leading us to propose that in metastatic BC the CTCs evaluation may be applied as liquid biopsy

since CTCs presence and relapse of the disease has already been shown with the CellSearch® system, and, in early BC the CTCs presence and persistence may help to identify patients with worst prognosis and in need of an adjuvant therapy [176]. Also, the evaluation of CTCs can help to identify cancer-specific markers, and the emerging of resistant clones, such as the HER2-positive clones [14].

Thus, technological platforms are being studied and optimized such as microfluidic devices, in order to increase sensitivity and attain a reliable CTC isolation of patients with BC, and once in the clinic, these devices may have the potential for many applications, like non-invasive monitoring of the tumour and identification of metastasis precursors [31].

In a near future, more assays on CTCs will be made, with higher sensitivity, and technologies will continue to further evolve, to achieve methods with precision for the detection of minimal cancer signs so that early detection of invasive and localized BC can be achieved. Nevertheless, liquid biopsy and the assessment of CTCs has all the potential as an innovating diagnostic tool, however, their utility needs to be improved and proven in clinical intervention studies, and, when all these challenges are overtaken, liquid biopsy may be routinely applied in clinical practice. This technology holds great promise and high hopes among the scientific community, for the better understanding and treatment of breast cancer patients.

CHAPTER 2: Objectives

2. Objectives

The main objective of this project is to optimize and validate a microfluidic device for the isolation and characterization of circulating tumour cells from whole blood in metastatic breast cancer. Also, to detect and assess the presence of HER2 biomarkers in the CTCs, relevant to stratify breast cancer patients.

Thus, the objectives are:

- Fabrication and functionalization of a microfluidic device, the RUBYchip™.
- Optimization and assessment of the capture efficiency of the device using breast cancer cell lines by flow dynamics.
- Optimization of the immunostaining protocol to allow standardization of the criteria set to be used in the analysis.
- Sampling and analysis of whole blood samples from patients with metastatic breast cancer by liquid biopsy.
- Comparison of CTC enumeration between technologies: a microfluidic device, the RUBYchip™ against the only FDA approved technology for CTC enumeration, the CellSearch®.
- Evaluation and analysis of HER2 expression in CTCs, as a relevant molecular markers in metastatic breast cancer patients in captured CTCs: HER2 and CK.
- Correlation of the clinical information with CTC enumeration and HER2 status.

CHAPTER 3: Techniques

3. Techniques

In this chapter, a brief description of the techniques used during this thesis will be made, for a better comprehension of their basic principles as well as the upcoming methods and results in the next chapters.

3.1. Micro and Nanofabrication techniques

The production of materials with small structures and features and the micro-and nanoscale offer unique opportunities for developments in science and technology. Micro and nanofabrication are now being applied in many fields, such as microfluidics, allowing the fabrication of small and low-cost devices with the desired characteristics [177].

3.1.1. Photolithography

The most common and successful technique used in micro and nanofabrication was developed in 1959 and is called photolithography or optical lithography. This technology combines high-intensity light, a photosensitive material and a photomask (which consists in a patterned Cr layer supported on a glass plate), in order to prepare a polymer network with a desired geometric shape, on top of a silicon wafer [178].

The first step in the photolithography process is to chemically clean the silicon wafer to remove any impurities or contamination it may have on its surface, followed by the heating of the wafer (at around 150 °C) to drive off any moisture left. Then a photosensitive polymer (photoresist) is used to coat the silicon wafer (Figure 4 A), this technique uses a high-speed centrifugal whirling of silicon wafers, to guarantee the formation of a thin flat layer of photoresist on top of the wafer. Following that, a soft-baking (at around 100 °C for 30 to 60 seconds) is done to eliminate the excess photoresist solvent from the coating. This step is extremely important, since it turns the photoresists photosensitive, for the following steps. [179].

The photoresist must be chosen accordingly to the desired pattern, it can be positive or negative.(Figure 4 C) Positive resists (composed by insoluble polymer) change their chemical structure when exposed to UV light, making them more soluble in developer (solution used to dissolve photoresist), this property allows for the removal of the exposed pattern, leaving the exposed areas without photoresist

on top of the wafer. Negative resists, when exposed to the UV light, become polymerized, therefore more difficult to dissolve, this resist remains on the exposed surface, and the unexposed portions are then removed with developer [178][179].

After the soft-baking step, a source of light is used to expose the photoresist layer. Several exposure systems can be used, such as, a mask aligner, a direct writing laser or an e-beam lithography system, only to name a few [178]. It is chosen according to the properties of the structures to be defined in the resist layer- the most commonly used for microfluidics is the mask aligner, this technique uses a physical mask, that contains the layout to be exposed, and after aligning the mask with the wafer, selective areas of the photoresist are exposed to a uniform UV light (Figure 4 B) [178][179].

Development is the following step, a developer solution is used to dissolve the areas of photoresist that were previously exposed to UV-light (positive resist), or the ones which were not (negative resist), depending on the properties of the photoresist (Figure 4 C) [178]–[180].

After development, the regions of the mask with no resist can be etched (Figure 4 D). There are two major types of etching, “wet” and “dry” etching. The “wet” etching consists in a chemical process used to remove layers from a wafer. The wafer is immersed in a solution that reacts specifically with the substrate however being inert to the mask material (photoresist), The “dry” etching, plasma etching or reactive ion etching (RIE) uses electromagnetic energy (usually radio frequency) applied to a gas that contains a reactive element. The wafer is bombarded with positively charged ions to remove materials and free radicals that react with the etched material forming volatile or non-volatile sub-products, this way a balance is found between physical and chemical etching because the physical bombardment is enough to remove the adequate material while chemical reactions occur to form volatile sub-products or protective deposits. This procedure is highly efficient because the electric charge of the ions leads them vertically towards the wafer so the etching is almost vertical and precise, and this is essentially due to the sophisticated designs of the today's chips [181].

Photoresists are, sometimes, used only as a protective and temporary mask. That said, the last step of photolithography is the photoresist removal also known as resist stripping (Figure 4 E), this process removes the resist without damaging the other materials. In this technique organic strippers (organic chemicals) can be used to modify the resist's structure so it no longer adheres to the substrate [181], [182].

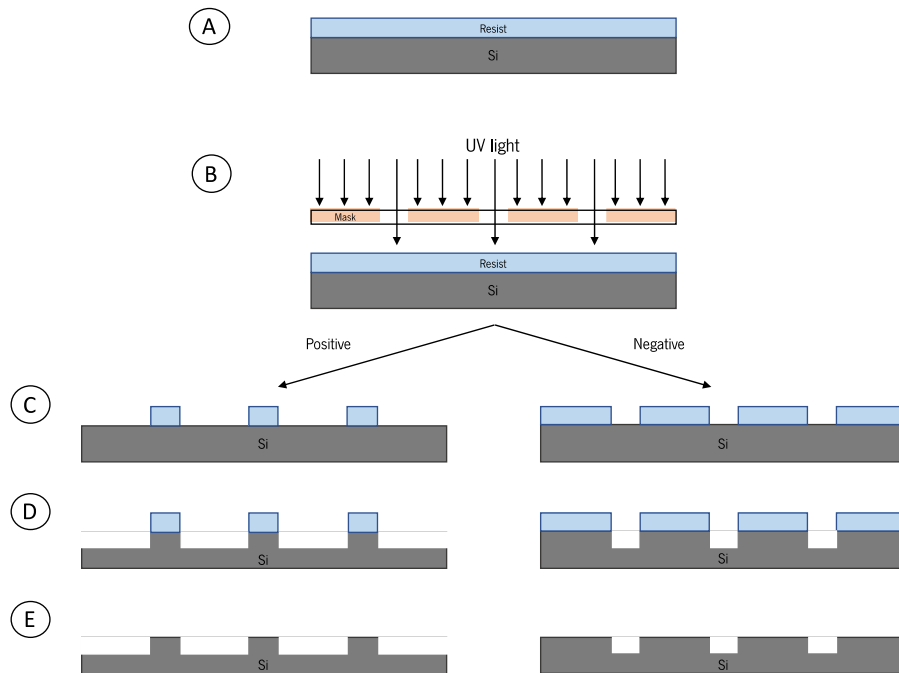


Figure 4: Schematic image of the photolithography process. (A) Resist coating; (B) Mask alignment and UV-light exposure; (C) Development: behavior of the positive and negative resists; (D) Etching; (E) Resist strip.

3.1.2. Soft lithography

Soft lithography was also used in this work, it is a low-cost, non-photolithographic technique for micro and nanofabrication, based on self-assembly and replica moulding, and currently used in several fields, such as photonics, biotechnology, electronics and microfluidics [177], [179].

Soft lithography is a collective name for many techniques, such as microcontact printing (μ CP), replica moulding (REM), microtransfer molding (μ TM), solvent-assisted micromolding (SAMIM), phase shifting edge lithography, nanotransfer printing, decal transfer lithography, nanoskiving and micromoulding in capillaries (MIMIC) [179], [183]. We will focus on replica moulding and related techniques since it is the one used in this work. The biggest advantage of soft lithography is the capability of fast production of replicas at low cost using a master, and this technique can be done in a regular laboratory environment, without requiring a cleanroom environment or expensive equipment, providing structures smaller than 100 nm [179] Photolithography and soft lithography can be used together to fabricate microstructures and microfluidic devices of polymeric materials. [177][184].

Replica moulding allows us to obtain a duplicate of the master, with the same shape and structures, using a wider range of materials. A liquid prepolymer of an elastomer is poured over the previously

silanized master (a microstructure silicon wafer fabricated using photolithography and used as a mould), the polymer is then cured and peeled off [179] (Figure 5).

The most commonly used elastomer is Poly(dimethylsiloxane) (PDMS), because of its advantageous and unique characteristics. Elastomers are used in this technique because they can make contact with relatively large areas, they have good elasticity and can be peeled off easily from the masters, even with complicated structures and patterns. PDMS, being an elastomer, has even more properties, such as a surface with low interfacial free energy and good chemical stability. Due to these characteristics, most polymer being moulded cannot adhere or react in an irreversible way to the PDMS surface. PDMS has good thermal stability, it can be cured thermally, is optically transparent down to approximately 300 nm, and is homogeneous and isotropic, meaning that the replicas made with this material can be deformed in order to manipulate the patterns in their surface, this replicas are also very durable once peeled off the master. Lastly, the surface of the PDMS can be treated with plasma to enable interactions with other materials like glass, allowing an irreversible plasma bonding between PDMS and other materials to produce, for example, microfluidic chips [179].

Overall, soft lithography is a technique that still needs improvements, but has many advantages, it allows for the duplication of complex structures from the master into multiple replicas, in a fast, simple and inexpensive way [179], [181].

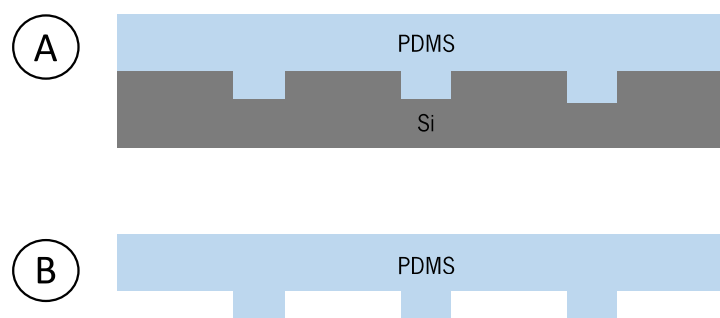


Figure 5: Schematic image of the soft lithography process, namely replica molding. (A) The elastomer Poly(dimethylsiloxane (PDMS) is poured over the master. (B) The replica is carefully peeled off, containing the exact same pattern of the master.

3.2. Fluorescence microscopy

Optical microscopy has been used in many fields and has a very important role in the study of the cell physiology, but it was the emergence of fluorescence microscopy that allowed a more complex study of cell biology, mostly using fluorescent labels [185][186].

A fluorescence microscope is an optical microscope which uses fluorescence, in addition to the usual optical microscopes, to study a certain specimen. It is usually composed by a light source (such as a mercury-vapour lamp or a xenon lamp), an excitation filter, a dichroic mirror and an emission filter[187], [188].

In the fluorescence process, the specimen is hit by light of a specific wavelength that is absorbed by the fluorescence indicators (fluorophores) which later emit light of a different wavelength. As expected, some of the energy is lost during the process, as a consequence, the emitted photon has less energy than the absorbed one, and it is known that light with a short wavelength (near blue) has more energy than light with long wavelength (near red), that means the light emitted in a fluorescence event, has longer wavelength than the excitation light (the Stokes shift) (Figure 6 and 7) [185], [187].

The main objective of the fluorescence microscope is to separate as better as possible, the emitted light from the excitation light. For that fluorophores with large Stokes shifts are preferentially used. In fact, the light separation is done with optical filters, and those must be selected based on the fluorophores used, because frequently, the excitation and emission spectra of different fluorophores overlap, so it is extremely important to choose the filters that guarantee the best compromise between the emitted and excitation light [187].

The microscope component that has the excitation and emission filter, as well as the dichroic mirror, is called the filter cube. This cube is responsible for directing light from the excitation source into the specimen and from this to the detector. That said, in order to obtain good quality images, it is very important that the filters are correctly orientated in the direction of the light path. Most fluorescence microscopes used nowadays are epifluorescence microscopes, which means that the excitation of the fluorophore and the detection of the respective fluorescence are done by the same light way, that is, the dichroic mirror separates the excitation and emission light [185], [189].

In life sciences, fluorescence studies are mostly carried out using two or more fluorophores simultaneously. The monitoring of those can be hard due to a phenomenon called “bleed through”, the overlap of the excitation and emission spectra, as previously said. The best way to contour this problem is to take separate images with different filters, each one of them designed for a specific fluorophore, and choose the appropriate dichroic mirror [185].

Although fluorescence microscopy is widely used and very important in life sciences research, it has its limitations, such as a phenomenon called photo bleaching, in which the fluorophores lose their capacity to fluoresce, as the molecules suffer constant damage while being illuminated by the excited electrons. This process is a limitation because it limits the time a sample can be observed, but it can be bypassed using more specific fluorophores and controlling the light intensity. Phototoxicity is also a problem, and this effect is unleashed when the cells are illuminated with a short wavelength light, resulting in reactive chemical species generated by the fluorescent molecules. Another limitation, a disadvantage in comparison to the reflected light microscopy, is the observation of the structures labelled with the fluorophores only, for example, using a fluorophore that targets the nucleus, only this organelle will be visible, preventing the observation of the complete cell [185], [190].

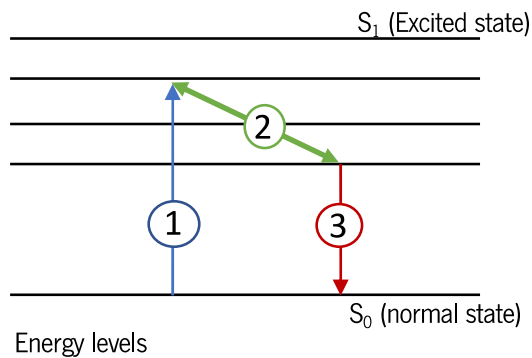


Figure 6: Schematic image representing the behavior of an electron during photon excitation and emission. The electron is excited by a laser light, transiting from S_0 level to a superior one S_1 , and after relaxation to lower energy levels, emits a photon with less energy.

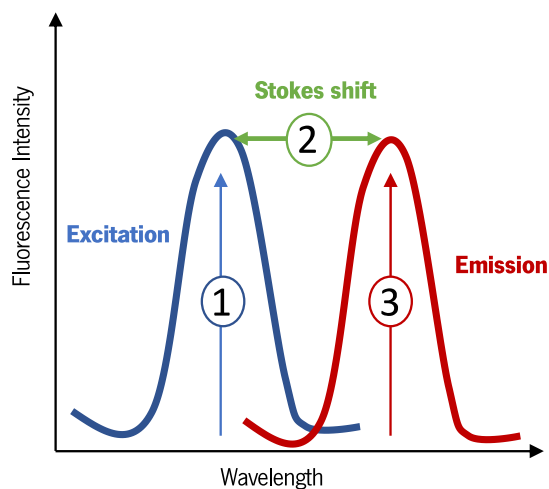


Figure 7: Schematic image of the Stokes shift. The light with short wavelength has more energy than the light with longer wavelength, this means that in a fluorescence event the light emitted has a longer wavelength and less energy than the excitation light.

3.3. Immunocytochemistry (ICC)

Studies of immunocytochemistry (ICC) began in 1942 and since then it has been used as an effective immunological detection method [191], [192].

In contrast with immunohistochemistry (IHC) that is performed in tissue samples processed into thin sections, ICC is performed on samples of cells grown in a monolayer or in suspension, that is, on cell smears, cell blocks and cell cultures [193]. Despite this difference, ICC relies on the same working process, using antibodies that bind to a specific antigen present in the cells. The cells can be prepared by many ways to be stained, depending on the analysis to be done as well as the sample characteristics, usually they are attached to a support to facilitate the later analysis. If adherent cells are used, their growth must be on a microscope slide, coverslip or other appropriate support, suspension cells can be centrifuged onto coverslips or glass slide or handled in suspension [194].

Because of their specificity, IHC and ICC have become crucial techniques in clinical diagnostics and laboratories, and are used to predict the prognostic of cancer tumours, identifying, for example, oncogenes, tumour suppressor genes, and tumour cells proliferation markers, thereby, allowing a more accurate diagnosis and prognostic, clinical staging, therapeutic decisions and disease grading, playing an important role in pathology. As these methods are able to identify certain oncogenes and tumour cell markers, they are also used to predict the response of a determinate patient to therapy, analysing the expression level of these markers [193].

3.4. Cell Culture

Cell culture is the name given to the growth of cells from an animal or plant, obtained directly from the tissue or from a cell line, in an artificial and controlled environment.

The first human cell line, studied by George Gey, was HeLa cell line, named after the lady from which the cells had their origin, Henrietta Lacks, who had cervical carcinoma, and in 1958 the first breast cancer cell line, BT-20, was established [195].

The first *in vitro* culture of the collected cells, grown under ideal conditions, is called primary culture, which can proliferate until confluence is reached and be subcultured, this means, divide the cells and pass or transfer them into a new vessel to provide more space for growth [196].

Once the primary culture is subcultured, it becomes known as a cell line. Cell lines can be classified, accordingly to their life span, into finite cell lines, cultures that can be subcultured a

determinate number of times, but at some point cease proliferation entering a stage of senescence, in which cell division does not occur, and at this point they should not be used; Continuous cell lines, cultures that are able to proliferate and be subcultured indefinitely, not showing senescence and, thereby, are stable for long-term, these cell lines usually have their origin in tumours or embryonic tissues; Stem cell lines, cultures with characteristics of stem cells, such as embryonic, which are able to produce diverse differentiated cells types, and, thereby, requiring a more careful maintenance. The cultures can either be adherent, growing as a monolayer on an artificial substrate, or float in the culture medium, growing as a suspension culture [197]. The maintenance of the cultures requires some important elements like cell medium, supplements, a suitable vessel and incubation conditions that vary taking into account each different cell type. The cell medium contains the essential nutrients, such as vitamins, minerals and amino acids, and in some cases can be supplemented with serum, essential for the maintenance and proliferation of many cell types, and antibiotics, to protect the cultures from contaminations. Thus, the medium should be precisely specified accordingly to the cell culture needs. As well as the medium, the temperature should be regulated accordingly to the type of cells in culture, and most human and mammalian cell lines are maintained at around 37°C for optimal growth, with a pH of 7.4 to mimic the physiological conditions [196], [197]. When the cells reach confluence, detachment solution like trypsin/EDTA is used to separate the cells from the substrate and from each other, in order to subculture the cell line [197].

Since this technique allows access to the cellular microenvironment in an easy and simple way, cell culture is a fundamental part of biology and biotechnology research, such as cancer research.

CHAPTER 4: Materials and Methods

4. Materials and methods

This chapter describes in detail the methods and techniques used for the design and fabrication of the microfluidic device, the RUBYchip™, as well as its characteristics. The cell culture procedures are also described, as well as the optimizations implemented in order to achieve the best performance of the RUBYchip™. The procedures and protocols for cell staining, image acquisition and image analysis are also explained. Some considerations on the procedures for sample collection, processing and analysis are demonstrated, as well as the RUBYchip™ operation on CTC isolation and enumeration.

4.1. Microfluidic device design and fabrication

The RUBYchip™ is the fourth generation of a microfluidic system designed to split the blood equally in 2 different rows, each row with 4 separated modules, which have the capacity to process a total of 7.5 ml of blood.

Each module has in its middle section a single row of anisotropic micropillars, diameter 25 μm and spaced 5 μm , which forms the cell filtering area. The size, geometry and aspect ratio of the micropillars, as well as the gap size, were carefully chosen to allow blood cells to deform and gently flow through, retaining, however, larger and more rigid cells in the filter. The pre-filters have 120 μm gaps to prevent clumps or debris from blocking the device. Each microfluidic device holds an approximate volume of 50 μl .

Surface coating is a very important and decisive process in both cell isolation and retrieval, because it prevents cell attachment to the surface, with the purpose to maximize cell purity and recovery.

The microfluidic masters were designed in 2D AutoCAD software (Autodesk) (Figure 8) and fabricated in a 200 mm silicon wafer using photolithography and deep reactive ion etching. Briefly, the silicon wafer (P/Boron, <100>, Sievert Wafer) was rinsed with deionized water, dehydrated at 150°C and exposed to hexamethyldisilazane (HDMS, Sigma Aldrich) vapour prime to improve the adhesion of the photoresist to the sample. Later, the wafer was spun coated with 2.2 μm of AZP4110 (Microchemicals GmbH), using a SÜSS MicroTec optical track (SÜSS MicroTec AG). The pattern was transferred onto the coated wafer using a Direct Write Laser system (DWL 2000 Heidelberg) with an Hg laser energy of 95% and focus -50. After the post bake, the exposed photoresist was developed with AZ400K (Microchemicals GmbH), and the wafer was rinsed with deionized water and dried. The pattern was then etched with sulphur hexafluoride (SF₆, Sigma Aldrich), by Silicon Deep Reactive Ion Etching (SPTS Pegasus), and

exposed areas passivated with octafluorocyclobutane (C₄F₈, Sigma Aldrich). Trench depth was measured in between steps using an optical profilometer (OPM profilometer, Ocean Optics NanoCalc XR) until the desired depth of 20 μm was reached. Residues were stripped using oxygen plasma and the master was characterized by Scanning Electron Microscopy (Quanta SEM, FEI). Finally, the wafer was diced into the individual masters using a Dicing Saw (DAD 3350, Disco) and cleaned with Isopropyl alcohol (IPA, Sigma Aldrich), rinsed with deionized water and dried at 150°C on a hot plate.

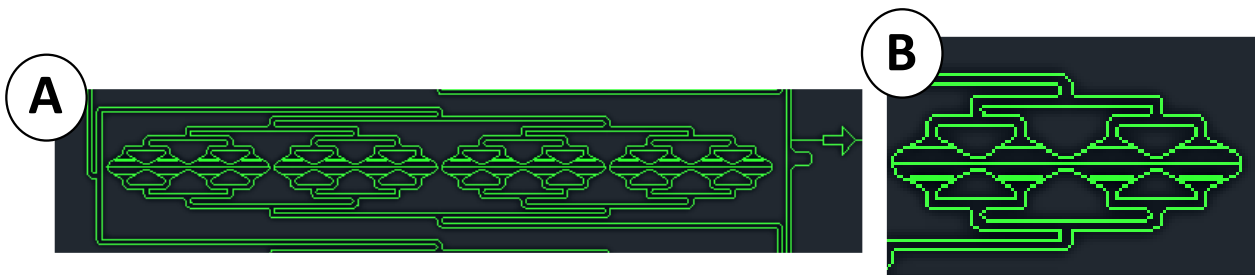


Figure 8: Schematic representation of part of the devices design in AutoCAD. (A) Represents one of the RUBYchip™ modules. (B) Represents an amplified area, corresponding to 25 fields, when acquiring the images in a microscope.

Before master replication, the wafer was hydrophobized with a vapour-phase treatment in trichloro(1H,1H,2H,2H-perfluorooctyl)silane (Sigma Aldrich) for one hour in a desiccator, and expose to a temperature of 65°C, for another hour in order to promote the vapour phase.

After hydrophobization, for rapid prototyping using soft lithography, polydimethylsiloxane prepolymer was mixed with a cross-linker (PDMS, SYLGARD™ 184 Silicone Elastomer, Dow Chemical Company) at 10:1 ratio, degassed, poured over the master, degassed again and cured at 65°C for 2h. The exposure to this temperature solidifies the PDMS. After the curing process, the PDMS replica was unmounted and both inlet and outlets were punched using a 1.25 mm biopsy puncher (World Precision Instruments). Finally, microscope glass slides (size 25x75 mm, ThermoFisher Scientific) previously cleaned with Hellmanex (Hellmanex III, Hellma Analytics), and the PDMS replicas were treated with oxygen plasma (Plasma Cleaner PDC-002-CE, HarrickPlasma) at medium power for 17s and brought in contact to produce irreversible bonding.

Afterwards, to process with device functionalization, ethyl vinyl acetate microtube (EVA, Cole-Parmer) was inserted, both in the inlet and outlet of the microfluidic devices, and a blunt needle (LS22K Luer Stub, Instech) was used in the inlet in order to connect the syringes to the microfluidic device. The

devices were connected to a syringe pump (NE-1200, New Era Syringe Pumps) and filled with 350 μl of ethanol (Sigma Aldrich) at 100 $\mu\text{l}/\text{min}$ to enhance the wettability, then rinsed with 350 μl of 10 mM Phosphate Buffer Saline (PBS, Sigma Aldrich) at 120 $\mu\text{l}/\text{min}$, and later treated with 4000 μl of 1% Pluronic F-127 (Sigma Aldrich) at 140 $\mu\text{l}/\text{min}$ for coating, to avoid unspecific attachment of cells onto the channel surface. For this last reagent the volume of solution used is considerable higher than needed, in order to stress test the device with a volume of solution used in the same order of magnitude of a blood sample (7.5 ml), such that efficient performance during blood sample processing is assured (figure 9).

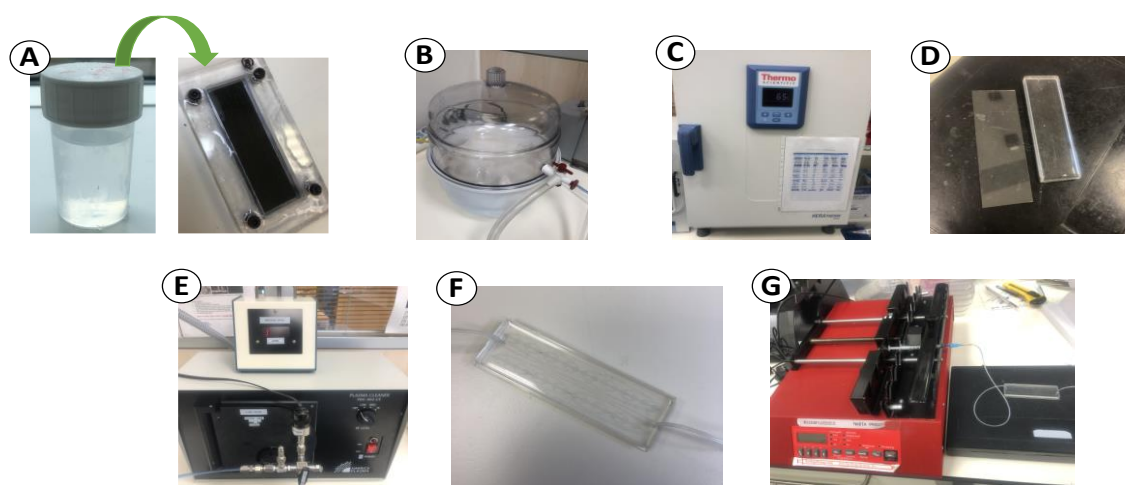


Figure 9: Workflow representation of the fabrication of a PDMS microfluidic device. (A) PDMS polymer is prepared by adding PDMS elastomer and crosslinker in a 10:1 ratio and vigorously mixed, afterwards the aerated mixture is degassed using vacuum, in the desiccator. Once degassed the PDMS is poured over the master. (B) The master is also put under vacuum to further degas the PDMS. (C) The master is brought to the oven, at 65°C for 2h to cure the PDMS. (D) Once the PDMS is cured, the replica is peeled off from the master, and inlet and outlet holes are punched. (E) Previously cleaned and inspected replica and glass slide are put under oxygen plasma treatment, to allow irreversible linkage between them. (F) EVA tubing is placed both in the inlets and outlets. (G) The device is connected to a syringe pump to proceed with device functionalization.

4.2. Cell Culture

The human breast cancer cell lines MCF-7 (ATCC, CRL-3435), MDA-MB-435 (ATCC, HTB-129) and SKBR3 (ATCC, HTB-30) were used for this study.

Both MDA-MB-435 and SKBR3 cell lines were cultured in Dulbecco's Modified Eagle's Medium (DMEM, Gibco), supplemented with 10% fetal bovine serum (FBS, Gibco) and 1% Penicillin/Streptomycin (Pen/Strep, Corning). MCF-7 cell line was cultured in DMEM, supplemented with 10% FBS and 1% Penicillin/Streptomycin and 0.1% human insulin (Sigma Aldrich). All the cell lines were cultured as a

monolayer at 37°C in a 5% CO₂ humidified atmosphere. The medium renewal was done 2 to 3 times per week.

Cells were routinely subcultured before reaching full confluence. The cell medium was removed, followed by a washing step with PBS to remove all traces of serum which contains trypsin inhibitor, afterwards the cell layer was rinsed with 0.25% (w/v) Trypsin-EDTA (BioConcept) and incubated for 4 minutes in order to disperse the cell layer and obtain a cell suspension. Posteriorly, complete growth medium was added to the cell suspension and cells were aspirated by gently pipetting, in order to avoid clumping and promoting cell separation, and also to neutralize the Trypsin-EDTA solution. Cell pellet was obtained by centrifugation, which was resuspended in fresh growth medium. Finally, appropriate volumes of cell suspension were added to new culture vessels with fresh growth medium and incubated at 37 °C.

4.3. Optimization studies

4.3.1. Spiking experiments

To optimize the performance of the RUBYchip™, the three different cell lines mentioned above were used in spiking experiments in order to assess the isolation efficiency of the microfluidic device. These cell lines were selected because they have different phenotypes, MCF-7 are epithelial, MDA-MB-435 have mesenchymal-like morphology, and SKBR3 have HER2 overexpression, thus, the use of different cell lines allowed a better understanding of the device performance in real scenario, using blood samples from patients with metastatic breast cancer.

Following the same steps as above, trypsinization was used to bring the cell layer into suspension. In order to calculate cell concentration (equation 1) and number (equation 2), the Neubauer hemocytometer method was used. A sample volume of 10 µl from the cell suspension were added to 10 µl of trypan blue solution (Corning), obtaining a dilution with a suitable concentration for cell counting. After pipetting and mixing the cell solution, 10 µl were carefully introduced into the Neubauer chamber (Hirschmann® EM Techcolor), placing the pipette tip against the edge of the cover slip and slowly expelling the solution. Finally, the Neubauer Chamber was taken to the microscope (Nikon Eclipse TS100, Nikon), and viable cells were counted.

Once known the cell concentration, a volume equivalent to 6x10⁵ cells was stained with Hoechst at a concentration of 10 µg/ml (Hoechst 33342, Trihydrochloride, Trihydrate – 10 mg/ml, Invitrogen®),

ThermoFisher Scientific) for 30 minutes, afterwards, serial dilutions were performed to obtain a working cell suspension of 100cells/100 μ l.

200 cells were then spiked in 7.5 ml of whole blood collected from healthy donors and injected at four different flow rates, 100, 120, 140 and 160 μ l/min, in the RUBYchip™ with a syringe pump (Figure 10). Trapped cells were rinsed with 350 μ l of 2% Bovine Serum Albumin (BSA, Sigma Aldrich) in filtered 0.01M PBS, fixed with 350 μ l of 4% Paraformaldehyde (PFA, Sigma Aldrich) for 20 minutes at room temperature (RT) and washed again with 350 μ l of 0.01M PBS.

Following the spiking processing, a fluorescence microscopy analysis of the trapped cells was performed using a fluorescence inverted Nikon- TI-E microscope, with the 20x objective. To assess the isolation efficiency of the RUBYchip™, the number of Hoechst positive cells trapped in the device was compared with the total number of cells spiked, as in equation 3.

Experiments were done in triplicate.

$$\text{Concentration (cells/ml)} = \text{average \# cells} \times \text{dilution factor} \times 10^4 \quad (\text{Eq. 1})$$

$$N^{\circ} \text{ of cells} = \text{average \# cells} \times \text{dilution factor} \times 10^4 \times \text{Volume of cell suspension} \quad (\text{Eq. 2})$$

$$\text{CTC isolation Efficiency (\%)} = \frac{\text{Trapped CTCs}}{\text{Spiked cells}} \times 100 \quad (\text{Eq. 3})$$

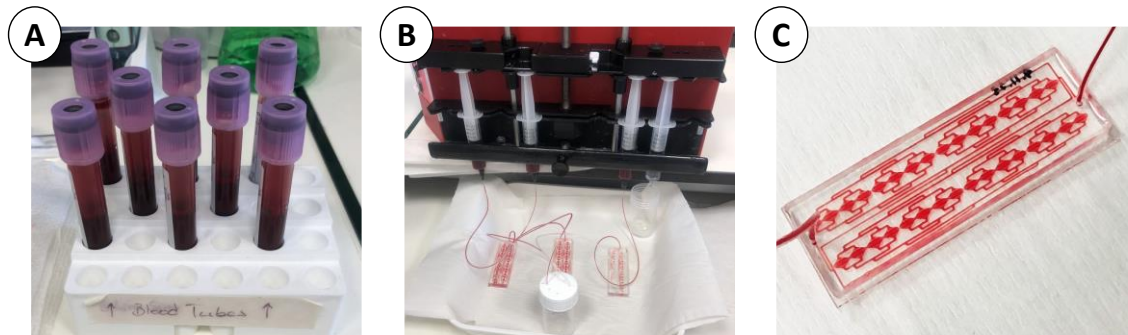


Figure 10: Representation of the benchtop setup for the spiking experiment. (A) Cultured cells are spiked in 7.5 ml of whole blood from healthy volunteers. (B) The blood containing the cells is transferred to a syringe. The syringe is properly placed in a syringe pump and the blood is pumped into the devices at a predetermined flow rate. (C) RUBYchip™ picture, once the blood is in the device, device design features become evident.

4.3.2. Immunofluorescence studies

In order to optimize the antibody (AB) panel used for this study in the RUBYchip™, several immunofluorescence (IF) studies were performed, namely, ICC performed in well plates (ICC-in-well), ICC performed in the microfluidic device (ICC-in-device) and negative control studies with healthy volunteers samples, also performed in the microfluidic device. Conjugated antibodies were used, meaning that direct IF studies were performed, in order to optimize the time of preparation and incubation of the antibodies, since protocols for direct IF are usually shorter as they only require one labelling step, and to minimize the risk of cross contamination, because when indirect IF is used, several secondary antibodies can bind to the primary antibody, resulting in an amplified signal, which does not happen in direct IF, since the fluorochrome is already conjugated to the primary antibody. The fluorochromes used were chosen based in the specificities of the equipment available for image acquisition, namely excitation and emission filters of the fluorescence microscope.

The panel was composed by Monoclonal Anti-Cytokeratin pan-FITC antibody (clone C-11, recognizes human cytokeratins 4, 5, 6, 8, 10, 13 and 18; Sigma Aldrich; F3418; 1.9 mg/ml) to target epithelial cells, FITC is excited at 365 nm having emission maximum at 530 nm; DyLight 550 Anti-ErbB2/HER2 (Immunostep®; 1399990570; 0.85 mg/ml) to target cells with HER2 overexpression, DyLight 550 is excited at 562 nm and emission maximum is 676 nm; and Cyanine5 Anti-Human CD45 (Immunostep®; 1399990730; 1 µg/ml) to target blood cells, thereby, used as a CTC exclusion criteria, Cyanine5 is excited at 625 nm and emission maximum is 670 nm; as well as with DAPI (Sigma Aldrich;

D9564; 1 mg/ml) to stain the nucleus, DAPI is excited at 340 nm and emission maximum is 488 nm (Figure 11). Using a fluorescence inverted Nikon- TI-E microscope, and using NIS® Software, it was possible to obtain multi-channel fluorescence images, with DAPI, CK, HER2 and CD45, in the blue, green, orange and red channels, respectively.

Since HER2 is a customized antibody, not being a catalogue available product, concentration is batch dependent, hence the preferred notation to refer to its concentration is in $\mu\text{g/ml}$, however, the respective dilution is also presented.

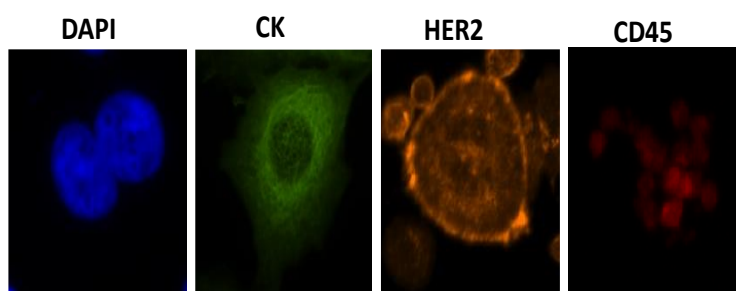


Figure 11: Representative images of the antibody panel used in the study. DAPI is used to stain the nucleus, CK used to target epithelial cells, HER2 used to target cells with the HER2 overexpression and CD45 used to target blood cells, used as CTC exclusion criteria.

4.3.2.1. Immunocytochemistry performed in well plate (ICC-in-well)

For this experiment, MCF-7, MDA-MB-435, SKBR3, and PBMCs (Peripheral Blood Mononuclear Cells) were used (Figure 12).

Cell lines were seeded on sterile glass coverslips (13 mm diameter), treated with Poly-Lysine, to facilitate the attachment of the cells to the glass surface, placed in 24-well plate at ideal densities, 1.2×10^5 cells per well for MDA-MB-435, 1.5×10^5 cells per well for MCF-7 and SKBR3, and grown for 24 h.

PBMCs were isolated by density gradient centrifugation using Histopaque® (Sigma Aldrich), for that, whole blood from a healthy donor was diluted in 2% PBS-FBS on a 1:1 proportion, and transferred into a falcon, being gently poured over Histopaque® on a 2:1 dilution, followed by a series of centrifugations, performed according to manufacturer's instructions. Afterwards, the different blood components were separated, and the buffy coat obtained was the fraction enriched in PBMCs and, therefore, PBMCs were collected and isolated. Posteriorly, PBMCs were washed with 2% PBS-FBS, and resuspended in PBS (Figure 13). The cells were counted by the same method as described above (section 4.3.1) and a density of 2×10^6 cells per eppendorf tube was used.

Since PBMCs are suspension cells, they do not present the ability to adhere to solid surfaces, that said, these cells were maintained in eppendorf tubes during the process, namely in the antibodies incubation.

Afterwards, cells were fixed with 4% PFA for 20 minutes, permeabilized with 0.25% Triton X-100 (Sigma Aldrich) in 0.01M PBS for 10 min and blocked with 2% BSA in filtered PBS for 30 min. Washing steps with PBS (10mM, pH 7.4) were performed between all the previous steps.

For immunofluorescence staining, the cells were incubated with the antibodies described above, at the dilutions to be tested (Table 2), for 1h and 15 min, at room temperature (RT). After antibody incubation, two washing steps with 0.5% BSA were performed at last.

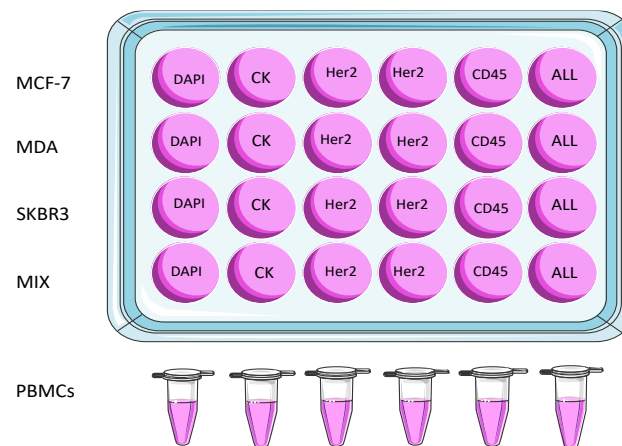


Figure 12: Representative image of the experimental design used to perform immunocytochemistry in well plate (ICC-in-well). Three different cell lines (MCF-7, MDA-MB-435 and SKBR3) and PBMCs from healthy volunteers were used separately and mixed. Cell lines were seeded on sterile glass coverslips, treated with Poly-Lysine to facilitate the cell attachment, and placed in a 24-well plate at ideal densities to grow for 24 h. PBMCs were isolated by density gradient centrifugation using Histopaque®, since PBMCs are suspension cells, they are not able to adhere to solid surfaces, so these cells were maintained in eppendorf tubes. For the mix, that is, all the cells present in a cover slip, a single drop of a solution containing the PBMCs was added to the mounting medium when mounting the glass slides, after the entire process including the antibody incubation. The antibodies (Cytokeratin (CK), HER2, and CD45) to be used in this study were tested, as well as DAPI, individually. A cocktail with all the antibodies was also tested (ALL in the well plate scheme).

To remove the solutions used in all the steps from the 24-well plate, an appropriate vacuum aspirator (Vacusafe, Integra) was used, while the eppendorf tubes containing the PBMCs were centrifuged, using a well plate centrifuge (Centrifuge 5810 R, Eppendorf), so that the supernatant was removed as well.

Finally, the coverslips were mounted with the cells facing towards a microscope slide on a drop of Aqueous Mounting Medium (Anti-Fade Fluorescence mounting Medium- Aqueous, Fluoroshield, Abcam) to immobilize coverslips and prevent fading of fluorescence, and visualized using Nikon-TI-E microscope, and the resulting images were analysed with NIS-Elements AR® Software from Nikon.

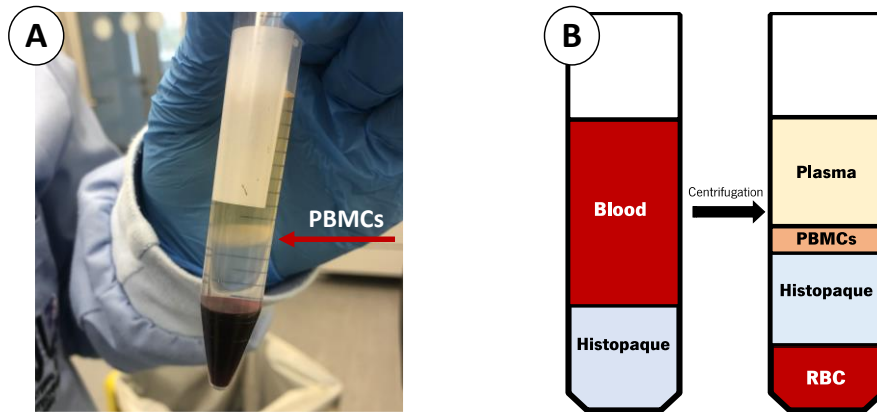


Figure 13: PBMCs isolation by density gradient centrifugation. (A) Centrifuged tube showing cells distributed in the solution in layers based in the differences in their density/size, buffy coat is the fraction enriched with PBMCs (Peripheral blood mononuclear cells). (B) Representative image of the PBMCs isolation. The blood from a healthy volunteer is gently poured over Histopaque® and centrifuged according to manufacturer's instructions. Afterwards, the different blood components are separated, and PBMCs can be isolated.

Table 2: Working dilutions tested for each of the selected antibodies and DAPI in this immunocytochemistry experiment in well, using adherent cells cultured on coverslips. (AB: antibodies)

DAPI	CK	HER2	CD45	ALL
1:5000	1:200	2 ug/ml (1:425)	6 ug/ml (1:142)	1:50
				Same AB dilutions

4.3.2.2. Immunocytochemistry performed in device (ICC-in-device)

For this experiment, as in the previous one described, MCF-7, MDA-MB-435, SKBR3 were used however, isolated PBMCs were not used, instead whole blood from a healthy volunteer was spiked with cell lines to mimic the processing conditions of cancer patient samples.

7.5 ml of whole blood samples were spiked with 200 cells of each cell line, using a working cell suspension of 100cells/100µl, and pumped at 120 µl/min in the RUBYchip™ using a syringe pump.

Standard ICC protocol was performed as described above in section 4.3.2.1., however, in the ICC-in-device, the cell become in contact with the reagents, such as the antibodies, by injection into the device.

Three optimization assays were made, namely ICC 1 (Table 3), 2 (Table 4) and 3 (Table 5), adjusting the antibody dilutions according to the results obtained in the previous assay.

The device was visualised, and images acquired using Nikon-TI-E microscope, those were analysed with NIS® Software.

Table 3: Working dilutions tested for each of the selected antibodies and DAPI in this immunocytochemistry experiment performed in device (ICC 1), using adherent cells cultured on coverslips.

DAPI	CK	HER2	CD45
1:5000	1:300	6 µg/ml (1:142)	1:50

Table 4: Working dilutions tested for each of the selected antibodies and DAPI in this immunocytochemistry experiment in device (ICC 2). Compared to the previous assay, ICC 1, CK and CD45 dilutions were increased.

DAPI	CK	HER2	CD45
1:5000	1:400	6 µg/ml (1:142)	1:100

Table 5: Working dilutions tested for each of the selected antibodies and DAPI in this immunocytochemistry experiment in device (ICC 3). The dilutions used for CK and CD45 are twice as high as ICC1.

DAPI	CK	HER2	CD45
1:5000	1:600	6 µg/ml (1:142)	1:200

4.3.2.3. Immunocytochemistry in healthy donors' blood

In order to have an expression negative control, no cancer cells present, whole blood from healthy donors was stained alone with the same selection of antibodies, 7.5 ml of blood was collected from three different healthy donors.

The blood was pumped at 120 $\mu\text{l}/\text{min}$ in the RUBYchip™ using a syringe pump, once sample processing was finished, standard ICC protocol was performed as described above, in section 4.3.2.1. (Table 6).

The devices were visualised and images acquired using Nikon-TI-E microscope, those were analysed with NIS® Software, as in section 4.3.2.2.

Table 6: Working dilutions tested for each of the selected antibodies and DAPI in this immunocytochemistry experiment as a negative control test.

DAPI	CK	HER2	CD45
1:5000	1:200	6 $\mu\text{g}/\text{ml}$ (1:142)	1:50

4.4. Immunofluorescence and CTC enumeration in the RUBYchip™

Cells from patient samples isolated using the RUBYchip™ were treated as in section 4.3.2.1. The immunofluorescence staining was made with the final antibody dilution selected based on the previous optimizations (Table 8).

Fluorescence microscopy analysis was performed using the same setup and software as described above.

Recurring to the CK, CD45, HER2 and DAPI immunostaining as well as to morphological properties, such as the nucleus size, the criteria to classify cells was developed. After excluding debris, irregular fluorescence shapes or with a dark outline, the clear events with cell-like morphology were classified. Cells classified as DAPI+/CK+/CD45- or DAPI+/CK+/HER2+/CD45- were considered for CTCs enumeration, otherwise DAPI+/CK-/CD45+ or DAPI+/CK-/HER2-/CD45+ as well as DAPI+/CK+/CD45+ or DAPI+/CK+/HER2+/CD45+ were excluded as CTCs. Cells with DAPI+/HER2+/CD45- staining were also excluded as CTCs (Table 7).

Table 7: Immunofluorescent staining characteristics for identifying CTCs. Cells isolated by the RUBYchip™ were classified according to immunostaining against CK, CD45, DAPI and HER2. Events DAPI+/CK+/CD45- OR DAPI+/CK+/HER2+/CD45- were defined as CTCs.

CHARACTERISTIC	TYPE
Irregular shape or dark outline	Debris
DAPI+/CK+/CD45-	CTC
DAPI+/CK+/HER2+/CD45-	
DAPI+/CK-/CD45+	WBC
DAPI+/CK-/HER2-/CD45+	
DAPI+/CK+/CD45+	Favour WBC
DAPI+/CK+/HER2+/CD45+	
DAPI+/HER2+/CD45+	

To achieve CTC counts, cells isolated in the RUBYchip™, were manually enumerated and randomized blind analysis was performed, meaning that the samples were analysed without any code that could identify the patient or the collection moment.

The presence of the HER2 mutation/HER2 overexpression was also tested by confirming the presence of DAPI+/CK+/HER2+/CD45- cells.

Table 8: Antibody dilution selected to be used in patient samples

DAPI	CK	HER2	CD45
1:5000	1:200	8 µg/ml (1:106)	1:100

4.5. Patient sample collection and analysis

In the present study, 14 patients diagnosed with metastatic breast cancer at the Hospital de Santa Maria, in Lisbon, were recruited and followed according to the Oncology Department guidelines for disease evaluation. All patients participated voluntarily and signed the IMM Biobank informed consent. IMM's

institutional review board provided ethical approval of the study, which complied with all the national regulations.

Clinicopathological information was recorded for all patients (Table 9). For each patient, 7.5 ml of peripheral blood was collected at two time points, at a baseline, before starting systemic treatment, and at monitoring follow-up monitoring, after 12 weeks of ongoing treatment. A double amounts of blood specimens were collected from each patient in order to process the samples with both technologies in parallel, the CellSearch® and the RUBYchip™, in a CellSave® preservative tube, with a cell preservative that is able to store cells for up to 96 hours at RT, to guarantee the blood samples were preserved until processing (CellSearch®, Janssen Diagnosis, USA- now owned by Menarini-Silicon Biosystems, Italy) and in a EDTA-coated tubes were used for sample collection, respectively. All the samples were anonymized and encoded prior to analysis.

The blood samples were collected and processed in loco by the RUBYchip™, within 24 hours, at Instituto de Biología Molecular (IMM), and later shipped to International Iberian Nanotechnology Laboratory (INL), to be analysed. The ones processed by the CellSearch® were shipped to the Liquid Biopsy Analysis Unit of the Health Research Institute of Santiago (IDIS), Spain, and processed within 48 hours, as previously described.

4.6. Statistical method

Statistical analysis was performed using GraphPad Prism software (GraphPad Software).

As CTCs counts in patients were not normally distributed, results were presented as absolute numbers and means with the corresponding percentages.

The Friedman test (a non-parametric statistical test), 95% confidence intervals, was used to compare CTC enumeration using CellSearch® test versus the RUBYchip™ technologies in metastatic breast cancer samples. Results were considered statistically significant if the p value was less than 0.05.

CHAPTER 5: Results and Discussion

5. Results and Discussion

5.1. RUBYchip™ performance in spiking experiments

Spiking experiments with 3 different cell lines were performed to assess the efficiency of the RUBYchip™ for the isolation of CTCs with different phenotypes in whole blood samples. Since the RUBYchip™ CTC isolation capacity relies on the cancer cell size deformability, the size and morphology of the cell lines was assessed inside the microchip.

The size of MCF-7 cells was 20-25 μm in average (Figure A1), some events of larger dimensions were found, 40-60 μm in diameter, possibly due to the different stages of the cell cycle and likely in mitosis. With a mesenchymal-like phenotype, MDA-MB-435 cells present a typical cell size of 14-25 μm (Figure A2), but some events of larger size were also observed, with 25-30 μm in diameter. The SKBR3 cells measured between 20-30 μm on average (Figure A 3), but larger cell sizes were observed with diameters between 50-60 μm . In conclusion, among the three cell lines studied, it was clearly observed that the SKBR3 had the largest size inside the microfluidic device (Figure 14).

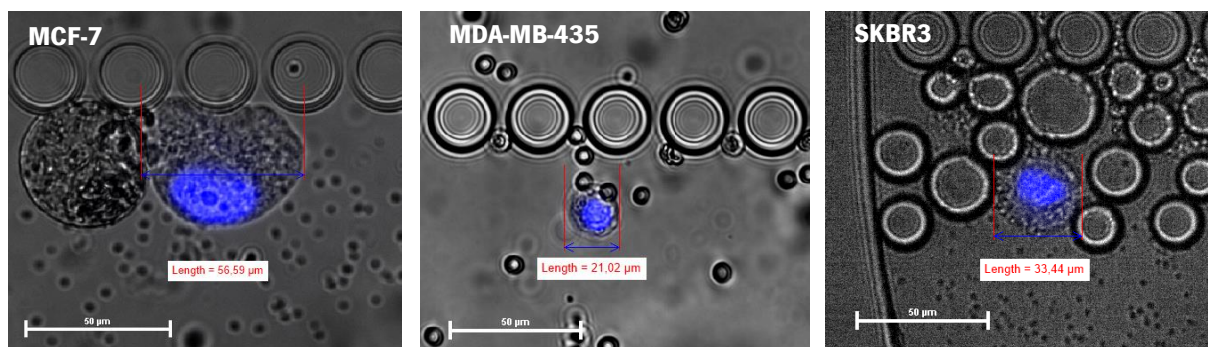


Figure 14: Representative image of the different cell lines trapped inside the RUBYchip™ after the spiking assay, in the micropillars that work as the filtering area, namely, MCF-7, MDA-MB-435 and SKBR3 with diameter 56.59 μm , 21.02 μm and 33.44 μm respectively. This image was visualised and acquired using Nikon-Ti-E microscope, and posterior measurements were done using NIS® Software. The images were acquired and observed with a 20x objective. The scale bars corresponds to 50 μm .

To study the isolation efficiency of the chip, a predetermined number of cultured cancer cells (200 cells) was spiked in a whole blood sample from healthy volunteers to mimic the circulation of CTCs in blood. Four different flow rates were tested, 100, 120, 140 and 160 $\mu\text{l}/\text{min}$, and the highest isolation efficiency was achieved at 120 $\mu\text{l}/\text{min}$, consistently for all the cell lines tested, such that the RUBYchip™

was able to isolate in average 53%, 59% and 56% of spiked MCF-7, MDA-MB-435 and SKBR3 breast cancer cells, respectively. The isolation efficiency decreased in all the others flow rates tested, either above or below the most efficient one (120 $\mu\text{l}/\text{min}$). The lowest isolation efficiency observed was at 160 $\mu\text{l}/\text{min}$ with an average of 33%, 16%, 25% of spiked MCF-7, MDA-MB-435 and SKBR3 cells isolated, respectively (Table 9).

Table 9: Isolation efficiency of the RUBYchip™ for four different flow rates tested.

Flow Rate ($\mu\text{l}/\text{min}$)	MCF-7	MDA-MB-435	SKBR3
100	41%	47%	38%
120	53%	59%	56%
140	44%	48%	44%
160	33%	16%	25%

The RUBYchip™ was designed to be used with unprocessed whole blood samples, and the design features of the microfluidic chip, namely the pre-filters layout, prevented flow obstructions by eventual cell debris or microclots. The geometry of the RUBYchip™, along with its surface treatment, creates a favourable environment for CTC entrapment eliminating most of the blood cells, such that a compromise

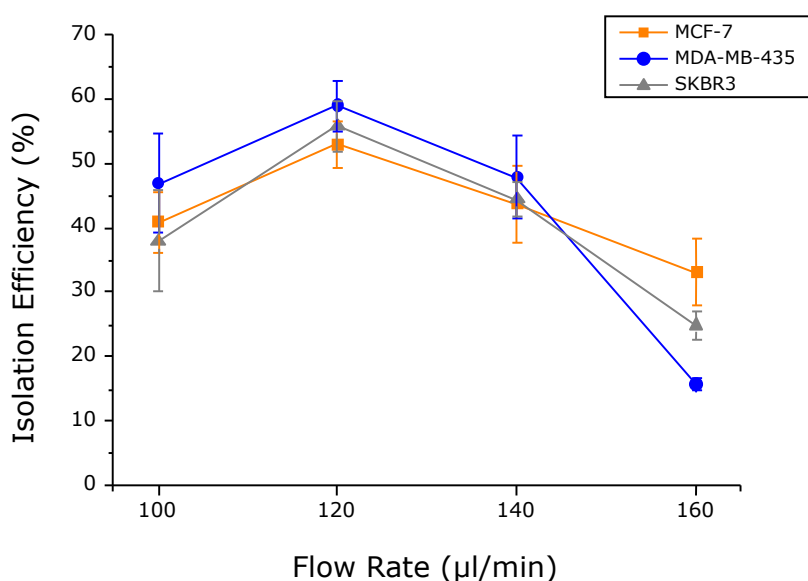


Figure 15 : Graphical representation of the isolation efficiency of the RUBYchip™ at four different flow rates, with three different cell lines, MCF-7, MDA-MB-435 and SKBR3. The highest results were achieved at 120 $\mu\text{l}/\text{min}$, for all the cell lines, with an isolation of 53%, 59% and 56% for MCF-7, MDA-MB-435 and SKBR3 breast cancer cells, respectively, showing consistency of the results.

between efficiency, speed and purity is obtained. The chip dimensions are ideal to allow deformable cells generally blood cells, to pass through the filter gaps, however retaining cells which cannot deform due to the smaller cytoplasm to nucleus ratio. These larger cells with bigger nucleus and cytoplasm are more likely to get trapped [198].

Despite cytomorphological differences between cell lines, the results were consistent for all the flow rates tested and similar values of isolation efficiency were observed for all the different cell lines (Figure 15). Also, knowing that CTCs may have a wide range of cell sizes and phenotypes, using three cell lines different in cell size and phenotype aimed at testing a reliable representation of CTCs in circulation in clinical samples and also to better understand the capacity of the size-based filter to isolate CTCs, guaranteeing a compromise between cell isolation efficiency and purity at the best flow rate, despite the morphological differences existent.

Considering these results, the flow rate of 120 $\mu\text{l}/\text{min}$ was selected for subsequent experiments and future patient sample processing. This flow rate allowed a fast sample processing, making it possible to process 7.5 ml of whole blood in less than 63 minutes.

5.2. Cell staining and analysis

5.2.1. Optimisation of cell labelling and analysis

The ICC performed in well was carried out using three different cell lines, MCF-7, MDA-MB-435 and SKBR3, as well as PBMCs, as described in section 4.3.2.1. These cells lines are expected to express

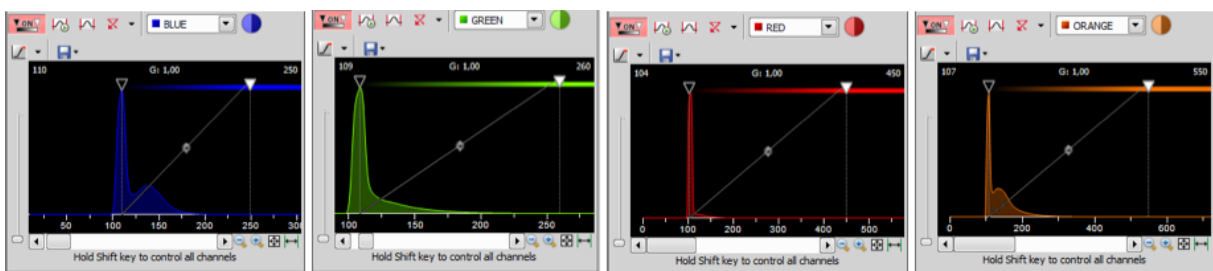


Figure 16: Histograms representing the frequency of pixels of an intensity value, for each colour channel. The left bar, with the black triangle on top, allows the regulation of the contrast, adjusted in the peak. The right bar, with the white triangle in top, allows the regulation of the brightness.

the selected markers (CK, HER; CD45) differently. According to the literature, SKBR3 cells exhibits cytoplasmatic CK expression and HER2 overexpression In the membrane, MCF7 cells express CK but are

negative for HER2, MDA-MB-435 do not express any of the selected markers and PBMCs cells express only CD45 [199]–[201].

Antibody conjugations was done following the different conditions summarised in section 4.3.2. In order to obtain images with a high resolution and without causing background, exposure times were established for each colour filter, namely, 500 ms for blue, 800 ms for green, 800 ms for orange and 1 s for red. After acquiring the images, the histogram was adjusted using the Look Up Table (LUT), to maximise signal while removing the background. In summary, the LUTs window was adjusted for the blue channel (110-250), green channel (100-260), orange channel (107-550) and red channel (104-450). These values were used in all the images, to allow a consistent evaluation and analysis throughout the study (Figure 16).

When observing the images obtained from MCF-7 cells, a very specific CK staining in the cytoskeleton was evident. The IMF confirmed that HER2 staining was not observed for any of the two dilutions tested, however, some CD45 expression was observed (Figure 17).

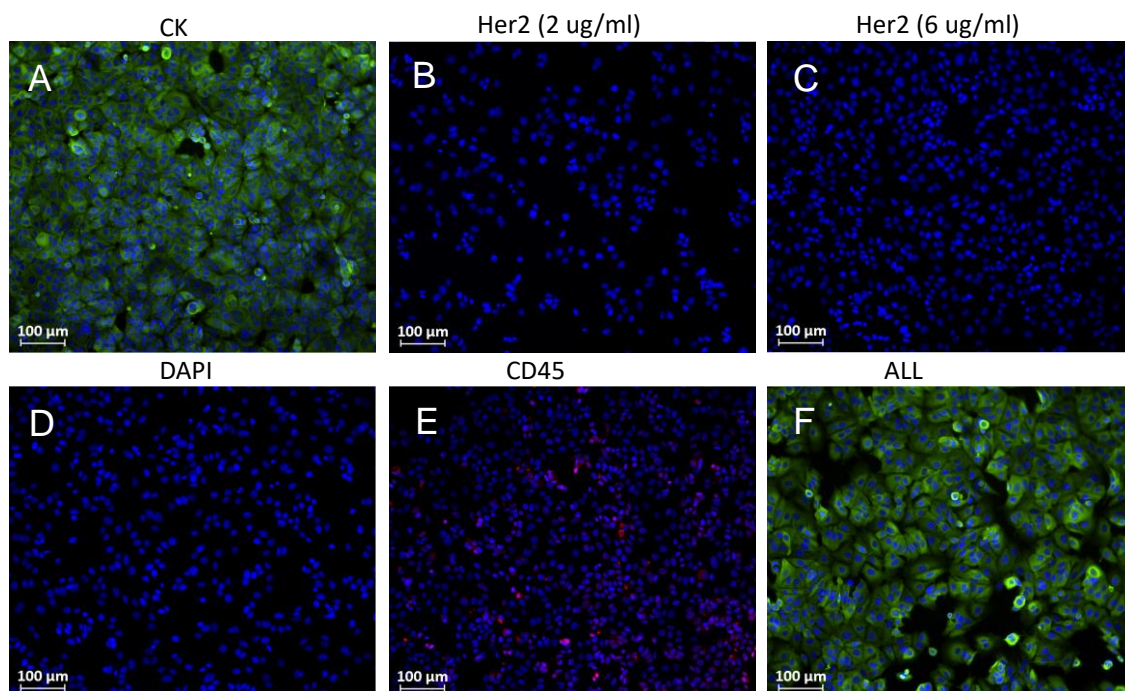


Figure 17: Immunocytochemistry in well of MCF-7 cells. (A) CK expression; (B) HER2 expression, at 2 µg/ml; (C) HER2 expression, at 6 µg/ml; (D) DAPI expression; (E) CD45 expression; (F) Cocktail of antibodies expression. DAPI is shown in all the images, staining the nucleus.

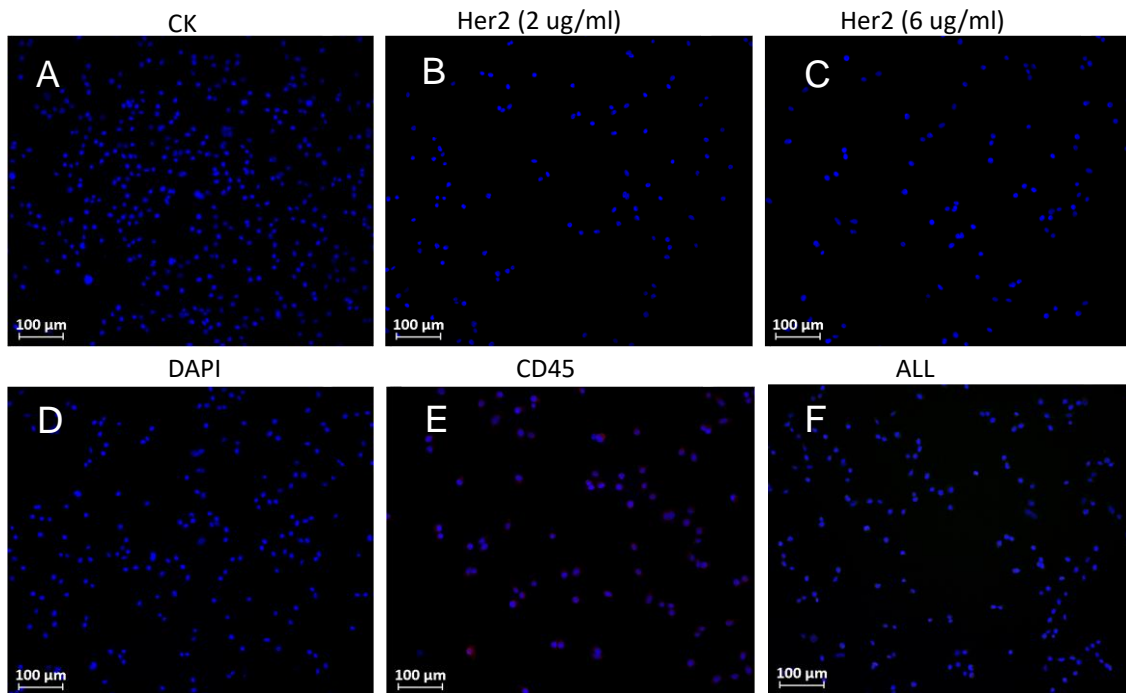


Figure 18: Immunocytochemistry in well of MDA-MB-435 cells. (A) CK expression; (B) HER2 expression, at 2 $\mu\text{g}/\text{ml}$; (C) HER2 expression, at 6 $\mu\text{g}/\text{ml}$; (D) DAPI expression; (E) CD45 expression; (F) Cocktail of antibodies expression. DAPI is shown in all the images, staining the nucleus.

MDA-MB-435 cells were not stained by CK or HER2 antibodies, for both dilutions tested. These results were expected, as described above, however, CD45 expression was observed, with a weaker signal (Figure 18).

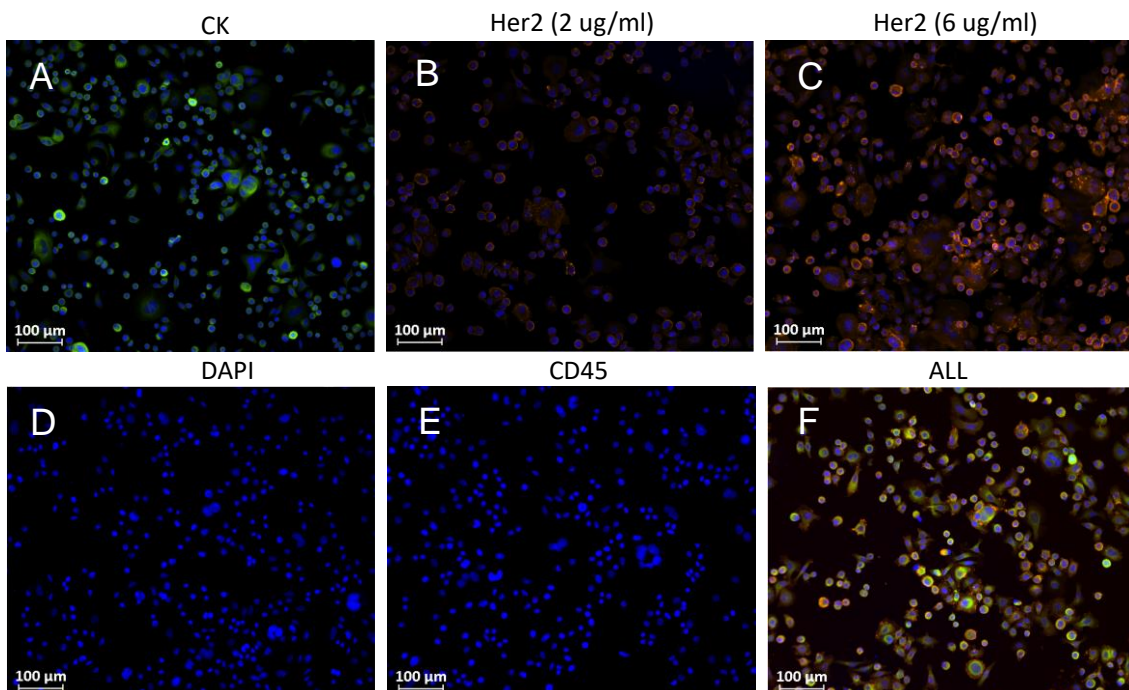


Figure 19: Immunocytochemistry in well of SKBR3 cells. (A) CK expression; (B) HER2 expression, at 2 $\mu\text{g}/\text{ml}$; (C) HER2 expression, at 6 $\mu\text{g}/\text{ml}$; (D) DAPI expression; (E) CD45 expression; (F) Cocktail of antibodies expression. DAPI is shown in all the images, staining the nucleus.

This assay also confirmed that SKBR3 cells expressed CK in the cytoskeleton. As expected, this was the only cell line that had HER2 expression, which was observed in the cell membrane, for the two dilutions tested, exhibiting a brighter signal at the concentration of 6 $\mu\text{g}/\text{ml}$. CD45 expression was not observed (Figure 19).

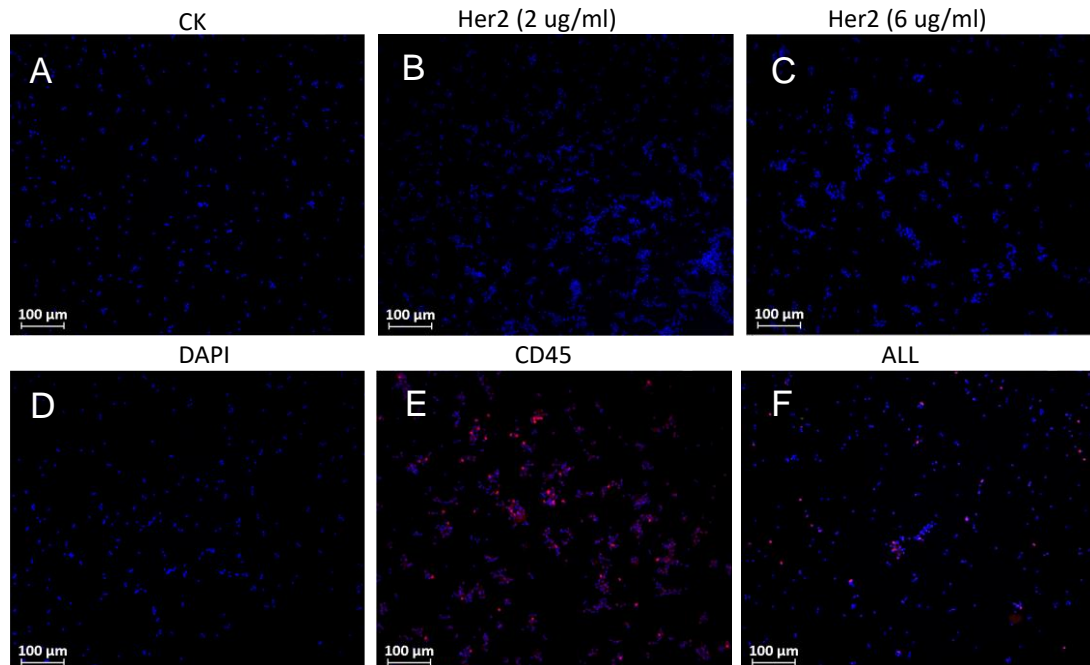


Figure 20: Immunocytochemistry in well of PBMCs- (A) CK expression; (B) HER2 expression, at 2 $\mu\text{g}/\text{ml}$; (C) HER2 expression, at 6 $\mu\text{g}/\text{ml}$; (D) DAPI expression; (E) CD45 expression; (F) Cocktail of antibodies expression. DAPI is shown in all the images, staining the nucleus.

PBMCs from healthy donors behaved also as expected, expressing CD45 specifically, and showing no presence of either CK or HER2 staining (Figure 20).

A final evaluation was made, having all the previous cell lines in the same well, to verify if each cell line could be distinguished by its specific antibody staining and to exclude that antibody cross-reactivity did not interfere with observations. It was clearly evident the specific expression of the different antibodies in each cell line, namely, epithelial marker CK expression by MCF-7 and SKBR3, both epithelial cell lines. However, MDA-MB-435 have mesenchymal-like phenotype, and CK expression was not observed. HER2 overexpression was noticeable in SKBR3 cells exclusively, as expected. The antibody signal was observed for both dilutions tested, being higher at for the concentration of 6 $\mu\text{g}/\text{ml}$. CD45 staining was observed in PBMCs, as anticipated, however it was noticed in MCF-7 and MDA-MB-435, with a weaker signal. This could be explained by using an unnecessarily high antibody concentration, leading to the need of adjustments in subsequent assays (Figure 21).

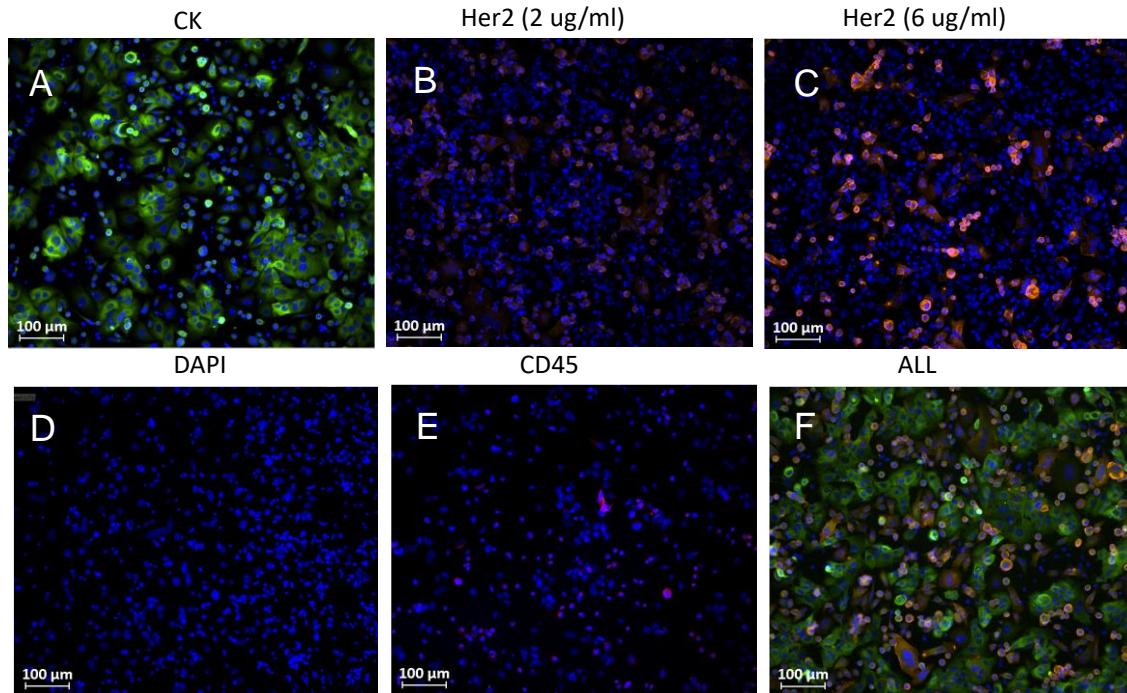


Figure 21: Immunocytochemistry in well of all the cells previously demonstrated, MCF-7, MDA-MB-435, SKBR3 and PBMCs. (A) CK expression; (B) HER2 expression, at 2 $\mu\text{g}/\text{ml}$; (C) HER2 expression, at 6 $\mu\text{g}/\text{ml}$; (D) DAPI expression; (E) CD45 expression; (F) Cocktail of antibodies expression.

After a careful analysis of the images obtained with the ICC-in-well, adjusting the exposure times and LUTs, the optimal dilutions were chosen for each antibody, in order to proceed with the ICC-in-device.

Since the DAPI staining had a clear and consistent signal, this dilution was adopted for subsequent assays. Despite the staining of CK worked fine, it was observed that the fluorochrome suffered some degradation over time, leading to adjustments in image acquisition, such as shorter LUTs window and higher exposure times than usual for the same antibody. Hence, with a new antibody vial, the dilution of CK was increased (lower concentration) for subsequent assays. CD45 dilution was also increased to remove the unspecific staining detected in MCF-7 and MDA-MB-435 cells. HER2 was tested with two different dilutions and the strongest signal was obtained using a final concentration of 6 $\mu\text{g}/\text{ml}$, this concentration was adopted for subsequent assays.

The representative images with higher resolution of this assay are shown in chapter 8 (Annexes A4 to A17).

5.2.2. Cell staining and analysis on chip

In this assay, the same cell lines were used to spike 7.5 ml of whole blood samples from healthy volunteers as described in section 4.3.2.2.

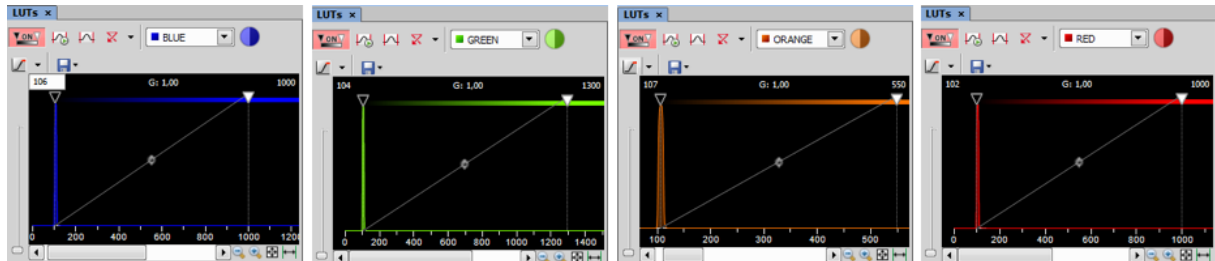


Figure 22: Histograms representing the frequency of pixels of an intensity value, for each colour channel. The left bar, with the black triangle on top, allows the regulation of the contrast, adjusted in the peak. The right bar, with the white triangle in top, allows the regulation of the brightness.

After cell isolation and staining, images of the device were acquired using a Nikon-Ti-E microscope, in 8 different large scans of 25 fields-of-view each, dividing the 2 rows of the device in 4 different areas (Figure 8). Knowing that the behaviour of the cells inside the device, as well as its fluorescence signal could present significant differences when compared to their behaviour in well, the exposure times were re-established for each colour filter, namely, 400 ms for blue, 200 ms for green, 800 ms for orange and 500 ms for red. Afterwards the LUTs window was adjusted for each channel, blue channel (106-1000), green channel (104-1300), orange channel (107-550) and red channel (102-1000) (Figure 22). Recurring to NIS-Elements AR® Software, it was possible to distinguish the different cell lines and PBMCs trapped inside the device, along the filtering area, and to detect clear fluorescence signals for the selected antibodies.

In the first assay (ICC 1), CK, DAPI, HER2 and CD45 staining was observed as different colour signals, in morphologically different cells. CK+/DAPI+ events were identified as MCF-7 cells, similarly events with cell-like morphology but exhibiting HER2 expression, were considered SKBR3 cells. Cells stained with DAPI and CD45, with smaller size were identified as PBMCs, and cellular events presenting larger nucleus without specific signal for the selected markers were identified as MDA-MB-435 cells (Figure 23).

After careful analysis of the device, the dilutions of antibodies were once again readjusted. HER2 staining was specific and had a good signal, such that the dilution was kept the same for subsequent

assays, however, CK and CD45 dilutions were increased because it was possible to observe that even with a shorter exposure time, in comparison to the previous assay, the signal for both antibodies was saturated.

For this purpose, two ICC experiments were performed next in the microdevice with adjusted dilutions for CK (1:400 and 1:600 for ICC2 and 3 respectively) and CD45 (1:100 and 1:200 for ICC1 and 3 respectively), while maintaining the exposure times and LUTs window, such that a comparison could be made with the compiled results in order to achieve the best compromise of dilutions to use.

In ICC 2 and 3, it was possible to observe, in comparison to ICC1, a decrease in the intensity of the signal for CK, more noticeable in ICC3 experiment, for the highest dilution tested, however, the specificity was maintained (Figure 23). CD45 signal intensity was also reduced in ICC2 and ICC3, notwithstanding the staining was specific, and expression was present in cells with smaller dimensions matching PBMCs typical morphology, however in ICC3 this signal was very poor.

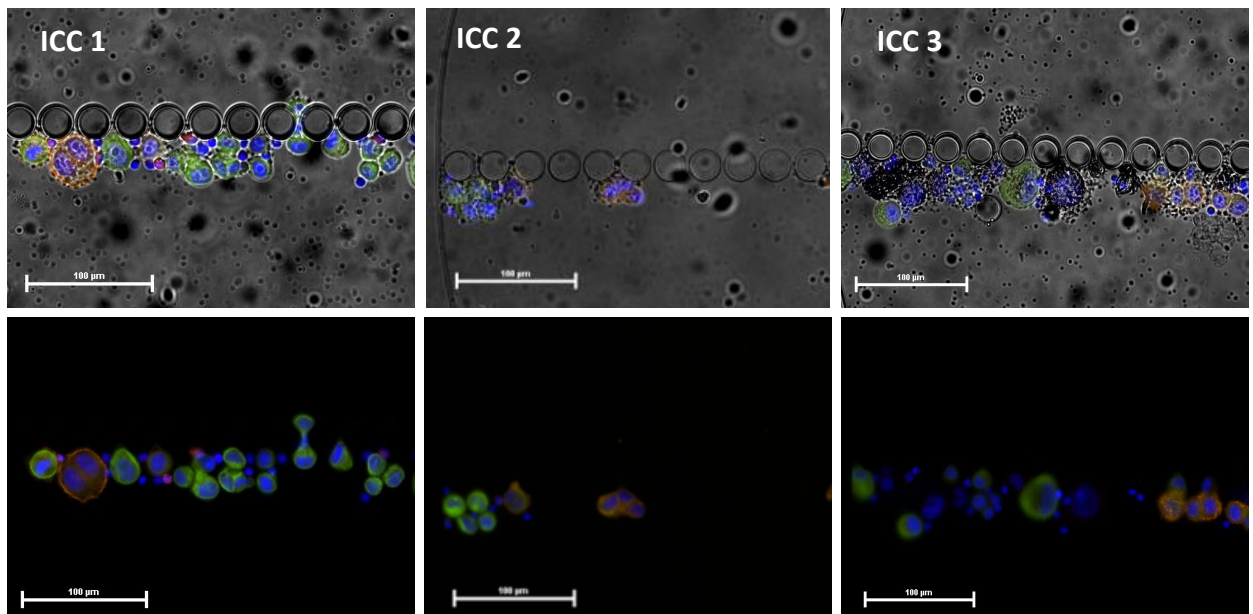


Figure 23: Images obtained from the immunocytochemistry in device assays (ICC 1, ICC 2 and ICC 3). Each ICC was made in separate devices with different antibodies dilutions, using all the cells previously demonstrated, MCF-7, MDA-MB-435, SKBR3 and PBMCs. It is possible to observe the cells trapped inside the device in the filtering area, and all the antibodies have expression in cells with distinct morphology, namely MCF-7 are CK+/DAPI+, MDA-MB-435 are DAPI+, SKBR3 are CK+/DAPI+/HER2+ and PBMCs are CD45+/DAPI+.

Afterwards, it was possible to define the dilutions for the antibody panel in study, to apply in future experiments, namely for the analysis of patient samples. The chosen conditions were 6 µg/ml for HER2, 1:300 for CK and 1:100 for CD45.

5.2.3. Controls in samples from healthy donors

As a negative control, with no cancer cells present, 7.5 ml of whole blood from healthy donors, were processed, stained and analysed following the protocol described in section 4.3.2.3. (experiments were performed in triplicate). The staining conditions were tested as follows: HER2 concentrations were maintained as described in the previous section, but the concentrations of CK and CD45 antibodies were increased (dilutions of 1:200 for CK and 1:50 for CD45) to test the behaviour of healthy cells in the most extreme conditions. The exposure times and LUTs window were maintained.

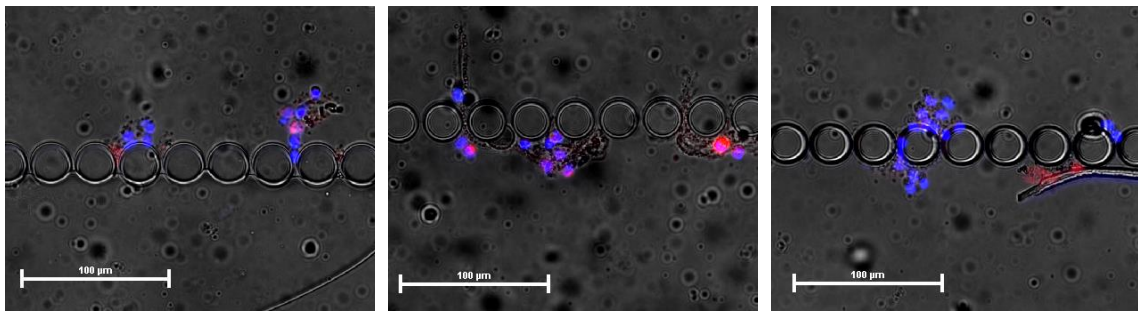


Figure 24: Images obtained from the immunocytochemistry assays using healthy donors blood. The assay was made in triplicate, (1), (2) and (3) represent images of the devices with PBMCs from the three different volunteers. As expected, only DAPI and CD45 staining is observed. No CTCs were detected in the blood of the healthy donors.

As expected, it was rare to find CK and HER2 staining, and only a very weak signal was observed in these rare events, furthermore the staining was not specific or cell like related. On the other hand, CD45 cell staining was very specific, but the signal varied from fairly weak to intense (Figure 24). It is important to refer that no CTCs were detected in healthy samples using the RUBYchip™.

Having completed the experiments for the optimization of the antibody cocktail and the immunofluorescence conditions, while validating the specificity of the antibody panel, it was possible to proceed with the study.

5.2.4. Patient sample staining and analysis

It is known, and has been described in literature, that the blood of cancer patients shows differences when compared to healthy donors blood, regarding degradation, density and clotting [202]. Similarly, CTCs behave differently than cultured cells. That said, patients' samples can influence cell isolation performance of the device, and to overcome this possibility, another assay was performed.

A sample from a luminal B MBC patient was collected and processed with the microchip to test the staining conditions previously defined, proceed with adjustments if needed, and to establish the optimal condition to be applied to the entire cohort.

After analysing the patient sample, CD45 dilutions were maintained, but CK and HER2 dilutions were decreased to 1:200 and 8 µg/ml, respectively.

5.3. Patient clinical characteristics

A total of 14 patients with metastatic breast cancer were recruited from Hospital de Santa Maria to participate in this study (Table 10). The mean age of the patients at metastases diagnosis was of 53.5 years, 9 of those patients (64%) had less than 60 years and 5 patients (36%) had 60 or more years. They were followed for an average of 94 days (approximately 3 months), while the study was ongoing. The main clinicopathological characteristics of the patient cohort are presented in table 10.

The cohort can be divided into three different groups of patients according to their breast cancer subtype. A total of 8 patients (57%) had Luminal A (ER+/PR+/HER2-) tumours, which is the most common subtype, followed by Luminal B (ER+/PR+/HER2+) occurring in 4 patients (29%), and triple negative breast cancer (ER-/PR-/HER2-) diagnosed in 2 patients (14%), having the lowest representation. Most patients had already had disease relapse (93%) or were recently diagnosed with metastatic disease (7%). As previously mentioned, each patient had blood collections at two time points, at a baseline and at monitoring follow-up, after 12 weeks of ongoing treatment.

Despite the baseline collection was intended before starting systemic treatment, 5 of the BC patients recruited for this study (Patients 1, 3, 9, 11 and 14) were already under systemic treatment at the first collection, due to patient recruitment limitations, similarly to the rest of the cohort, all were metastatic at first collection. Therefore, in these cases “baseline collection” was loosely adopted terminology, referring to the first collection of the study. The effect of ongoing therapy is specially considered in these cases and further discussed in following sections.

The longest time elapsed between the first diagnosis and the metastasis diagnosis was of 13 years (patient 6) and the shorter time was of 5 months (patient 14), averaging 68 months until disease relapse occurred (6 years).

Metastases were found in different sites and the highest incidence was in bone (5 patients, 36%), followed by liver and lung, both present in 2 patients each (14%). 1 patient had cutaneous metastases (7%), and metastases in the central nervous system were found in 1 of the patients (7%). Metastases in

multiple sites were found in 3 patients, namely, bone and lung (1 patient, 7%), lung and lymph node (1 patient, 7%), liver and cutaneous (1 patient, 7%).

Overall cancer treatment was provided as per the institutional guidelines and was in compliance with the international oncology society guidelines. The majority of the patients received conjugated systemic therapy, except for two patients (10 and 12) which received alternative therapies, such as radiotherapy, adequate for each of the patients. Out of the 14 patients, half of them (50%) received systemic chemotherapy (neoadjuvant and/or adjuvant), and hormone therapy was administrated to the other half (50%). Also, 3 of the 4 patients with HER2 positive primary tumours (21% of the 14 patients) were treated with Anti-HER2 therapy, and 3 patients (21%) received cyclin inhibitor therapy. Bone target therapy was administrated in 3 patients (21%), whom had bone metastases.

Table 10 : Clinicopathological characteristics of patients enrolled in this study.

Patients	Age	Breast Cancer subtype	Metastases	Therapy	Time until relapse	
1	40	ER+/PR+/HER2+	Luminal B	Cutaneous	Chemotherapy; Anti-P13K/AKT/mTOR; Anti-HER2	3 years
2	64	ER+/PR+/HER2-	Luminal A	Lung; Bone	Hormone therapy	12 years
3	61	ER+/PR+/HER2-	Luminal A	Bone	Chemotherapy; Hormone therapy; Cyclin inhibitor; Bone target therapy	7 years
4	69	ER+/PR+/HER2+	Luminal B	Liver; Cutaneous	Chemotherapy; Anti-HER2	2 years
5	54	ER+/PR-/HER2-	Luminal A	Bone	Bone target therapy	12 years
6	69	ER+/PR+/HER2-	Luminal A	Lung	Chemotherapy	13 years
7	50	ER+/PR+/HER2-	Luminal A	Bone	Chemotherapy; Hormone therapy	5 years
8	61	ER+/PR-/HER2+	Luminal B	Liver	Chemotherapy; Anti-HER2	5 years
9	53	ER+/PR+/HER2-	Luminal A	Lung	Hormone therapy	10 years
10	50	ER+/PR-/HER2+	Luminal B	Lung; Lymph node	N/D	No relapse/ first diagnosis
11	46	ER+/PR-/HER2-	Luminal A (ER)	Liver	Hormone therapy	1 year
12	34	ER-/PR-/HER2-	Basal (TNBC)	CNS (central nervous system)	N/D	1 year
13	44	ER-/PR-/HER2-	Basal (TNBC)	Bone	Hormone therapy; Cyclin inhibitor	2 years
14	54	ER+/PR+/HER2-	Luminal A	Bone	Chemotherapy; Hormone therapy; Cyclin inhibitor; Bone target therapy	5 months

5.4. Comparative analysis: Isolation of CTCs by the RUBYchip™ versus CellSearch®

Considering the effective performance of the RUBYchip™ in spiking experiments and having the staining and analysis conditions established, the performance of the RUBYchip™ in the clinic was next evaluated by comparing this technology with the gold standard and FDA approved system for CTCs enumeration, CellSearch®.

As described in section 4.5., 2 samples were collected at baseline from each of the 14 MBC patients to perform CTC enumeration by both the RUBYchip™ and the CellSearch®, and another 2 samples were collected at the follow-up time point. After isolations, immunocytochemistry, staining and immunofluorescence analysis was performed to identify CTCs in the RUBYchip™, as explained in section 4.4., namely, DAPI+/CK+/HER2-/CD45- and DAPI+/CK+/HER+/CD45- cells were identified in a blind analysis and results obtained from both technologies were compared.

Table 11: Technology comparison, RUBYchip™ versus CellSearch®, results for both baseline and follow-up collection times. Results showing the enumeration of CTCs by each technology are presented, as well as the number of samples above the threshold established for breast cancer (≥ 5 CTCs).

	N=14			
	Baseline		Follow-Up	
	RUBYchip™	CellSearch®	RUBYchip™	CellSearch®
Presence of CTCs (CTC+)	14 (100%)	7 (50%)	13 (93%)	4 (29%)
Threshold (≥ 5 CTCs)	12 (86%)	3 (21%)	8 (57%)	1 (7%)

Analysis of the microchip-processed samples was performed manually using NIS-Elements AR® Software, as previously mentioned. The number of CTCs identified by the RUBYchip™ and the CellSearch® were compared head to head including all samples, without discrimination of time-points. Also, to further investigate disease progression monitoring, baseline and follow-up collections were compared for each patient.

Results showed that the RUBYchip™ detected CTCs in all 14 samples at baseline (100%), however, only 7 samples (50%) had CTCs detected by the CellSearch®. Regarding CTC enumeration, at the

baseline collection, the average number isolated by the RUBYchip™ was 14.5 CTCs (range, 1-36) and by the CellSearch® 3.8 CTCs (range, 0-28).

Taking into account the threshold established by CellSearch® to evaluate disease progression in breast cancer, ≥ 5 CTCs/7.5 ml of whole blood [96], the RUBYchip™ was able to isolate equal or more than 5 CTCs in 12 of the samples (86%), while the CellSearch® only detected 3 samples (21%) with CTCs counts above threshold.

At follow-up collection, the average number of CTCs isolated by the RUBYchip™ was 13.5 (range, 0-43), and by the CellSearch® 4.2 CTCs (range, 0-56). Similarly, to the baseline results, 13 samples (93%) had CTCs isolated by the RUBYchip™, contrasting with the 4 samples (29%) with CTCs detected by the CellSearch®. Regarding the threshold values, the RUBYchip™ detected equal or more than 5 CTCs in 8 of the samples (57%), against 1 sample (7%) in the CellSearch®.

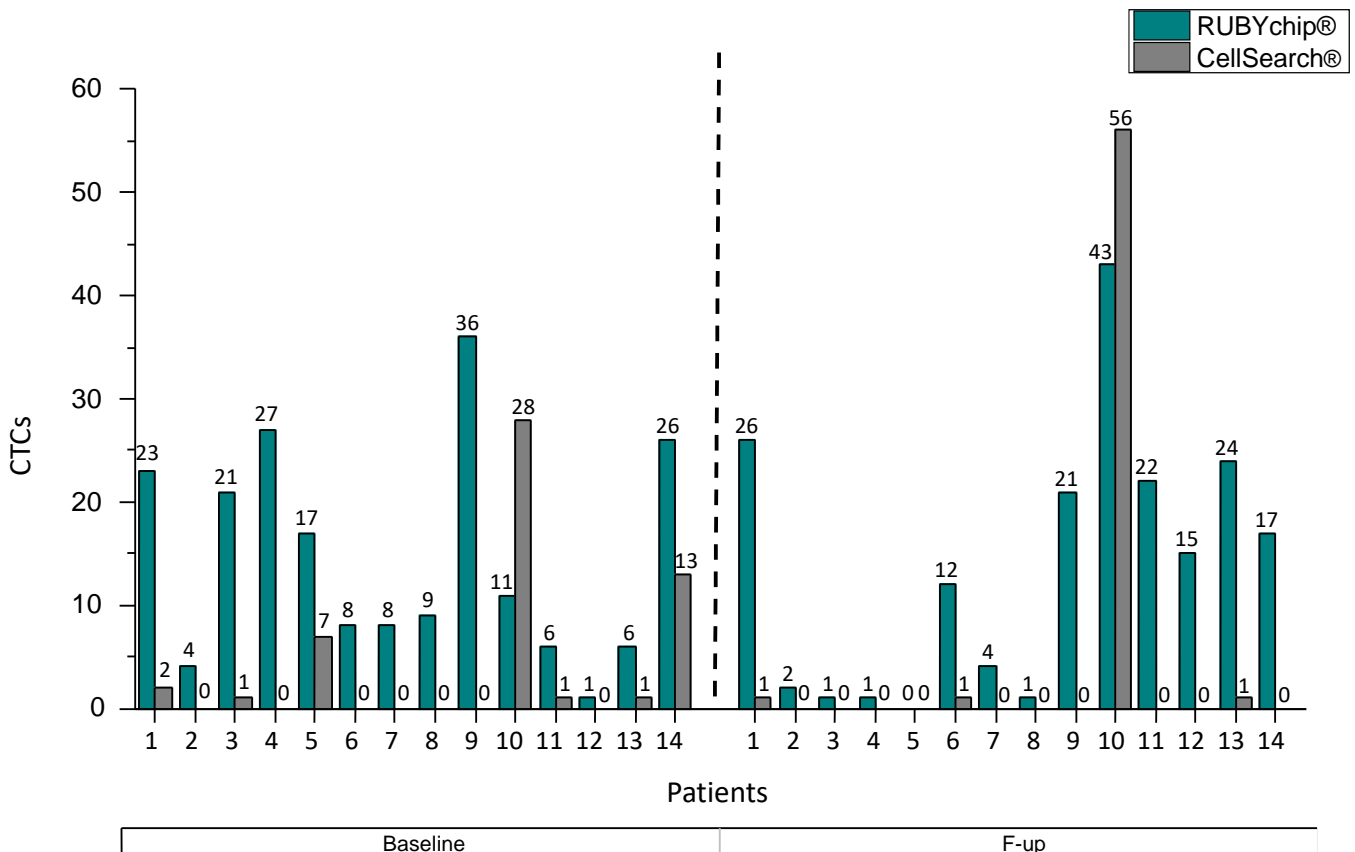


Figure 25: Comparative bar chart demonstrating the enumeration of CTCs using the RUBYchip™, in green *versus* the CellSearch® system, in grey, for all the 14 patient’s samples analysed in both time points. Baseline results are shown on the left side of the graphic, and follow-up results on the right.

The comparative study of 14 patients with MBC demonstrated considerable discrepancies between both technologies in CTCs isolation and enumeration.

It is important to point out that 16 of the 28 samples (57%) had CTCs isolated only by the RUBYchip™ and, for the remaining other 12 samples, the RUBYchip™ isolated a higher number of CTCs

in 9 samples (75%), demonstrating that the isolation of epithelial CTCs using the RUBYchip™ is more efficient and sensitive than the CellSearch®, both in the baseline and in the follow-up ($p=0.0046$), highlighting the better performance and clinical potential of this device.

The noticeable discrepancies in the number of CTCs isolated by the two different systems, in most of the samples (Figure 25), can be explained by the loss of CTCs by the CellSearch® system during sample pre-processing steps, as explained in section 1.3.1., while whole blood samples are introduced and filtered directly in the RUBYchip™, decreasing the possibility of cell loss [203][92].

Also, the CellSearch® system targets EpCAM+ CTCs only, missing out other CK+ CTCs with low EpCAM expression. In addition to the detection of epithelial-like CTCs (DAPI+/CK+/CD45-), DAPI+/CK-/CD45-/HER2+ cells were identified in the RUBYchip™, suggesting that this device is able to entrap cells with different phenotypes, increasing even further the number of isolated CTCs and providing additional important information of the disease status. In fact, other studies described the isolation of CK-/HER2+ CTCs in breast cancer recurring to liquid biopsy systems [204]. Still, further studies would be needed to confirm that the DAPI+/CK-/CD45-/HER2+ cells isolated by the RUBYchip™ are indeed from cancer origin. Nonetheless, the immunofluorescence staining of trapped cells allowed to confirm the purity of

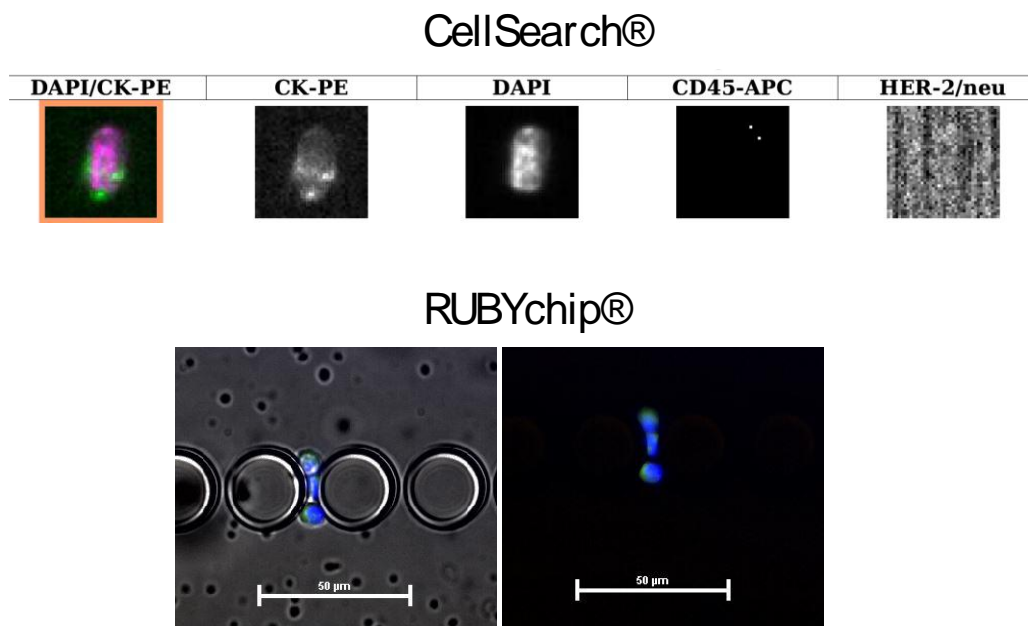


Figure 26: Representative images obtained with the different technologies, CellSearch® on the top, and RUBYchip™ at the bottom. With the RUBYchip™ is possible to obtain high resolution images, when compared to those obtained with the CellSearch®. In this particular case, it is possible to observe CTCs (DAPI+/CK+/CD45-). The RUBYchip™ images show 3 CTCs, both in a merged image (bright field and fluorescence) and fluorescence only.

CTCs, providing good quality images, compared to those obtained with the CellSearch®, making the analysis and validation steps easier, faster and more reliable (Figure 26).

Considering the threshold established for poor disease progression in MBC, the results obtained by the CellSearch® were negative for 11 (79%) of the patients, meaning that the number of CTCs was

below the threshold, making it difficult to evaluate disease progression and most importantly rendering the technology ineffective for patient stratification. In contrast, the results obtained by RUBYchip™ were positive for 13 (93%) of the patients, allowing a more accurate evaluation of the disease progression for each patient.

The fact that most of the patient samples analysed using CellSearch® had a number of CTCs below threshold, that is, a low number of CTCs, could lead to a misleading classification of the patients as having good prognosis, however, when comparing with the RUBYchip™ system, it was possible to observe that the same patient samples had a much higher number of CTCs isolated, meaning that a wrong correlation could be made between the CTCs number using CellSearch® and the disease progression, and proving that the RUBYchip™ had a much better performance and allowed a more trustworthy evaluation of the disease progression and patient prognosis (Table 11).

5.5. Tissue biopsy *versus* Liquid Biopsy: HER2 status

The tissue biopsy, usually made at the time of the first diagnostic, gives molecular information about the tumour, including the disease subtype and the grade. Consequently, the therapy administered to each patient is defined based on this biopsy. When disease relapse happens, the clinical decisions in the hospital where the patients were recruited, are made based on the first tissue biopsy made, even if the relapse occurs many years after the first diagnostic. A new tissue biopsy is only made occasionally if the patients does not present any response to therapy. The evaluation of disease progression by the oncologist is made based on the clinical and biochemical analysis, as well as imagiological examination (such and Computed Axial Tomography made every three months).

However, as already explained, cancer is a heterogeneous and dynamic disease, meaning that the tumour characteristics can change over time. Also, tumours are heterogeneous and molecular characteristics can be different in different tumour locations. Hence, tissue biopsy often fails to represent intra-tumour and inter-tumour heterogeneity, as it relies on a limited sample of tumour tissue. Liquid biopsy gives the possibility to access the molecular characteristics of the various tumours in real-time, by isolating and characterising CTCs present in the patient samples, being a reproducible and minimally invasive technique [202].

Following CTC isolation, it was important to characterize the HER2 status of the isolated cells, in order to assess their prognostics and predictive potential. One of the main aims of the study was to evaluate the presence of HER2+ CTCs in the patient samples and compare these findings with the HER2

status of the tissue biopsy sample. For this purpose, HER2+ CTCs (DAPI+/CK+/HER2+/CD45-) were enumerated by both technologies and later compared against tissue biopsy results (Table 12).

Concerning the number and characteristics of the CTCs isolated with each technology, it was observed that the RUBYchip™ was able to isolate HER2+ CTCs in 5 patients (36%) (Figure 27), while CellSearch® detected these cells in 4 patients (29%). The technologies are in agreement in 2 of the cases, where HER2+ CTCs were found in patient 1, at the baseline, and patient 13, at the follow-up moment.

The results showed that not only the RUBYchip™ is able to isolate and detect HER2+ CTCs in a higher number of samples, but also the number of HER2+ CTCs captured is higher, with an average of 3.2 CTCs, whereas average number of HER2+ CTCs isolated by CellSearch® is 1, proving once again that RUBYchip™ has a better performance.

Table 12: Evaluation of the HER2 status in the patients' tumours and CTCs. The presence (✓) or absence (✗) of this biomarker were assessed in tissue biopsy and liquid biopsy, based on patient clinical reports and results obtained with the RUBYchip™ and the CellSearch®. Presented data refers to pool of patients that exhibited HER2 positivity in at least one of the assessments or time points. (0 stands for the samples with no CTCs isolated)

PATIENTS	TISSUE BIOPSY	RUBYCHIP™		CELLSEARCH®	
		Baseline	Follow-up	Baseline	Follow-Up
1	✓	✓	✗	✓	✗
3	✗	✗	✓	✗	0
4	✓	✓	✗	0	0
6	✗	✗	✗	0	✓
7	✗	✗	✓	0	0
8	✓	✗	✗	0	0
10	✓	✗	✗	✗	0
11	✗	✗	✗	✓	0
13	✗	✓	✓	✗	✓

Analysing the clinical reports on tissue biopsy data, it was observed that in total, 4 patients were diagnosed as having HER2+ tumours, namely, patients 1, 4, 8 and 10. In these cases, tissue biopsy was made at the time of the first diagnosis, meaning that in 3 of these patients this diagnosis was made several years ago, as shown in table 9, and may reflect an inaccurate assessment of the real time disease HER2 status.

After obtaining all the results from the liquid biopsies, it was possible to correlate these findings with the tissue biopsy diagnostic. HER2+ cells were found in 2 out of 4 patients (50%) positive for tissue biopsy, by the RUBYchip™, and in 1 out of 4 patients (25%), by the CellSearch®, interestingly consensus regarding HER2 status among the three methodologies was found in patient 1 only.

A group of patients (Patients 1, 4 and 8) diagnosed by tissue biopsy has having HER2+ tumours (table 12), were treated with Anti-HER2 therapy between the two moments of collection, as shown in table 10, and the RUBYchip™ was able to isolate HER2+ CTCs in 2 of these patients (patient 1 and 4). Looking carefully at the results concerning the cases of patient 1 and 4, a relevant finding is that according to the RUBYchip™, both patients are positive for HER2+ at the baseline, however, HER2+ CTCs were not found at the follow-up, matching well with the fact that these patients were under anti-HER2 targeted therapy. CellSearch® is in agreement in the case of patient 1. On the other hand, in agreement with CellSearch® findings, patient 1, even with no HER2+ CTCs found at the follow-up, had a total number of CTCs increased.

The fact that both technologies are in agreement supports the importance of CTCs isolation and characterization, which allows an accurate diagnosis for successful therapy selection.

Since the number of HER2+ cells decreases between times of collection in patients under Anti-HER2 targeted therapy, it may be indicative of a positive response to therapy. The higher number of CTCs in total by one of the patients (patient 1), may be an indicative that the tumour burden is still high but tumour phenotypical characteristics have changed, ideally even to a less invasive and more well managed subtype, because it is known, and has been described in chapter 1, that HER2+ tumours are more aggressive and associated with a worst prognosis [205].

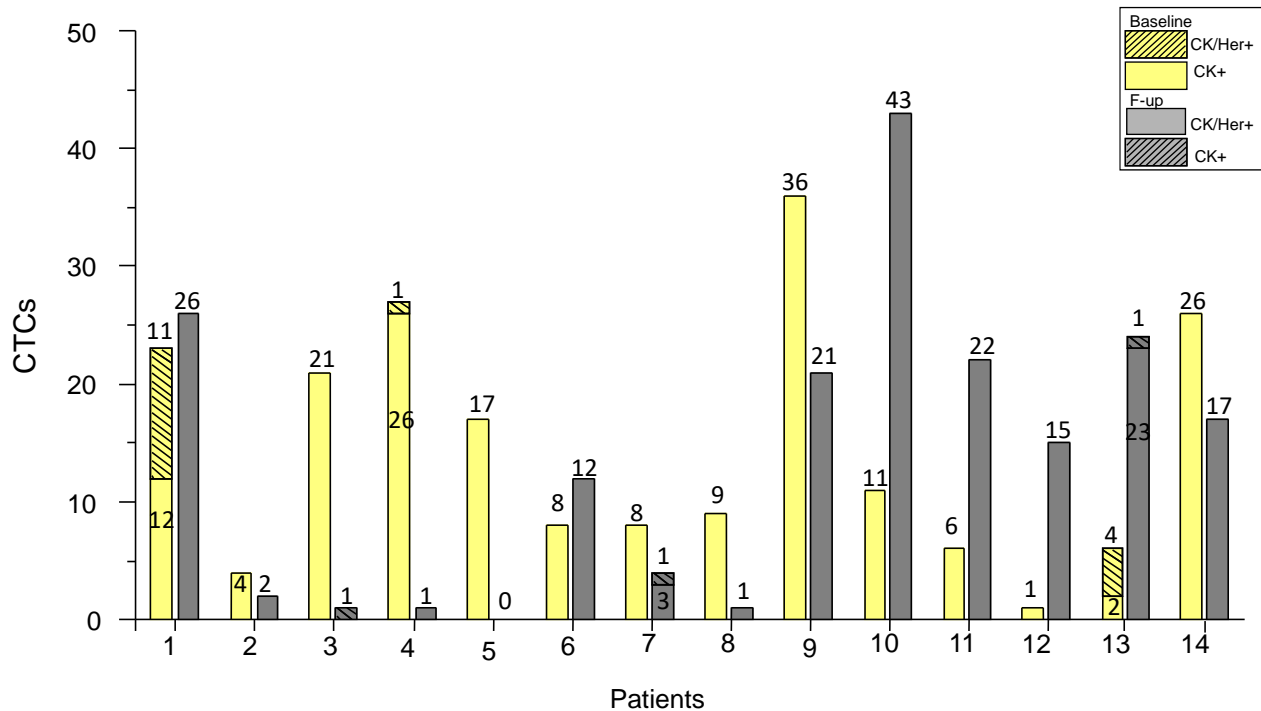


Figure 27 : Bar chart demonstrating the number of CTCs isolated by the RUBYchip™ in 14 metastatic breast cancer patients, in both moments of collection, baseline (before starting systemic therapy, in yellow bars) and follow-up (after 12 weeks of systemic treatment, in grey bars). It is also possible to observe the presence of HER2+ cell, represented by striped bars.

The presence of HER2+ cells, isolated by the RUBYchip™, in patients that were not diagnosed as having HER2+ tumours by the tissue biopsy diagnostic, as well as the absence of HER2+ cell in the RUBYchip™ in patients diagnosed as having HER2+ was observed. As mentioned in the beginning of this section, cancer is a dynamic and heterogeneous disease [8], the tumour state of each patient can change over time, such that an HER2+ tumour diagnosed 5 years ago (patient 8) could change to HER2- in the elapsed time due to therapeutic intervention or clonal evolution. And the other way around, patients diagnosed as having a Luminal A (patients 3 and 7) or TNBC (patient 13) tumours, can suffer alterations over time, presenting HER2+ cells in the current collections as detected by the RUBYchip™.

Additionally, it is long discussed that HER2 testing on the core biopsy in some circumstances may be unreliable or unrepresentative of the tumour [206], it could be argued that these patients could harbour HER2+ mutation, however since the tissue biopsy is made to a restrict part of the tumour, the presence of HER2 could have been missed out. Tumour misclassification can bring risks and consequences to the patients, namely, decrease of added life expectancy because no target therapy is administrated, which could also lead to an increased change of recurrence and evolution to metastatic disease [207].

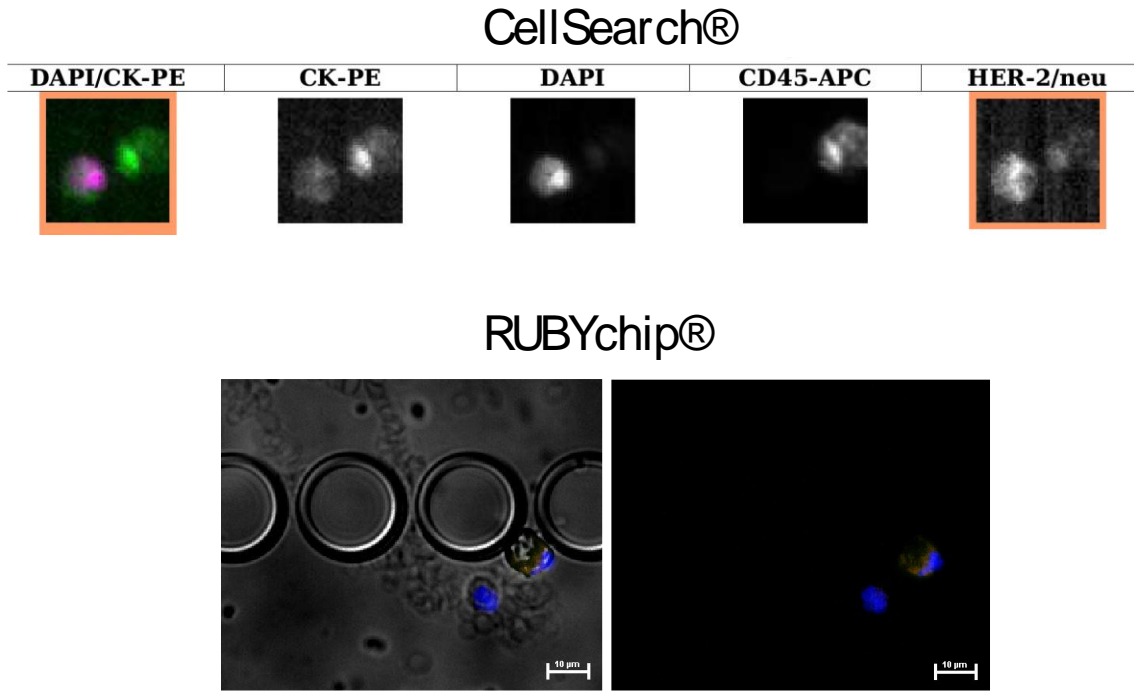


Figure 28: Representative images obtained with the different technologies, CellSearch® on the top, and RUBYchip™ at the bottom. RUBYchip™ technology image quality is considerably higher than those obtained with the CellSearch®. In this particular case, it is possible to observe HER2+ CTCs (DAPI+/CK+/HER2+/CD45-). The RUBYchip™ images show 1 CTC with HER2 presence, both in a merged image (bright field and fluorescence) and fluorescence only.

That said, it was possible to confirm that liquid biopsy and CTC isolation, representing a real-time snapshot of the tumour burden, offer unique opportunity for minimally invasive sampling in cancer patients. The RUBYchip™ is able to efficiently isolate CTCs and characterize their different phenotypes, namely, HER2+ CTCs, a very important group since HER2 mutation in breast cancer is associated with a worst prognosis. Thus, liquid biopsy can be an alternative or complementary to current clinical disease monitoring practices.

The study of CTCs and the implementation of relevant technologies in the field of liquid biopsy, such as the RUBYchip™ as a complement to current clinical practices, is of utmost importance in combating metastatic cancer and metastases formation because it provides up-to-date information on disease status, allowing targeted and personalized therapy to be applied to each patient individually, consequently improving therapeutic outcomes.

5.6. Correlation of clinicopathological information with CTC enumeration

To further evaluate the implications of CTCs in metastatic breast cancer setting, it was evaluated whether CTC enumeration and HER2 status findings were associated with relevant clinicopathological characteristics, including BC subtype, HER2 status in primary BC, administered treatment/therapeutic options and clinical stage in patients with metastatic breast cancer.

The correlation of the clinical information with CTC enumeration was made as a case by case approach since a small population sample size and cross-sectional experimental design didn't allow appropriate statistical analysis.

For that, it was observed how the number of isolated CTCs evolved during course of the disease, taking into account the therapy administered in the elapsed time. Regarding the five patients whom entered the study when they were already under treatment, as explained in section 5.3., information about the therapy administered before the baseline collection was also available and considered.

Six patients (43%) had increased CTC counts at follow-up when compared to the baseline collection to the follow-up, namely, patients 1, 6, 10, 11, 12 and 13, (Figure 27). HER2+ CTCs were detected by the RUBYchip™ in patients 1 and 13, and, as referred in the previous section, patient 1, which was diagnosed as having an HER2+ tumour, received anti-HER2 therapy, before and after baseline collection until follow-up, and although an increase in the total number of CTCs is observed, the number of HER2 positive CTCs decreased. On the other hand, patient 13 that was diagnosed as having a TNBC tumour, had an increase of 18 CTCs at follow-up (3x higher than baseline). This increase can be an indicator of a possible resistance to therapy and worst prognosis. A considerable increase in the total number of CTCs at follow-up was also observed in patients 10, 11 and 12. As reported in table 10, patient 12, with TNBC, did not received systemic therapy. This patient presented metastases in the central nervous system, since this type of therapy would not be able to penetrate the blood brain barrier, radiotherapy was chosen to be administered to the patient. The increase in the number of CTCs between collection may be explained by that, and as known, brain metastasis are the most aggressive and difficult to treat, correlated with a worst prognosis [208].

All the other patients showed a decrease in the number of total CTCs, most noticeable cases of decreased number of CTC at follow-up compared to baseline, were observed in patients 3 (20x less CTCs), 4 (26x less) and 5 (from 17 to 0. CTCs).

Both patient 3 and 5, which presented bone metastases, were treated with bone target therapy between collections, and the considerably decrease in the number of CTC at follow-up may be an indicator of response to therapy [209].

According to the clinical data information regarding the disease progression, based on the physical, biochemical and mainly imagiological assessment, none of the patients was reported to be in disease progression at the time-points comprised in this study. Conversely, CTC enumeration results obtained with the RUBYchip™, showed that six patients (43%) had an increase in the total number of CTCs at the follow-up, which could be indicative of disease progression. Even though traditionally, imaging technologies have been used to measure the effectiveness of treatment in patients with metastatic breast cancer, this approach is not exempt of inaccuracy, and may not detect early or low signs of cancer spreading. Hence, it can be argued that seeming discrepancies in the evaluation of metastatic disease status, may reflect different detection limits of the technologies, higher thus less sensitive for conventional imaging than CTC enumeration, particularly considering an experimental design with a timeframe that can be restrictive to display considerable metastatic tumour development.

Accumulating studies have reported that the CTC count is reproducible and is associated with disease progression status. Besides, often showing useful results at an earlier time point. A more accurate and earlier determination of treatment effectiveness in the course of therapy might spare patient toxicity from futile therapy and allow treatment to be changed to a more effective regimen. In sum, RUBYchip™ results highlight that simpler, informative and more effective technologies which are capable of assessing the effectiveness of therapy are needed to allow optimal treatment of patients.

CHAPTER 6: Conclusion and Future Perspectives

The main goal of this work was to optimize and validate the RUBYchip™ for the isolation and characterization of circulating tumour cells from whole blood in metastatic breast cancer, and also to assess the relevance of HER2 expression in CTC for patient stratification.

The results of this thesis demonstrate that the RUBYchip™ can isolate CTCs from whole blood samples from MBC patients with higher sensitivity, than the only FDA approved CellSearch® system, not only enumerating a higher number of CTCs for most patients (CTCs were detected exclusively by the RUBYchip™ in 57% of the samples (16 out of 28 samples) and for the other samples, it had higher CTC counts in 75% of the samples). RUBYchip™ showed more efficient detection of different subpopulations, namely HER2 expression.

The RUBYchip™ was able to detect HER2+ CTCs in 36% of the samples. Moreover, the device isolated HER2+ CTCs in 50% of the patients positive for tissue biopsy, at the baseline. These patients received anti-HER2 targeted therapy, and it was possible to observe that no HER2+ CTCs were found at the follow-up. Characterization of such molecular markers could be differentially associated with patients' clinical outcome and provide relevant information with clinical relevance for therapeutic reasoning.

Noticing that most HER2 studies have established a scoring grade to classify the receptor overexpression, future work ought to include additional ICC studies in which cell lines with different HER2 expression levels will be used, so that a new criteria can be established to classify HER2 in grades, similar to criteria established and approved in clinical practice. Once a more comprehensive and consensual classification criteria is established, a more accurate assessment can be achieved.

As a general conclusion, the use of the RUBYchip™ in the clinic allows to obtain better information of patients' prognosis. This minimally invasive strategy can be used to continuously gather information about the state of the tumour in real time, overcoming tumour dynamics and heterogeneity. Finally, the implementation of CTCs as a routine clinical tool for the management of MBC is expected to assist in patient stratification and prognosis, enabling personalized therapy.

In the future, workflow is expected to be improved, with the objective to minimize the time sample-to-result. For this purpose, future work includes the validation of a software optimized for automatic cell counting, in order to improve the reproducibility of the results, remove inter-user variability, avoid biased analysis and reduce the time of analysis.

Ultimately, we expect to validate the technology in the clinic to achieve CE marking as a certified *in vitro* diagnostics system for MBC, and to later expand the utility of the system to other cancer types.

CHAPTER 7: References

- [1] A. Jemal, F. Bray, M. M. Center, J. Ferlay, E. Ward, and D. Forman, "Global cancer statistics.," *CA. Cancer J. Clin.*, vol. 61, no. 2, pp. 69–90, 2011.
- [2] J. Ferlay, H.-R. Shin, F. Bray, D. Forman, C. Mathers, and D. M. Parkin, "Estimates of worldwide burden of cancer in 2008: GLOBOCAN 2008.," *Int. J. cancer*, vol. 127, no. 12, pp. 2893–2917, Dec. 2010.
- [3] H. Esmaeilsabzali, T. V. Beischlag, M. E. Cox, A. M. Parameswaran, and E. J. Park, "Detection and isolation of circulating tumor cells: Principles and methods," *Biotechnol. Adv.*, vol. 31, no. 7, pp. 1063–1084, 2013.
- [4] S. McGuire, "World Cancer Report 2014. Geneva, Switzerland: World Health Organization, International Agency for Research on Cancer, WHO Press, 2015.," *Adv. Nutr.*, vol. 7, no. 2, pp. 418–419, Mar. 2016.
- [5] D. Hanahan and R. A. Weinberg, "Hallmarks of cancer: the next generation.," *Cell*, vol. 144, no. 5, pp. 646–674, Mar. 2011.
- [6] J. S. Bertram, "Molecular aspects of medicine," *Mol. Aspects Med.*, vol. 8, no. 2, p. 1, 1985.
- [7] W. J. Irvin and L. A. Carey, "What is triple-negative breast cancer?," *Eur. J. Cancer*, vol. 44, no. 18, pp. 2799–2805, 2008.
- [8] N. V. Cherdyntseva, N. V. Litviakov, E. V. Denisov, P. A. Gervas, and E. S. Cherdyntsev, "Circulating tumor cells in breast cancer: Functional heterogeneity, pathogenetic and clinical aspects," vol. 39, no. 1, pp. 2–11, 2017.
- [9] D. Massihnia *et al.*, "A headlight on liquid biopsies: a challenging tool for breast cancer management," *Tumor Biol.*, vol. 37, no. 4, pp. 4263–4273, Apr. 2016.
- [10] A. Bombonati and D. C. Sgroi, "The molecular pathology of breast cancer progression.," *J. Pathol.*, vol. 223, no. 2, pp. 307–317, Jan. 2011.
- [11] R. L. Siegel, K. D. Miller, and A. Jemal, "Cancer statistics, 2015.," *CA. Cancer J. Clin.*, vol. 65, no. 1, pp. 5–29, 2015.
- [12] D. Fanale, V. Amodeo, L. R. Corsini, S. Rizzo, V. Bazan, and A. Russo, "Breast cancer genome-wide association studies: there is strength in numbers.," *Oncogene*, vol. 31, no. 17, pp. 2121–2128, Apr. 2012.
- [13] Z. Li and Y. Kang, "Emerging therapeutic targets in metastatic progression: A focus on breast cancer," *Pharmacol. Ther.*, vol. 161, pp. 79–96, 2016.
- [14] C. Alix-Panabières and K. Pantel, "Clinical applications of circulating tumor cells and circulating tumor DNA as liquid biopsy," *Cancer Discov.*, vol. 6, no. 5, pp. 479–491, 2016.
- [15] R. Wang, X. Li, H. Zhang, K. Wang, and J. He, "Cell-free circulating tumor DNA analysis for breast cancer and its clinical utilization as a biomarker," *Oncotarget*, vol. 8, no. 43, pp. 75742–75755, 2017.
- [16] C. Curtis *et al.*, "The genomic and transcriptomic architecture of 2,000 breast tumours reveals novel subgroups," *Nature*, vol. 486, p. 346, Apr. 2012.
- [17] B. Weigelt, F. C. Geyer, and J. S. Reis-Filho, "Histological types of breast cancer: How special are they?," *Mol. Oncol.*, vol. 4, no. 3, pp. 192–208, 2010.

- [18] B. Weigelt *et al.*, "Breast cancer molecular profiling with single sample predictors: a retrospective analysis," *Lancet. Oncol.*, vol. 11, no. 4, pp. 339–349, Apr. 2010.
- [19] J. S. Parker *et al.*, "Supervised risk predictor of breast cancer based on intrinsic subtypes.," *J. Clin. Oncol.*, vol. 27, no. 8, pp. 1160–1167, Mar. 2009.
- [20] N. C. Turner and J. S. Reis-Filho, "Basal-like breast cancer and the BRCA1 phenotype.," *Oncogene*, vol. 25, no. 43, pp. 5846–5853, Sep. 2006.
- [21] S. Badve *et al.*, "Basal-like and triple-negative breast cancers: a critical review with an emphasis on the implications for pathologists and oncologists.," *Mod. Pathol. an Off. J. United States Can. Acad. Pathol. Inc*, vol. 24, no. 2, pp. 157–167, Feb. 2011.
- [22] P. Klingbeil *et al.*, "CD44 is overexpressed in basal-like breast cancers but is not a driver of 11p13 amplification.," *Breast Cancer Res. Treat.*, vol. 120, no. 1, pp. 95–109, Feb. 2010.
- [23] J. Peppercorn, C. M. Perou, and L. A. Carey, "Molecular subtypes in breast cancer evaluation and management: divide and conquer.," *Cancer Invest.*, vol. 26, no. 1, pp. 1–10, Feb. 2008.
- [24] L. Pusztai, C. Mazouni, K. Anderson, Y. Wu, and W. F. Symmans, "Molecular classification of breast cancer: limitations and potential.," *Oncologist*, vol. 11, no. 8, pp. 868–877, Sep. 2006.
- [25] B. Weigelt, F. L. Baehner, and J. S. Reis-Filho, "The contribution of gene expression profiling to breast cancer classification, prognostication and prediction: a retrospective of the last decade.," *J. Pathol.*, vol. 220, no. 2, pp. 263–280, Jan. 2010.
- [26] B. S. Yadav, P. Chanana, and S. Jhamb, "Biomarkers in triple negative breast cancer: A review.," *World J. Clin. Oncol.*, vol. 6, no. 6, pp. 252–263, Dec. 2015.
- [27] S. Hurvitz and M. Mead, "Triple-negative breast cancer: advancements in characterization and treatment approach.," *Curr. Opin. Obstet. Gynecol.*, vol. 28, no. 1, pp. 59–69, Feb. 2016.
- [28] D. Carlisi *et al.*, "The oxygen radicals involved in the toxicity induced by parthenolide in MDA-MB-231 cells.," *Oncol. Rep.*, vol. 32, no. 1, pp. 167–172, Jul. 2014.
- [29] L. Xi, D. G. Nicastrì, T. El-Hefnawy, S. J. Hughes, J. D. Luketich, and T. E. Godfrey, "Optimal markers for real-time quantitative reverse transcription PCR detection of circulating tumor cells from melanoma, breast, colon, esophageal, head and neck, and lung cancers.," *Clin. Chem.*, vol. 53, no. 7, pp. 1206–1215, Jul. 2007.
- [30] J.-Y. Pierga, F.-C. Bidard, M. G. Denis, and P. de Cremoux, "Prognostic value of peripheral blood double detection of CK19 and MUC1 mRNA positive cells detected by RT-quantitative PCR in 94 breast cancer patients with a follow up of 9 years," *Mol. Oncol.*, vol. 1, no. 3, pp. 267–268, Dec. 2007.
- [31] M. Yu, S. Stott, M. Toner, S. Maheswaran, and D. A. Haber, "Circulating tumor cells: Approaches to isolation and characterization," *J. Cell Biol.*, vol. 192, no. 3, pp. 373–382, 2011.
- [32] B. Thierry, M. Kurkuri, J. Y. Shi, L. E. M. P. Lwin, and D. Palms, "Herceptin functionalized microfluidic polydimethylsiloxane devices for the capture of human epidermal growth factor receptor 2 positive circulating breast cancer cells," *Biomicrofluidics*, vol. 4, no. 3, pp. 1–10, 2010.

- [33] J. Mazières *et al.*, “Lung cancer that harbors an HER2 Mutation: Epidemiologic characteristics and therapeutic perspectives,” *J. Clin. Oncol.*, vol. 31, no. 16, pp. 1997–2003, 2013.
- [34] C. M. Connell and G. J. Doherty, “Activating HER2 mutations as emerging targets in multiple solid cancers,” *ESMO Open*, vol. 2, no. 5, p. e000279, 2017.
- [35] L. Angeles, “HER2 Mutation and Response to Trastuzumab Therapy in Non – Small-Cell Lung Cancer,” *Int. J. Technol. Assess. Health Care*, pp. 2619–2621, 2006.
- [36] T. Wang *et al.*, “HER2 somatic mutations are associated with poor survival in HER2-negative breast cancers,” *Cancer Sci.*, vol. 108, no. 4, pp. 671–677, 2017.
- [37] M. J. Wagner, M. M. Stacey, B. A. Liu, and T. Pawson, “Molecular mechanisms of SH2- and PTB-domain-containing proteins in receptor tyrosine kinase signaling,” *Cold Spring Harb. Perspect. Biol.*, vol. 5, no. 12, p. a008987, Dec. 2013.
- [38] M. A. Lemmon, J. Schlessinger, and K. M. Ferguson, “The EGFR family: not so prototypical receptor tyrosine kinases.,” *Cold Spring Harb. Perspect. Biol.*, vol. 6, no. 4, p. a020768, Apr. 2014.
- [39] Y. Yarden and G. Pines, “The ERBB network: at last, cancer therapy meets systems biology.,” *Nature reviews. Cancer*, vol. 12, no. 8. England, pp. 553–563, Jul-2012.
- [40] N. L. Spector and K. L. Blackwell, “Understanding the mechanisms behind trastuzumab therapy for human epidermal growth factor receptor 2-positive breast cancer.,” *J. Clin. Oncol.*, vol. 27, no. 34, pp. 5838–5847, Dec. 2009.
- [41] H. Greulich *et al.*, “Functional analysis of receptor tyrosine kinase mutations in lung cancer identifies oncogenic extracellular domain mutations of ERBB2.,” *Proc. Natl. Acad. Sci. U. S. A.*, vol. 109, no. 36, pp. 14476–14481, Sep. 2012.
- [42] R. Bose *et al.*, “Activating HER2 mutations in HER2 gene amplification negative breast cancer.,” *Cancer Discov.*, vol. 3, no. 2, pp. 224–237, Feb. 2013.
- [43] Y. Endo *et al.*, “HER2 mutation status in Japanese HER2-negative breast cancer patients.,” *Jpn. J. Clin. Oncol.*, vol. 44, no. 7, pp. 619–623, Jul. 2014.
- [44] P. J. Stephens *et al.*, “The landscape of cancer genes and mutational processes in breast cancer.,” *Nature*, vol. 486, no. 7403, pp. 400–404, May 2012.
- [45] S. Banerji *et al.*, “Sequence analysis of mutations and translocations across breast cancer subtypes.,” *Nature*, vol. 486, no. 7403, pp. 405–409, Jun. 2012.
- [46] V. Serra *et al.*, “Clinical response to a lapatinib-based therapy for a Li-Fraumeni syndrome patient with a novel HER2V659E mutation.,” *Cancer Discov.*, vol. 3, no. 11, pp. 1238–1244, Nov. 2013.
- [47] B. N. Rexer *et al.*, “Human breast cancer cells harboring a gatekeeper T798M mutation in HER2 overexpress EGFR ligands and are sensitive to dual inhibition of EGFR and HER2.,” *Clin. Cancer Res.*, vol. 19, no. 19, pp. 5390–5401, Oct. 2013.
- [48] R. K. Kancha, N. von Bubnoff, N. Bartosch, C. Peschel, R. A. Engh, and J. Duyster, “Differential sensitivity of ERBB2 kinase domain mutations towards lapatinib.,” *PLoS One*, vol. 6, no. 10, p. e26760, 2011.

- [49] J. W. Lee *et al.*, "Somatic mutations of ERBB2 kinase domain in gastric, colorectal, and breast carcinomas.," *Clin. Cancer Res.*, vol. 12, no. 1, pp. 57–61, Jan. 2006.
- [50] M. J. Ellis *et al.*, "Whole-genome analysis informs breast cancer response to aromatase inhibition.," *Nature*, vol. 486, no. 7403, pp. 353–360, Jun. 2012.
- [51] S. P. Shah *et al.*, "Mutational evolution in a lobular breast tumour profiled at single nucleotide resolution.," *Nature*, vol. 461, no. 7265, pp. 809–813, Oct. 2009.
- [52] Z. Kan *et al.*, "Diverse somatic mutation patterns and pathway alterations in human cancers.," *Nature*, vol. 466, no. 7308, pp. 869–873, Aug. 2010.
- [53] S. P. Shah *et al.*, "The clonal and mutational evolution spectrum of primary triple-negative breast cancers.," *Nature*, vol. 486, no. 7403, pp. 395–399, Apr. 2012.
- [54] I. Smith *et al.*, "2-year follow-up of trastuzumab after adjuvant chemotherapy in HER2-positive breast cancer: a randomised controlled trial.," *Lancet (London, England)*, vol. 369, no. 9555, pp. 29–36, Jan. 2007.
- [55] R. Colomer *et al.*, "Biomarkers in breast cancer: A consensus statement by the Spanish Society of Medical Oncology and the Spanish Society of Pathology," *Clin. Transl. Oncol.*, pp. 1–12, 2017.
- [56] R. W. Carlson *et al.*, "HER2 testing in breast cancer: NCCN Task Force report and recommendations.," *J. Natl. Compr. Canc. Netw.*, vol. 4 Suppl 3, pp. S1-22; quiz S23-4, Jul. 2006.
- [57] D. C. Zaha, "Significance of immunohistochemistry in breast cancer," *World J. Clin. Oncol.*, vol. 5, no. 3, p. 382, 2014.
- [58] A. C. Wolff *et al.*, "American Society of Clinical Oncology/College of American Pathologists guideline recommendations for human epidermal growth factor receptor 2 testing in breast cancer.," *Arch. Pathol. Lab. Med.*, vol. 131, no. 1, pp. 18–43, 2007.
- [59] D. G. Hicks and R. R. Tubbs, "Assessment of the HER2 status in breast cancer by fluorescence in situ hybridization: a technical review with interpretive guidelines.," *Hum. Pathol.*, vol. 36, no. 3, pp. 250–261, Mar. 2005.
- [60] L. Lima *et al.*, "Sialyl-Tn identifies muscle-invasive bladder cancer basal and luminal subtypes facing decreased survival, being expressed by circulating tumor cells and metastases," *Urol. Oncol. Semin. Orig. Investig.*, vol. 35, no. 12, pp. 675.e1-675.e8, 2017.
- [61] D. Madhavan *et al.*, "Circulating miRNAs with prognostic value in metastatic breast cancer and for early detection of metastasis," *Carcinogenesis*, vol. 37, no. 5, pp. 461–470, 2016.
- [62] S. Maheswaran and D. A. Haber, "Circulating tumor cells: a window into cancer biology and metastasis.," *Curr. Opin. Genet. Dev.*, vol. 20, no. 1, pp. 96–99, Feb. 2010.
- [63] K. Pantel and C. Alix-Panabieres, "Circulating tumour cells in cancer patients: challenges and perspectives.," *Trends Mol. Med.*, vol. 16, no. 9, pp. 398–406, Sep. 2010.
- [64] H. Sihto *et al.*, "Breast cancer biological subtypes and protein expression predict for the preferential distant metastasis sites: A nationwide cohort study," *Breast Cancer Res.*, vol. 13, no. 5, p. R87, 2011.

- [65] H. Kennecke *et al.*, “Metastatic behavior of breast cancer subtypes,” *J. Clin. Oncol.*, vol. 28, no. 20, pp. 3271–3277, 2010.
- [66] A. J. D. Cohen *et al.*, “Detection and localization of surgically resectable cancers with a multi-analyte blood test,” *Science (80-.)*, vol. 3247, no. January, pp. 1–10, 2018.
- [67] T. J. Semrad, A. R. Fahrni, I.-Y. Gong, and V. P. Khatri, “Integrating Chemotherapy into the Management of Oligometastatic Colorectal Cancer: Evidence based Approach Using Clinical Trial Findings,” *Ann. Surg. Oncol.*, vol. 22, no. 0 3, pp. 855–862, Dec. 2015.
- [68] A. C. Huang *et al.*, “T-cell invigoration to tumour burden ratio associated with anti-PD-1 response.,” *Nature*, vol. 545, no. 7652, pp. 60–65, May 2017.
- [69] I. Bozic *et al.*, “Evolutionary dynamics of cancer in response to targeted combination therapy.,” *Elife*, vol. 2, p. e00747, Jun. 2013.
- [70] L. J. van ’t Veer *et al.*, “Gene expression profiling predicts clinical outcome of breast cancer.,” *Nature*, vol. 415, no. 6871, pp. 530–536, Jan. 2002.
- [71] I. Van Der Auwera *et al.*, “The presence of circulating total DNA and methylated genes is associated with circulating tumour cells in blood from breast cancer patients,” *Br. J. Cancer*, vol. 100, no. 8, pp. 1277–1286, 2009.
- [72] Y. Kang *et al.*, “A multigenic program mediating breast cancer metastasis to bone,” *Cancer Cell*, vol. 3, no. 6, pp. 537–549, 2003.
- [73] C. Alix-Panabières and K. Pantel, “Circulating tumor cells: Liquid biopsy of cancer,” *Clin. Chem.*, vol. 59, no. 1, pp. 110–118, 2013.
- [74] H. W. Hou, A. A. S. Bhagat, W. C. Lee, S. Huang, J. Han, and C. T. Lim, *Microfluidic Devices for Blood Fractionation*, vol. 2, no. 3. 2011.
- [75] P. Starostik, “Clinical mutation assay of tumors: new developments.,” *Anticancer. Drugs*, vol. 28, no. 1, pp. 1–10, Jan. 2017.
- [76] S. Perakis and M. R. Speicher, “Emerging concepts in liquid biopsies,” *BMC Med.*, vol. 15, no. 1, p. 75, 2017.
- [77] K. Pantel and C. Alix-Panabières, “Real-time liquid biopsy in cancer patients: Fact or fiction?,” *Cancer Res.*, vol. 73, no. 21, pp. 6384–6388, 2013.
- [78] I. G. Domínguez-Vigil, A. K. Moreno-Martínez, J. Y. Wang, M. H. A. Roehrl, and H. A. Barrera-Saldaña, “The dawn of the liquid biopsy in the fight against cancer,” *Oncotarget*, vol. 9, no. 2, pp. 2912–2922, Jan. 2018.
- [79] C. M. Hugen, D. E. Zainfeld, and A. Goldkorn, “Circulating Tumor Cells in Genitourinary Malignancies: An Evolving Path to Precision Medicine,” *Front. Oncol.*, vol. 7, p. 6, Jan. 2017.
- [80] G. Siravegna, S. Marsoni, S. Siena, and A. Bardelli, “Integrating liquid biopsies into the management of cancer.,” *Nat. Rev. Clin. Oncol.*, vol. 14, no. 9, pp. 531–548, Sep. 2017.
- [81] P. Hofman and H. H. Popper, “Pathologists and liquid biopsies: to be or not to be?,” *Virchows Arch.*, vol. 469, no. 6, pp. 601–609, Dec. 2016.

- [82] P. Mehlen and A. Puisieux, "Metastasis: a question of life or death.," *Nat. Rev. Cancer*, vol. 6, no. 6, pp. 449–458, Jun. 2006.
- [83] A. van de Stolpe, K. Pantel, S. Sleijfer, L. W. Terstappen, and J. M. J. den Toonder, "Circulating tumor cell isolation and diagnostics: toward routine clinical use.," *Cancer research*, vol. 71, no. 18. United States, pp. 5955–5960, Sep-2011.
- [84] G. Barriere, P. Fici, G. Gallerani, F. Fabbri, W. Zoli, and M. Rigaud, "Circulating tumor cells and epithelial, mesenchymal and stemness markers: characterization of cell subpopulations.," *Ann. Transl. Med.*, vol. 2, no. 11, p. 109, 2014.
- [85] Y. Husemann *et al.*, "Systemic spread is an early step in breast cancer.," *Cancer Cell*, vol. 13, no. 1, pp. 58–68, Jan. 2008.
- [86] C. A. Klein, "Parallel progression of primary tumours and metastases.," *Nature reviews. Cancer*, vol. 9, no. 4. England, pp. 302–312, Apr-2009.
- [87] Y. Kang and K. Pantel, "Tumor cell dissemination: emerging biological insights from animal models and cancer patients.," *Cancer Cell*, vol. 23, no. 5, pp. 573–581, May 2013.
- [88] L. Dieguez, M. A. Winter, K. J. Pocock, K. E. Bremmell, and B. Thierry, "Efficient microfluidic negative enrichment of circulating tumor cells in blood using roughened PDMS.," *Analyst*, vol. 140, no. 10, pp. 3565–3572, May 2015.
- [89] P. Chen, Y.-Y. Huang, K. Hoshino, and X. Zhang, "Multiscale immunomagnetic enrichment of circulating tumor cells: from tubes to microchips.," *Lab Chip*, vol. 14, no. 3, pp. 446–458, Feb. 2014.
- [90] M. M. Ferreira, V. C. Ramani, and S. S. Jeffrey, "Circulating tumor cell technologies.," *Mol. Oncol.*, vol. 10, no. 3, pp. 374–394, Mar. 2016.
- [91] A. Tadimety, A. Syed, Y. Nie, C. R. Long, K. M. Kready, and J. X. J. Zhang, "Liquid biopsy on chip: a paradigm shift towards the understanding of cancer metastasis.," *Integr. Biol. (Camb)*, vol. 9, no. 1, pp. 22–49, Jan. 2017.
- [92] J. M. Jackson, M. A. Witek, J. W. Kamande, and S. A. Soper, "Materials and microfluidics: enabling the efficient isolation and analysis of circulating tumour cells.," *Chem. Soc. Rev.*, vol. 46, no. 14, pp. 4245–4280, Jul. 2017.
- [93] C. Alix-Panabieres, H. Schwarzenbach, and K. Pantel, "Circulating tumor cells and circulating tumor DNA.," *Annu. Rev. Med.*, vol. 63, pp. 199–215, 2012.
- [94] D. R. Parkinson *et al.*, "Considerations in the development of circulating tumor cell technology for clinical use.," *J. Transl. Med.*, vol. 10, p. 138, Jul. 2012.
- [95] D. Issadore *et al.*, "Ultrasensitive clinical enumeration of rare cells ex vivo using a micro-hall detector.," *Sci. Transl. Med.*, vol. 4, no. 141, p. 141ra92, Jul. 2012.
- [96] M. Cristofanilli *et al.*, "Circulating tumor cells, disease progression, and survival in metastatic breast cancer.," *N. Engl. J. Med.*, vol. 351, no. 8, pp. 781–791, Aug. 2004.
- [97] K. C. Andree, G. van Dalum, and L. W. M. M. Terstappen, "Challenges in circulating tumor cell detection by the CellSearch system," *Mol. Oncol.*, vol. 10, no. 3, pp. 395–407, Mar. 2016.

- [98] L. Dieguez *et al.*, "Efficient microfluidic negative enrichment of circulating tumor cells in blood using roughened PDMS.," *Analyst*, vol. 140, no. 10, pp. 3565–3572, May 2015.
- [99] M. C. Miller, G. V. Doyle, and L. W. M. M. Terstappen, "Significance of Circulating Tumor Cells Detected by the CellSearch System in Patients with Metastatic Breast Colorectal and Prostate Cancer.," *J. Oncol.*, vol. 2010, p. 617421, 2010.
- [100] M. G. Krebs *et al.*, "Evaluation and prognostic significance of circulating tumor cells in patients with non-small-cell lung cancer.," *J. Clin. Oncol.*, vol. 29, no. 12, pp. 1556–1563, Apr. 2011.
- [101] J. Kraan *et al.*, "External quality assurance of circulating tumor cell enumeration using the CellSearch((R)) system: a feasibility study.," *Cytometry B. Clin. Cytom.*, vol. 80, no. 2, pp. 112–118, Mar. 2011.
- [102] M. Cristofanilli, "Circulating tumor cells, disease progression, and survival in metastatic breast cancer.," *Semin. Oncol.*, vol. 33, no. 3 Suppl 9, pp. S9-14, Jun. 2006.
- [103] R. Catarino *et al.*, "Quantification of free circulating tumor DNA as a diagnostic marker for breast cancer.," *DNA Cell Biol.*, vol. 27, no. 8, pp. 415–421, Aug. 2008.
- [104] S. Riethdorf *et al.*, "Detection of circulating tumor cells in peripheral blood of patients with metastatic breast cancer: a validation study of the CellSearch system.," *Clin. Cancer Res.*, vol. 13, no. 3, pp. 920–928, Feb. 2007.
- [105] E. W. Thompson and I. Haviv, "The social aspects of EMT-MET plasticity.," *Nature medicine*, vol. 17, no. 9. United States, pp. 1048–1049, Sep-2011.
- [106] C. L. Chaffer and R. A. Weinberg, "A Perspective on Cancer Cell Metastasis," *Science (80-.).*, vol. 331, no. 6024, pp. 1559 LP – 1564, Mar. 2011.
- [107] K. Polyak and R. A. Weinberg, "Transitions between epithelial and mesenchymal states: acquisition of malignant and stem cell traits.," *Nat. Rev. Cancer*, vol. 9, no. 4, pp. 265–273, Apr. 2009.
- [108] M. Yu *et al.*, "Circulating Breast Tumor Cells Exhibit Dynamic Changes in Epithelial and Mesenchymal Composition," *Science*, vol. 339, no. February, pp. 580–584, Feb. 2013.
- [109] F. Le Du, N. T. Ueno, and A. M. Gonzalez-Angulo, "Breast cancer biomarkers: Utility in clinical practice," *Curr. Breast Cancer Rep.*, vol. 5, no. 4, pp. 284–292, 2013.
- [110] S. Kasimir-Bauer, O. Hoffmann, D. Wallwiener, R. Kimmig, and T. Fehm, "Expression of stem cell and epithelial-mesenchymal transition markers in primary breast cancer patients with circulating tumor cells.," *Breast Cancer Res.*, vol. 14, no. 1, p. R15, Jan. 2012.
- [111] X. Zheng *et al.*, "Epithelial-to-mesenchymal transition is dispensable for metastasis but induces chemoresistance in pancreatic cancer.," *Nature*, vol. 527, no. 7579, pp. 525–530, Nov. 2015.
- [112] K. R. Fischer *et al.*, "Epithelial-to-mesenchymal transition is not required for lung metastasis but contributes to chemoresistance.," *Nature*, vol. 527, no. 7579, pp. 472–476, Nov. 2015.
- [113] R. Kalluri and R. A. Weinberg, "The basics of epithelial-mesenchymal transition.," *J. Clin. Invest.*, vol. 119, no. 6, pp. 1420–1428, Jun. 2009.

- [114] A. M. Sieuwerts *et al.*, "Anti-epithelial cell adhesion molecule antibodies and the detection of circulating normal-like breast tumor cells.," *J. Natl. Cancer Inst.*, vol. 101, no. 1, pp. 61–66, Jan. 2009.
- [115] C. G. Rao *et al.*, "Expression of epithelial cell adhesion molecule in carcinoma cells present in blood and primary and metastatic tumors.," *Int. J. Oncol.*, vol. 27, no. 1, pp. 49–57, Jul. 2005.
- [116] T. M. H. Gall and A. E. Frampton, "Gene of the month: E-cadherin (CDH1).," *J. Clin. Pathol.*, vol. 66, no. 11, pp. 928–932, Nov. 2013.
- [117] S. A. Joosse *et al.*, "Changes in keratin expression during metastatic progression of breast cancer: impact on the detection of circulating tumor cells.," *Clin. Cancer Res.*, vol. 18, no. 4, pp. 993–1003, Feb. 2012.
- [118] E. A. Runkle and D. Mu, "Tight junction proteins: from barrier to tumorigenesis.," *Cancer Lett.*, vol. 337, no. 1, pp. 41–48, Aug. 2013.
- [119] L. E. Lindley and K. J. Briegel, "Molecular characterization of TGFbeta-induced epithelial-mesenchymal transition in normal finite lifespan human mammary epithelial cells.," *Biochem. Biophys. Res. Commun.*, vol. 399, no. 4, pp. 659–664, Sep. 2010.
- [120] R. H. Hovhannisyan and R. P. Carstens, "Heterogeneous ribonucleoprotein m is a splicing regulatory protein that can enhance or silence splicing of alternatively spliced exons.," *J. Biol. Chem.*, vol. 282, no. 50, pp. 36265–36274, Dec. 2007.
- [121] C. C. Warzecha and R. P. Carstens, "Complex changes in alternative pre-mRNA splicing play a central role in the epithelial-to-mesenchymal transition (EMT).," *Semin. Cancer Biol.*, vol. 22, no. 5–6, pp. 417–427, Oct. 2012.
- [122] C. C. Warzecha, S. Shen, Y. Xing, and R. P. Carstens, "The epithelial splicing factors ESRP1 and ESRP2 positively and negatively regulate diverse types of alternative splicing events.," *RNA Biol.*, vol. 6, no. 5, pp. 546–562, 2009.
- [123] M. A. Khan, H. Chen, D. Zhang, and J. Fu, "Twist: a molecular target in cancer therapeutics.," *Tumour Biol.*, vol. 34, no. 5, pp. 2497–2506, Oct. 2013.
- [124] L. Li, S. A. L. Bennett, and L. Wang, "Role of E-cadherin and other cell adhesion molecules in survival and differentiation of human pluripotent stem cells.," *Cell Adh. Migr.*, vol. 6, no. 1, pp. 59–70, 2012.
- [125] A. Satelli and S. Li, "Vimentin in cancer and its potential as a molecular target for cancer therapy.," *Cell. Mol. Life Sci.*, vol. 68, no. 18, pp. 3033–3046, Sep. 2011.
- [126] G. Barrière, A. Riouallon, J. Renaudie, M. Tartary, and M. Rigaud, *Mesenchymal and stemness circulating tumor cells in early breast cancer diagnosis*, vol. 12, no. 1. BioMed Central Ltd, 2012.
- [127] S. Ansieau, A.-P. Morel, G. Hinkal, J. Bastid, and A. Puisieux, "TWISTing an embryonic transcription factor into an oncoprotein.," *Oncogene*, vol. 29, no. 22, pp. 3173–3184, Jun. 2010.
- [128] Y.-J. Liang, Y. Ding, S. B. Lavery, M. Lobaton, K. Handa, and S. Hakomori, "Differential expression profiles of glycosphingolipids in human breast cancer stem cells vs. cancer non-stem cells.," *Proc. Natl. Acad. Sci. U. S. A.*, vol. 110, no. 13, pp. 4968–4973, Mar. 2013.

- [129] V. L. Battula *et al.*, “Ganglioside GD2 identifies breast cancer stem cells and promotes tumorigenesis.,” *J. Clin. Invest.*, vol. 122, no. 6, pp. 2066–2078, Jun. 2012.
- [130] L. Xu *et al.*, “Optimization and evaluation of a novel size based circulating tumor cell isolation system,” *PLoS One*, vol. 10, no. 9, pp. 1–23, 2015.
- [131] H. A. Stone and S. Kim, “Microfluidics : Basic Issues , Applications , and Challenges,” vol. 47, no. 6, pp. 1250–1254.
- [132] T. M. Squires and S. R. Quake, “Microfluidics: Fluid physics at the nanoliter scale,” *Rev. Mod. Phys.*, vol. 77, no. 3, pp. 977–1026, Oct. 2005.
- [133] K.-A. Hyun and H.-I. Jung, “Advances and critical concerns with the microfluidic enrichments of circulating tumor cells.,” *Lab Chip*, vol. 14, no. 1, pp. 45–56, Jan. 2014.
- [134] G. M. Whitesides, “The origins and the future of microfluidics.,” *Nature*, vol. 442, no. 7101, pp. 368–373, Jul. 2006.
- [135] Y. Dong *et al.*, “Microfluidics and circulating tumor cells.,” *J. Mol. Diagn.*, vol. 15, no. 2, pp. 149–157, Mar. 2013.
- [136] S. Nagrath *et al.*, “Isolation of rare circulating tumour cells in cancer patients by microchip technology.,” *Nature*, vol. 450, no. 7173, pp. 1235–1239, Dec. 2007.
- [137] A. A. S. Bhagat, H. Bow, H. W. Hou, S. J. Tan, J. Han, and C. T. Lim, “Microfluidics for cell separation.,” *Med. Biol. Eng. Comput.*, vol. 48, no. 10, pp. 999–1014, Oct. 2010.
- [138] E. D. Pratt, C. Huang, B. G. Hawkins, J. P. Gleghorn, and B. J. Kirby, “Rare Cell Capture in Microfluidic Devices.,” *Chem. Eng. Sci.*, vol. 66, no. 7, pp. 1508–1522, Apr. 2011.
- [139] A.-E. Saliba *et al.*, “Microfluidic sorting and multimodal typing of cancer cells in self-assembled magnetic arrays.,” *Proc. Natl. Acad. Sci. U. S. A.*, vol. 107, no. 33, pp. 14524–14529, Aug. 2010.
- [140] H. W. Hou *et al.*, “Isolation and retrieval of circulating tumor cells using centrifugal forces,” *Sci. Rep.*, vol. 3, pp. 1–8, 2013.
- [141] J. P. Gleghorn *et al.*, “Capture of circulating tumor cells from whole blood of prostate cancer patients using geometrically enhanced differential immunocapture (GEDI) and a prostate-specific antibody.,” *Lab Chip*, vol. 10, no. 1, pp. 27–29, Jan. 2010.
- [142] A. A. Adams *et al.*, “Highly efficient circulating tumor cell isolation from whole blood and label-free enumeration using polymer-based microfluidics with an integrated conductivity sensor.,” *J. Am. Chem. Soc.*, vol. 130, no. 27, pp. 8633–8641, Jul. 2008.
- [143] G. Spizzo *et al.*, “High Ep-CAM expression is associated with poor prognosis in node-positive breast cancer.,” *Breast Cancer Res. Treat.*, vol. 86, no. 3, pp. 207–213, Aug. 2004.
- [144] K.-A. Hyun, T. Y. Lee, and H.-I. Jung, “Negative enrichment of circulating tumor cells using a geometrically activated surface interaction chip.,” *Anal. Chem.*, vol. 85, no. 9, pp. 4439–4445, May 2013.

- [145] L. Yang *et al.*, "Optimization of an enrichment process for circulating tumor cells from the blood of head and neck cancer patients through depletion of normal cells.," *Biotechnol. Bioeng.*, vol. 102, no. 2, pp. 521–534, Feb. 2009.
- [146] A. E. Ring, L. Zabaglo, M. G. Ormerod, I. E. Smith, and M. Dowsett, "Detection of circulating epithelial cells in the blood of patients with breast cancer: comparison of three techniques," *Br. J. Cancer*, vol. 92, p. 906, Feb. 2005.
- [147] S. J. Tan, L. Yobas, G. Y. H. Lee, C. N. Ong, and C. T. Lim, "Microdevice for the isolation and enumeration of cancer cells from blood.," *Biomed. Microdevices*, vol. 11, no. 4, pp. 883–892, Aug. 2009.
- [148] H. Mohamed, M. Murray, J. N. Turner, and M. Caggana, "Isolation of tumor cells using size and deformation.," *J. Chromatogr. A*, vol. 1216, no. 47, pp. 8289–8295, Nov. 2009.
- [149] T. A. Yap, D. Lorente, A. Omlin, D. Olmos, and J. S. De Bono, "Circulating tumor cells: A multifunctional biomarker," *Clin. Cancer Res.*, vol. 20, no. 10, pp. 2553–2558, 2014.
- [150] E. S. Lianidou, A. Markou, and A. Strati, "The Role of CTCs as Tumor Biomarkers.," *Adv. Exp. Med. Biol.*, vol. 867, pp. 341–367, 2015.
- [151] E. Cortesi, M. Palleschi, V. Magri, and G. Naso, "The promise of liquid biopsy in cancer: a clinical perspective.," *Chin. J. Cancer Res.*, vol. 27, no. 5, pp. 488–490, Oct. 2015.
- [152] F.-C. C. Bidard, C. Proudhon, and J.-Y. Y. Pierga, "Circulating tumor cells in breast cancer," *Mol. Oncol.*, vol. 10, no. 3, pp. 418–430, 2016.
- [153] M. Banys-paluchowski, N. Krawczyk, and F. Meier-stiegen, "Critical Reviews in Oncology / Hematology Circulating tumor cells in breast cancer – current status and perspectives," vol. 97, pp. 22–29, 2016.
- [154] T. Fehm *et al.*, "Detection and characterization of circulating tumor cells in blood of primary breast cancer patients by RT-PCR and comparison to status of bone marrow disseminated cells.," *Breast Cancer Res.*, vol. 11, no. 4, p. R59, 2009.
- [155] J.-Y. Tseng, C.-Y. Yang, S.-C. Liang, R.-S. Liu, J.-K. Jiang, and C.-H. Lin, "Dynamic changes in numbers and properties of circulating tumor cells and their potential applications.," *Cancers (Basel)*, vol. 6, no. 4, pp. 2369–2386, Dec. 2014.
- [156] E. F. Solomayer *et al.*, "Comparison of HER2 status between primary tumor and disseminated tumor cells in primary breast cancer patients.," *Breast Cancer Res. Treat.*, vol. 98, no. 2, pp. 179–184, Jul. 2006.
- [157] N. Krawczyk *et al.*, "HER2 status on persistent disseminated tumor cells after adjuvant therapy may differ from initial HER2 status on primary tumor.," *Anticancer Res.*, vol. 29, no. 10, pp. 4019–4024, Oct. 2009.
- [158] T. Fehm *et al.*, "ERalpha-status of disseminated tumour cells in bone marrow of primary breast cancer patients," *Breast Cancer Res.*, vol. 10, no. 5, p. R76, 2008.
- [159] M. Banys *et al.*, "The influence of removal of primary tumor on incidence and phenotype of circulating tumor cells in primary breast cancer," *Breast Cancer Res. Treat.*, vol. 132, no. 1, p. 121–129, 2012.

- [160] D. F. Hayes *et al.*, “Circulating tumor cells at each follow-up time point during therapy of metastatic breast cancer patients predict progression-free and overall survival.,” *Clin. Cancer Res.*, vol. 12, no. 14 Pt 1, pp. 4218–4224, Jul. 2006.
- [161] G. T. Budd *et al.*, “Circulating tumor cells versus imaging—predicting overall survival in metastatic breast cancer.,” *Clin. Cancer Res.*, vol. 12, no. 21, pp. 6403–6409, Nov. 2006.
- [162] F.-C. Bidard *et al.*, “Clinical validity of circulating tumour cells in patients with metastatic breast cancer: a pooled analysis of individual patient data.,” *Lancet. Oncol.*, vol. 15, no. 4, pp. 406–414, Apr. 2014.
- [163] J. B. Smerage *et al.*, “Circulating tumor cells and response to chemotherapy in metastatic breast cancer: SWOG S0500.,” *J. Clin. Oncol.*, vol. 32, no. 31, pp. 3483–3489, Nov. 2014.
- [164] F.-C. Bidard *et al.*, “Time-Dependent Prognostic Impact of Circulating Tumor Cells Detection in Non-Metastatic Breast Cancer: 70-Month Analysis of the REMAGUS02 Study.,” *Int. J. Breast Cancer*, vol. 2013, p. 130470, 2013.
- [165] Z. Shen, A. Wu, and X. Chen, “Current detection technologies for circulating tumor cells,” *Chem. Soc. Rev.*, vol. 46, no. 8, pp. 2038–2056, Apr. 2017.
- [166] K. Pachmann *et al.*, “Monitoring the Response of Circulating Epithelial Tumor Cells to Adjuvant Chemotherapy in Breast Cancer Allows Detection of Patients at Risk of Early Relapse,” *J. Clin. Oncol.*, vol. 26, no. 8, pp. 1208–1215, Mar. 2008.
- [167] A. Lucci *et al.*, “Circulating tumour cells in non-metastatic breast cancer: a prospective study,” *Lancet Oncol.*, vol. 13, no. 7, pp. 688–695, Jul. 2012.
- [168] B. Rack *et al.*, “Circulating Tumor Cells Predict Survival in Early Average-to-High Risk Breast Cancer Patients,” *JNCI J. Natl. Cancer Inst.*, vol. 106, no. 5, pp. dju066–dju066, May 2014.
- [169] S. Abalde-Cela, P. Piairol, L. Dieguez, and L. Diéguez, “The Significance of Circulating Tumour Cells in the Clinic,” *Acta Cytol.*, vol. 63, no. 6, pp. 466–478, 2019.
- [170] T. Fehm *et al.*, “HER2 status of circulating tumor cells in patients with metastatic breast cancer: a prospective, multicenter trial.,” *Breast Cancer Res. Treat.*, vol. 124, no. 2, pp. 403–412, Nov. 2010.
- [171] T. Fehm, V. Müller, C. Alix-Panabières, and K. Pantel, “Micrometastatic spread in breast cancer: detection, molecular characterization and clinical relevance,” *Breast Cancer Res.*, vol. 10, no. Suppl 1, pp. S1–S1, Apr. 2008.
- [172] M. Ignatiadis *et al.*, “HER2-positive circulating tumor cells in breast cancer.,” *PLoS One*, vol. 6, no. 1, p. e15624, Jan. 2011.
- [173] S. Riethdorf *et al.*, “Detection and HER2 expression of circulating tumor cells: prospective monitoring in breast cancer patients treated in the neoadjuvant GeparQuattro trial.,” *Clin. Cancer Res.*, vol. 16, no. 9, pp. 2634–2645, May 2010.
- [174] B. A. S. Jäger *et al.*, “Estrogen Receptor and HER2 Status on Disseminated Tumor Cells and Primary Tumor in Patients with Early Breast Cancer,” *Transl. Oncol.*, vol. 8, no. 6, pp. 509–516, Dec. 2015.

- [175] F.-C. Bidard and J.-Y. Pierga, "Clinical utility of circulating tumor cells in metastatic breast cancer.," *Journal of clinical oncology : official journal of the American Society of Clinical Oncology*, vol. 33, no. 14. United States, p. 1622, May-2015.
- [176] M. A. Olayioye, R. M. Neve, H. A. Lane, and N. E. Hynes, "The ErbB signaling network: receptor heterodimerization in development and cancer.," *EMBO J.*, vol. 19, no. 13, pp. 3159–3167, Jul. 2000.
- [177] X. Zhao, Y. Xia, and G. M. Whitesides, "Soft lithographic methods for nano-fabrication," vol. 7, pp. 1069–1074, 1997.
- [178] K. L. Berkowski, K. N. Plunkett, Q. Yu, and J. S. Moore, "Introduction to Photolithography : Preparation of Microscale Polymer Silhouettes W," vol. 82, no. 9, 2005.
- [179] Y. Xia and G. M. Whitesides, "SOFT LITHOGRAPHY," no. 12, 1998.
- [180] B. S. Yilbas, A. Al-Sharafi, and H. Ali, "Chapter 3 - Surfaces for Self-Cleaning," B. S. Yilbas, A. Al-Sharafi, and H. B. T.-S.-C. of S. and W. D. M. Ali, Eds. Elsevier, 2019, pp. 45–98.
- [181] D. Maily, C. Vieu, and G. Considerations, "Lithography and Etching Processes."
- [182] P. Films and A. Media, "Photoresist removal."
- [183] D. Qin, Y. Xia, and G. M. Whitesides, "Soft lithography for micro- and nanoscale patterning," *Nat. Protoc.*, vol. 5, no. 3, pp. 491–502, 2010.
- [184] J. A. Rogers and R. G. Nuzzo, "Recent progress in soft lithography," *Mater. Today*, vol. 8, no. 2, pp. 50–56, 2005.
- [185] M. J. Sanderson, I. Smith, I. Parker, and M. D. Bootman, "Fluorescence Microscopy," vol. 2014, no. 10, 2016.
- [186] B. N. G. Giepmans, S. R. Adams, M. H. Ellisman, and R. Y. Tsien, "The fluorescent toolbox for assessing protein location and function.," *Science*, vol. 312, no. 5771, pp. 217–224, Apr. 2006.
- [187] D. M. Spring KR, "Introduction to Fluorescence Microscopy," *Nikon Microsc.*
- [188] M. S. E. H. Worlds, "The Fluorescence Microscope," . *Nobel Found.*
- [189] S. W. Hell, "Microscopy and its focal switch.," *Nat. Methods*, vol. 6, no. 1, pp. 24–32, Jan. 2009.
- [190] D. Axelrod, "Total internal reflection fluorescence microscopy in cell biology.," *Traffic*, vol. 2, no. 11, pp. 764–774, Nov. 2001.
- [191] M. S. Kim, S. Kwon, T. Kim, E. Sook, and J. Park, "Biomaterials Quantitative proteomic profiling of breast cancers using a multiplexed microfluidic platform for immunohistochemistry and immunocytochemistry," *Biomaterials*, vol. 32, no. 5, pp. 1396–1403, 2011.
- [192] M. A. Miller, "When Tissue Antigens and Antibodies Get Along : Revisiting the Technical Aspects of Immunohistochemistry – The Red , Brown , and Blue Technique," vol. 51, no. 1, pp. 42–87, 2014.
- [193] J. Duraiyan, R. Govindarajan, and M. Palanisamy, "Applications of immunohistochemistry The Principle of IHC Neurodegenerative Disorders IHC in Muscle Diseases Research Application."
- [194] R. W. Burry, "Controls for Immunocytochemistry : An Update," 2011.

- [195] D. L. Holliday and V. Speirs, "Choosing the right cell line for breast cancer research," 2011.
- [196] Invitrogen, "CELL CULTURE BASICS Handbook."
- [197] S. Coecke *et al.*, "Guidance on Good Cell Culture Practice Guidance on Good Cell Culture Practice A Report of the Second ECVAM Task Force on Good Cell Culture Practice," no. June 2014, 2007.
- [198] J. S. Bagnall *et al.*, "Deformability of Tumor Cells versus Blood Cells," *Sci. Rep.*, vol. 5, no. November, pp. 1–11, 2015.
- [199] S. Ribeiro-Samy *et al.*, "Fast and efficient microfluidic cell filter for isolation of circulating tumor cells from unprocessed whole blood of colorectal cancer patients," *Sci. Rep.*, vol. 9, no. 1, pp. 1–12, 2019.
- [200] R. Riahi *et al.*, "A novel microchannel-based device to capture and analyze circulating tumor cells (CTCs) of breast cancer," *Int. J. Oncol.*, vol. 45, no. 6, pp. 1870–1878, 2014.
- [201] W. Chen *et al.*, "Detection of HER2-positive Circulating Tumor Cells Using the LiquidBiopsy System in Breast Cancer," *Clin. Breast Cancer*, vol. 19, no. 1, pp. e239–e246, 2019.
- [202] J.-Y. Pierga *et al.*, "Pathological Response and Circulating Tumor Cell Count Identifies Treated HER2⁺ Inflammatory Breast Cancer Patients with Excellent Prognosis: BEVERLY-2 Survival Data," *Clin. Cancer Res.*, vol. 21, no. 6, pp. 1298 LP – 1304, Mar. 2015.
- [203] E. A. Rakha *et al.*, "Updated UK recommendations for HER2 assessment in breast cancer," *J. Clin. Pathol.*, vol. 68, no. 2, pp. 93–99, 2015.
- [204] L. P. Garrison, J. B. Babigumira, A. Masaquel, B. C. M. Wang, D. Lalla, and M. Brammer, "The Lifetime Economic Burden of Inaccurate HER2 Testing: Estimating the Costs of False-Positive and False-Negative HER2 Test Results in US Patients with Early-Stage Breast Cancer," *Value Heal.*, vol. 18, no. 4, pp. 541–546, 2015.
- [205] N. U. Lin, J. R. Bellon, and E. P. Winer, "CNS Metastases in Breast Cancer," *J. Clin. Oncol.*, vol. 22, no. 17, pp. 3608–3617, Sep. 2004.
- [206] W.-T. Yan *et al.*, "Circulating tumor cell status monitors the treatment responses in breast cancer patients: a meta-analysis," *Sci. Rep.*, vol. 7, p. 43464, Mar. 2017.

CHAPTER 8: Annexes

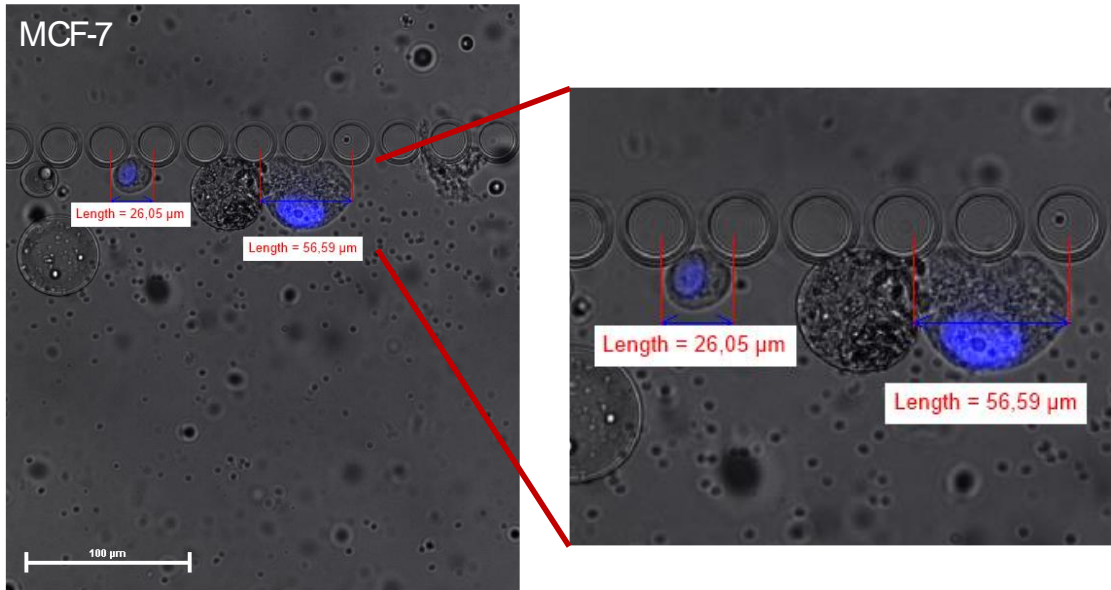


Figure A 1 : Two MCF-7 cells trapped inside the RUBYchip™, in the micropillars that work as the filtering area. One of the cells in the picture measures 26.05 μm , the average size for this cell line, while the other measures 56.59 μm , a much larger size, that occurs due cells being in different phases of the cell cycle. This image was visualised and acquired using Nikon-Ti-E microscope, and posterior measurements were done using NIS-Elements AR® Software.

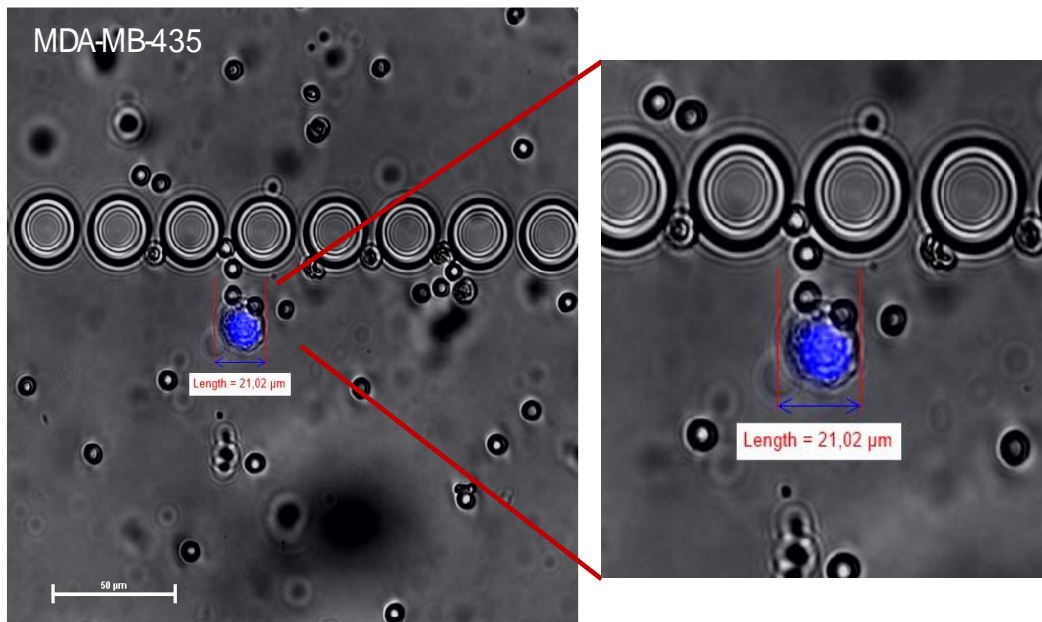


Figure A 2: MDA-MB-435 cell trapped inside the RUBYchip™, next to the micropillars. This cell has the usual size observed in this cell line, 21.02 μm . This image was visualised and acquired using Nikon-Ti-E microscope, and posterior measurements were done using NIS-Elements AR® Software.

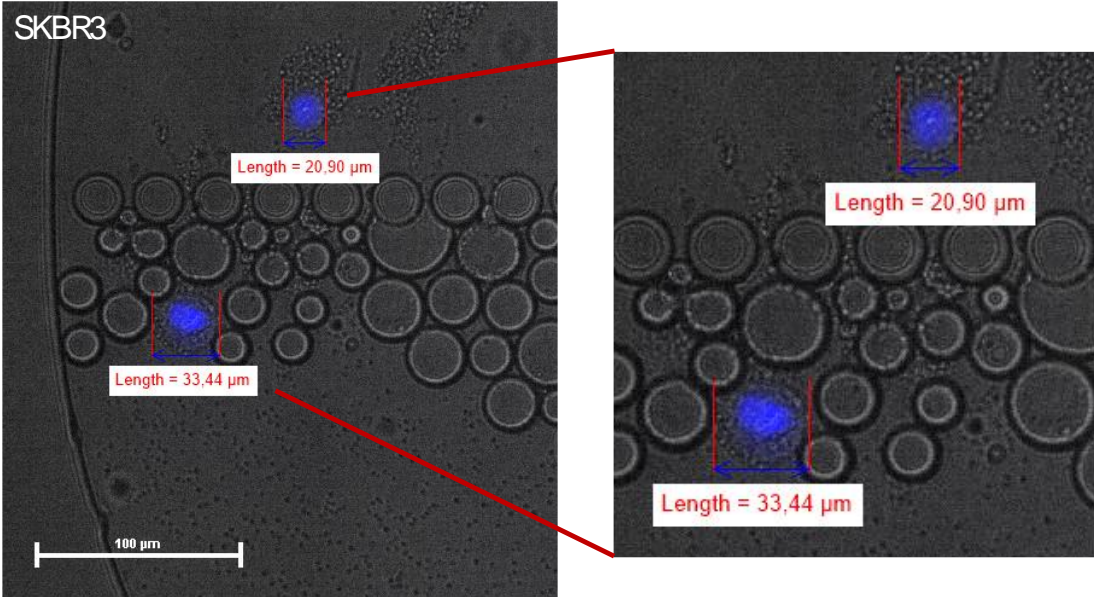


Figure A 3: SKBR3 cells trapped inside the RUBYchip™, near the filtering area. One of the cells in the picture measures 20.09 µm, the average size for this cell line, while the other measures 33.44 µm, a larger size, differences found in cell size are due to cells being at different phases of the cell cycle. This image was visualised and acquired using Nikon-TI-E microscope, and posterior measurements were done using NIS-Elements AR® Software.

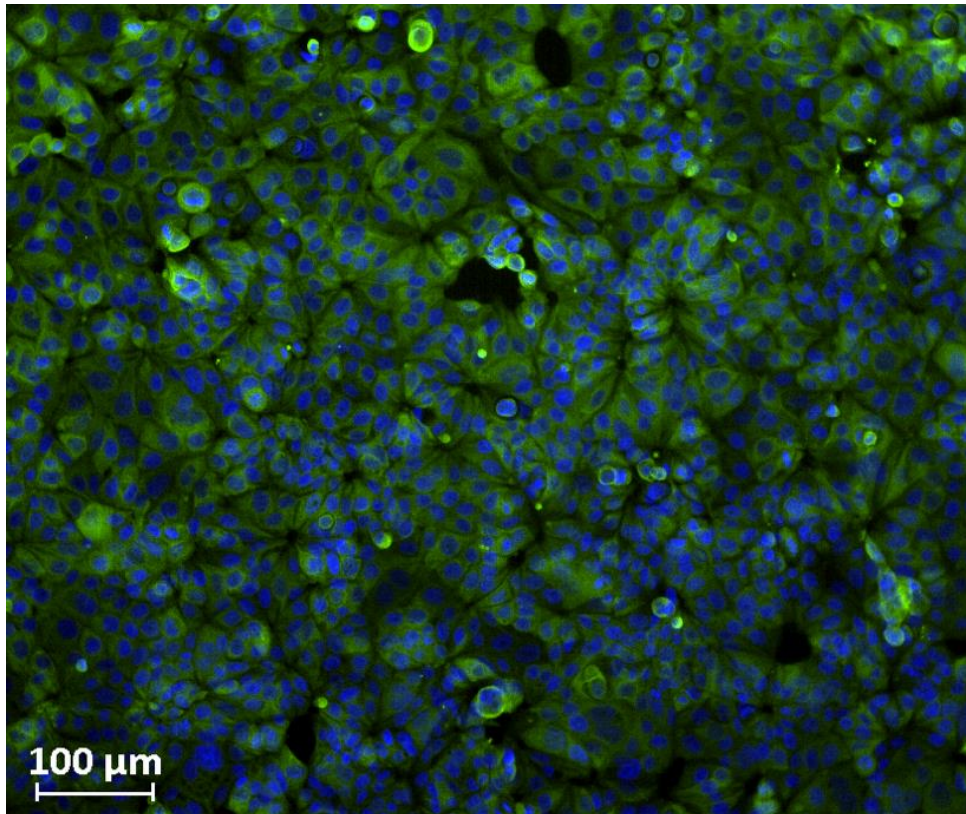


Figure A 4 : Immunofluorescence image of MCF-7 breast cancer cells, CK presence and DAPI stain can be found in the cytoskeleton and nucleus, respectively.

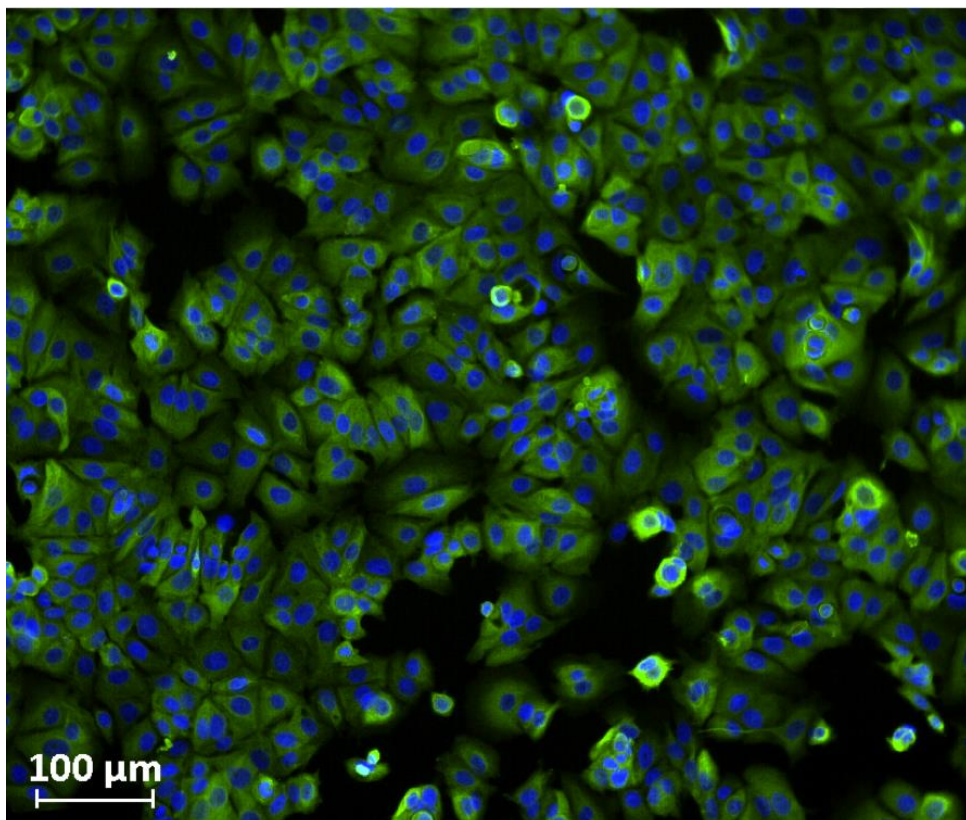


Figure A 5 : Immunofluorescence image of MCF-7 breast cancer cells, incubated with an antibody cocktail containing all the antibodies used in this study, only CK expression can be found and DAPI, as expected.

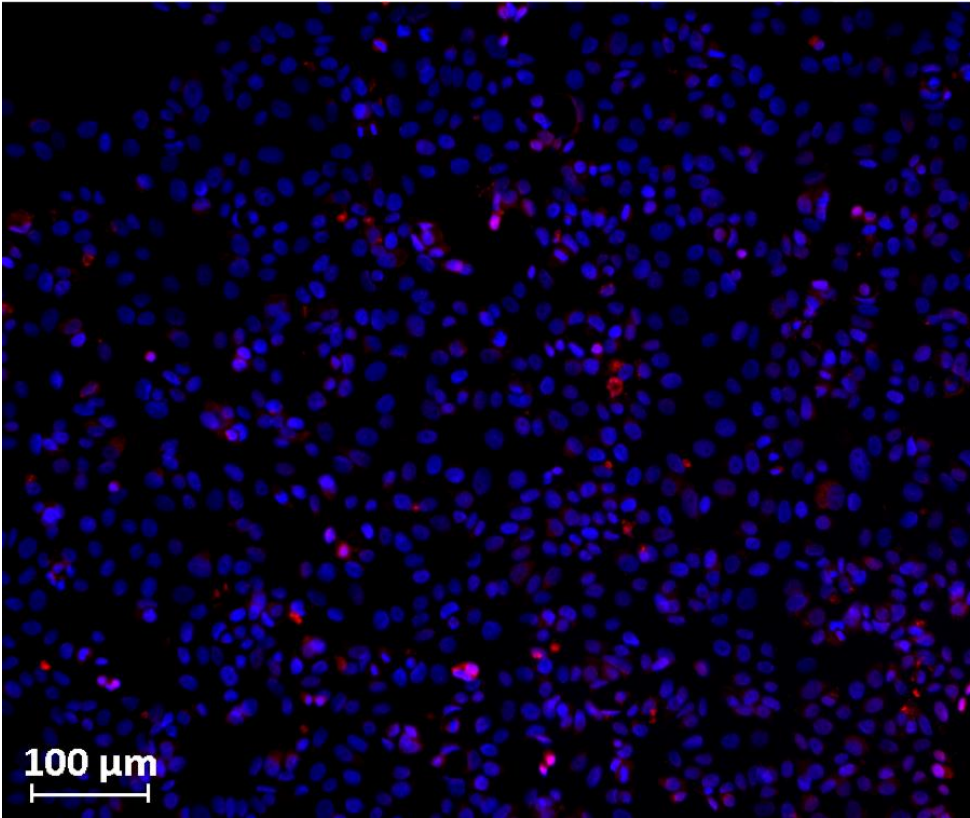


Figure A 6 : Immunofluorescence image of MCF-7 breast cancer cells, incubated with anit-CD45 antibody and DAPI. CD45 unspecific staining can be found, whichh could be due to the use of an antibody concentration higher than needed.

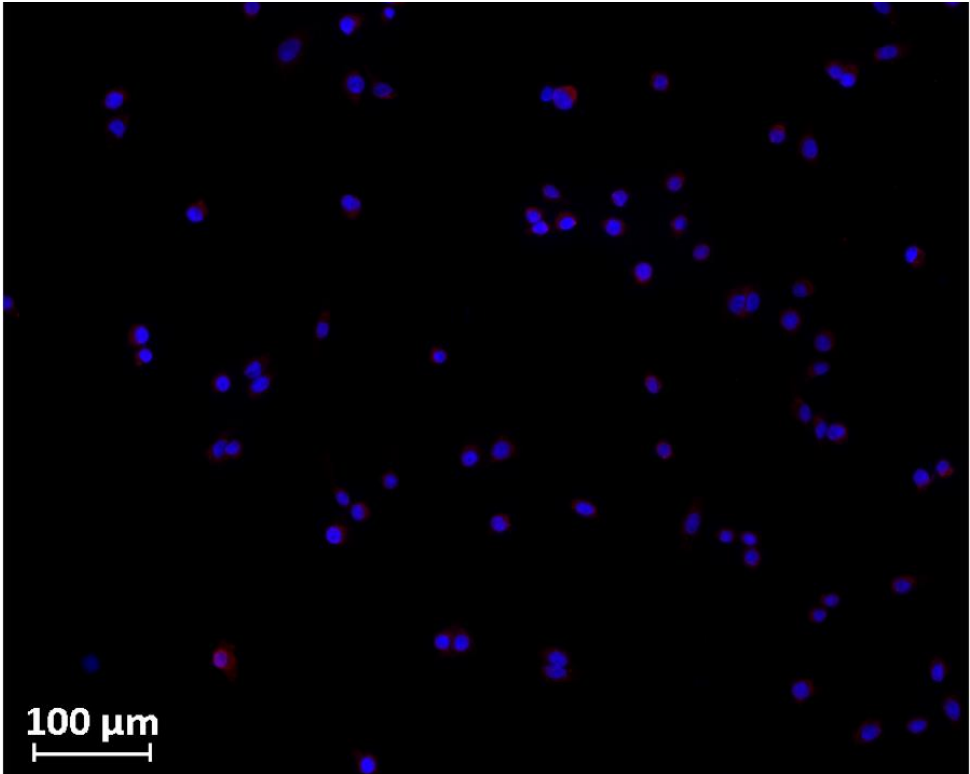


Figure A 7: Immunofluorescence image of MDA-MB-435 breast cancer cells, incubated with anit-CD45 antibody and DAPI. CD45 unspecific staining can be found, whichh could be due to the use of an antibody concentration higher than needed.

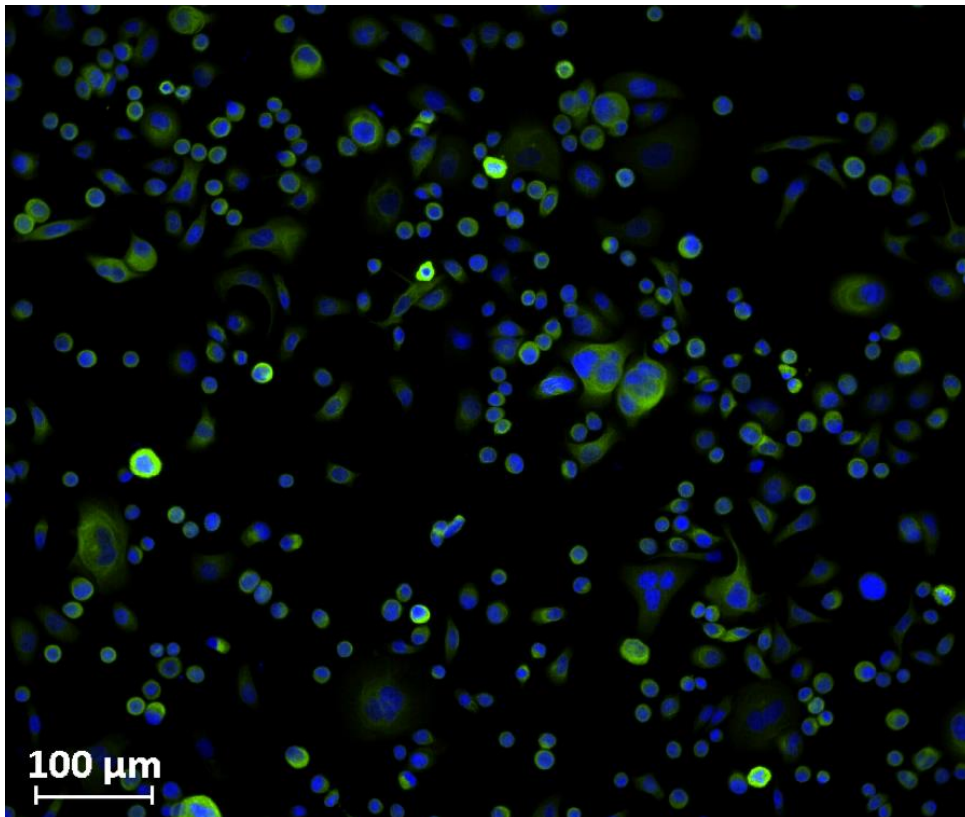


Figure A 8: Immunofluorescence image of SKBR3 breast cancer cells, incubated with anti-CK antibody. CK presence and DAPI stain can be found in the cytoskeleton and nucleus, respectively.

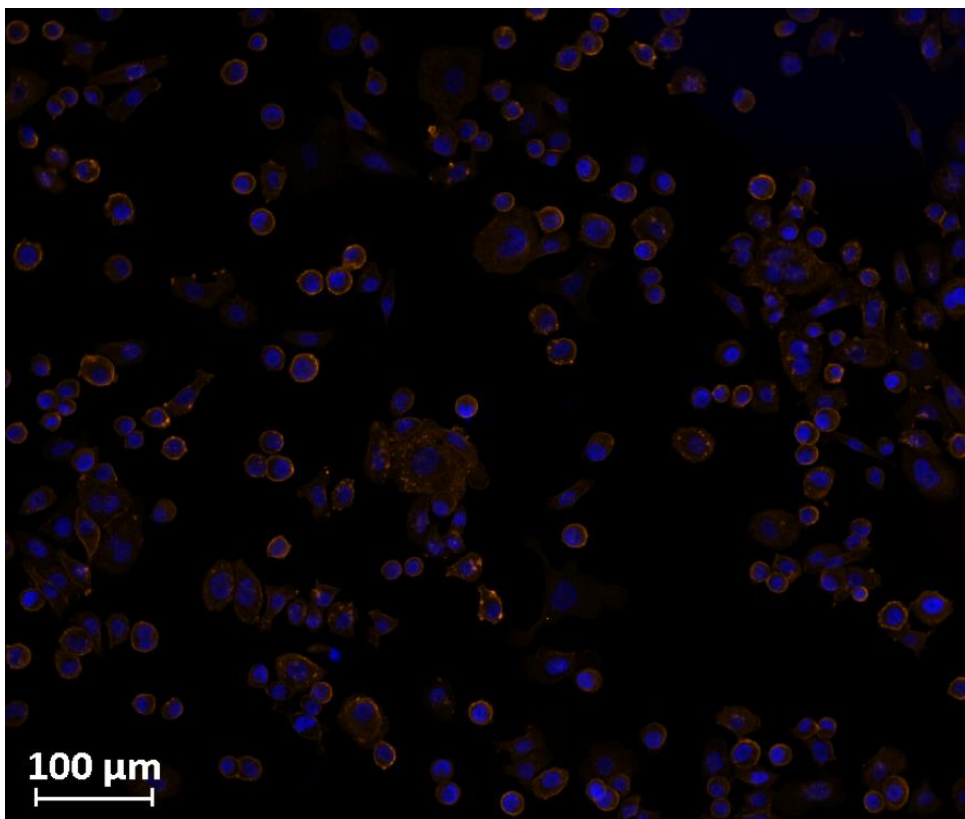


Figure A 9: : Immunofluorescence image of SKBR3 breast cancer cells, incubated with anti-HER2, at 2 g/ml, HER2 presence and DAPI stain can be found in the cell membrane and nucleus, respectively.

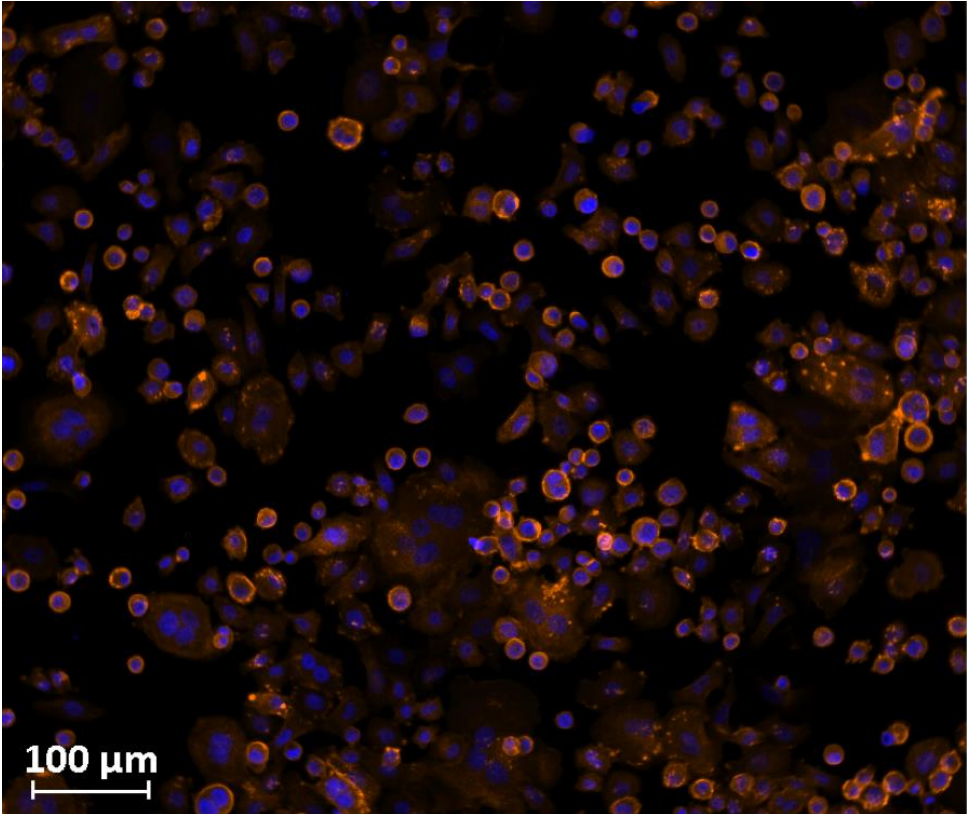


Figure A 10: Immunofluorescence image of SKBR3 breast cancer cells, incubated with anti-HER2, at 6 g/ml, HER2 presence and DAPI stain can be found in the cell membrane and nucleus, respectively..

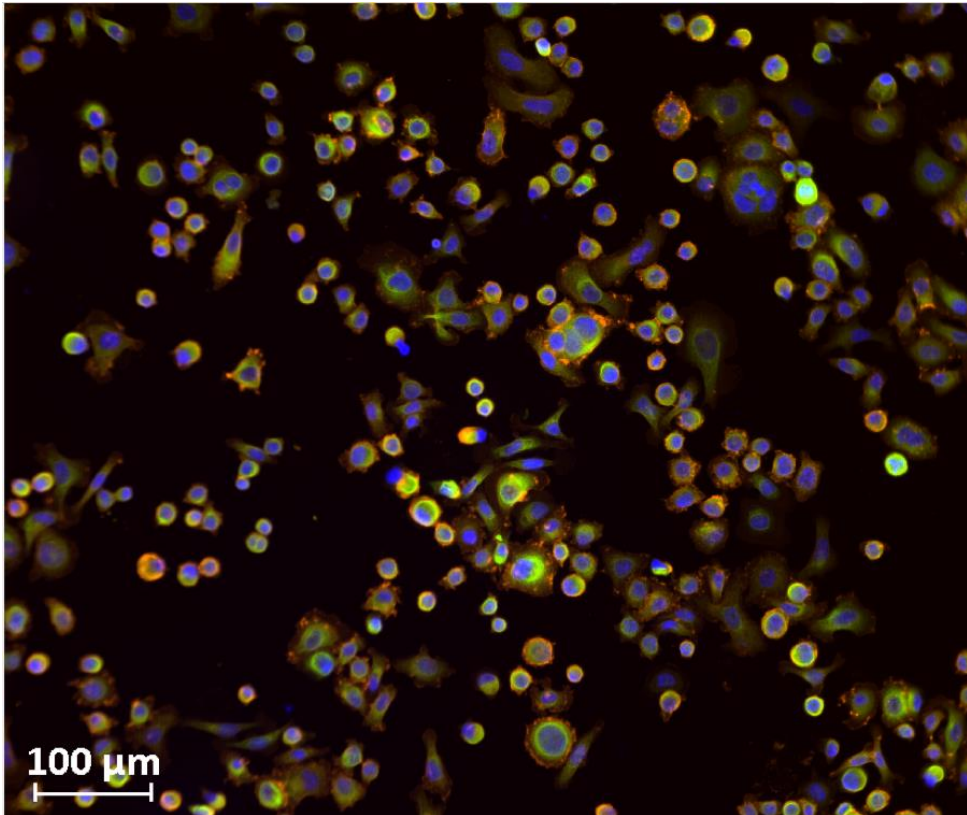


Figure A 11: Immunofluorescence image of SKBR3 breast cancer cells, incubated with an antibody cocktail containing all the antibodies used in this study, CK, HER2 expression and DAPI is observed, as expected

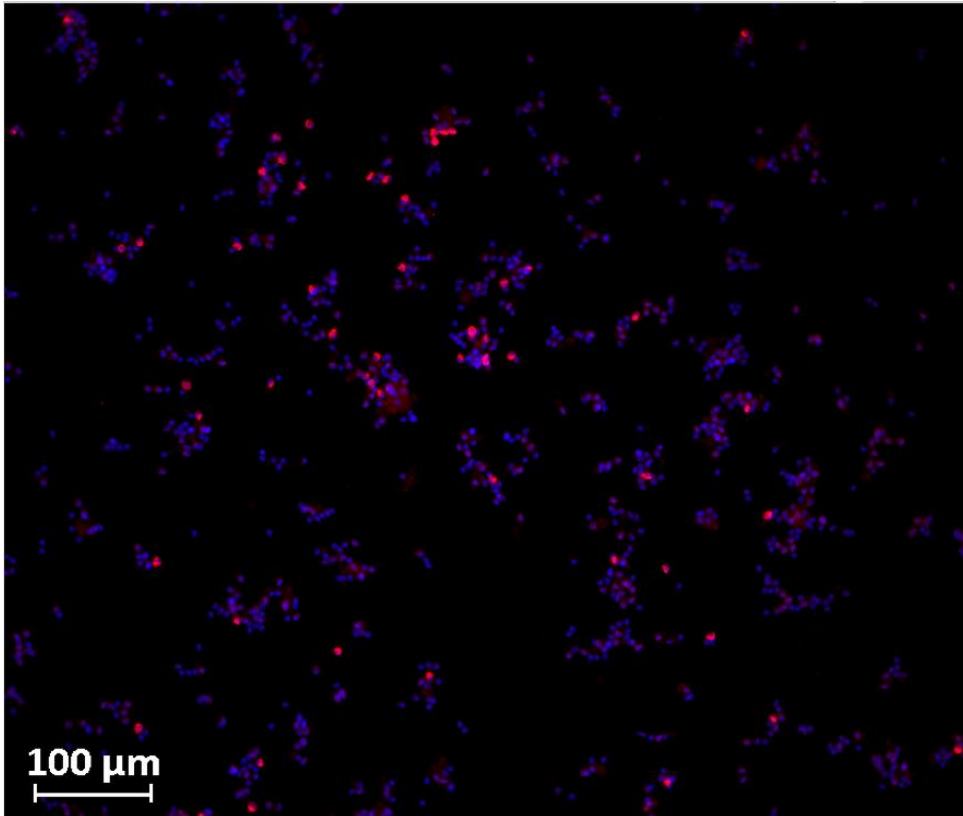


Figure A 12: Immunofluorescence image of PBMCs Incubated with anti-CD45 antibody, CD45 and DAPI stainings are observed

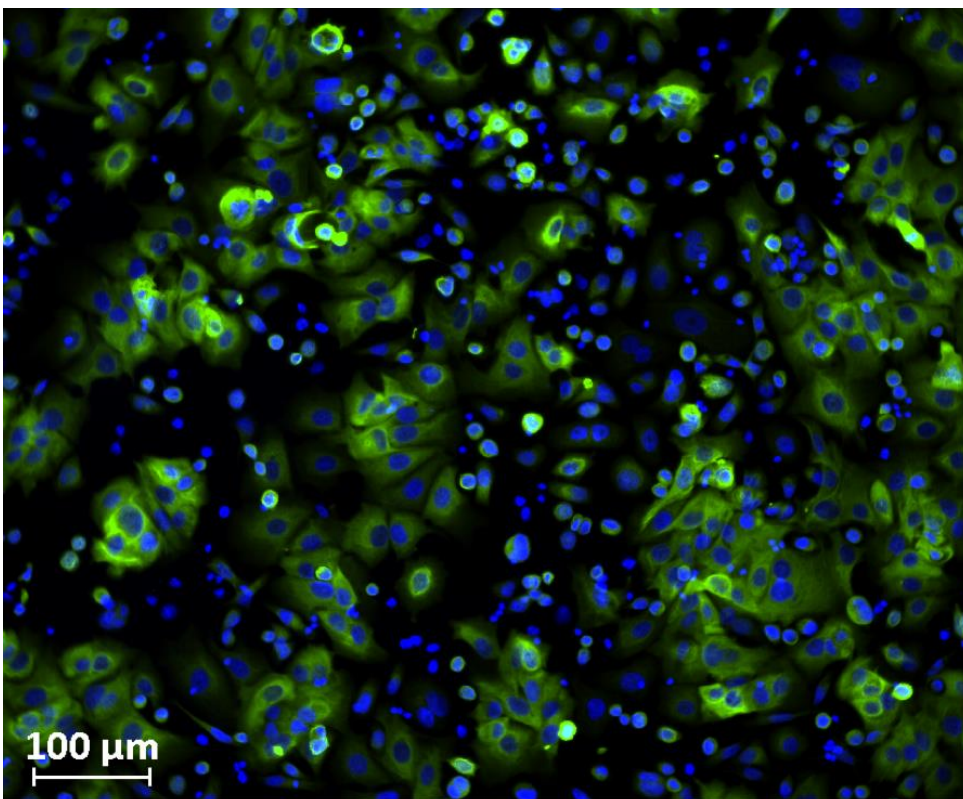


Figure A 13: Immunofluorescence image of all the cell lines (MCF-7, MDA-MB-435 and SKBR3) and PBMCs, incubated with anti-CK antibody and DAPI. CK is expressed by MCF-7 and SKBR3 cells, since CK targets epithelial cells only.

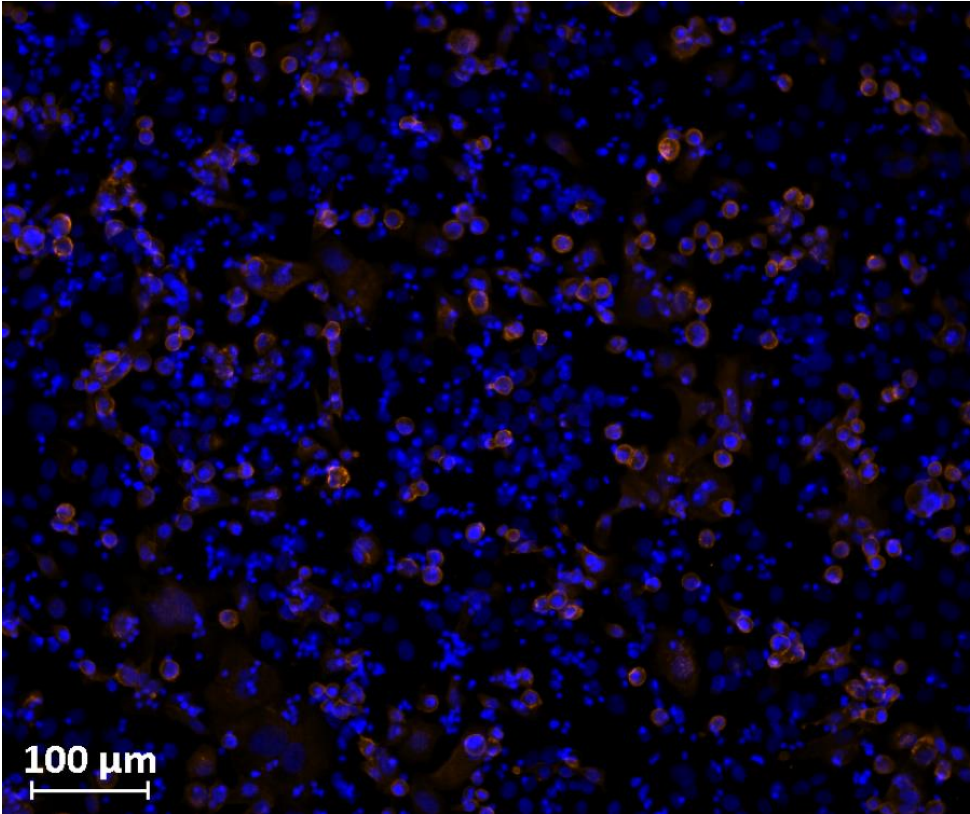


Figure A 14: Immunofluorescence image of all the cell lines (MCF-7, MDA-MB-435 and SKBR3) and PBMCs, incubated with anti-HER2 antibody, at 2 µg/ml, and DAPI, HER2 expression can be found in cell membranes.

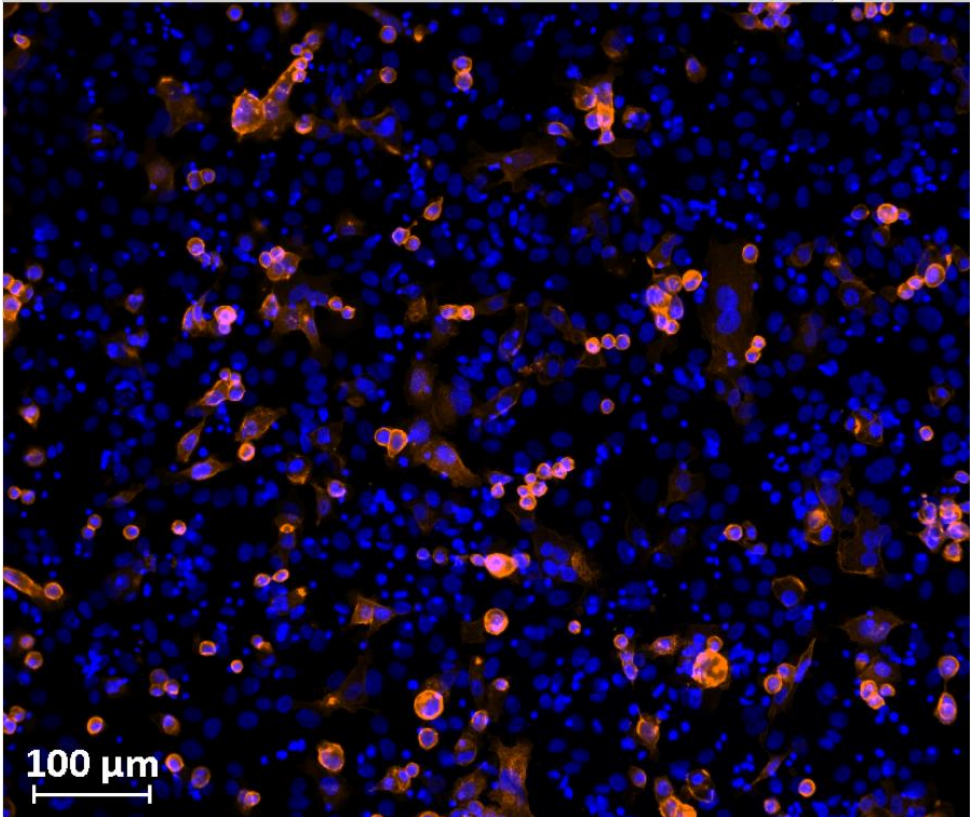


Figure A 15: Immunofluorescence image of all the cell lines (MCF-7, MDA-MB-435 and SKBR3) and PBMCs, incubated with anti-HER2 antibody, at 6 µg/ml, and DAPI, HER2 expression can be found in cell membranes. Staining is more noticeable at this concentration than the previous.

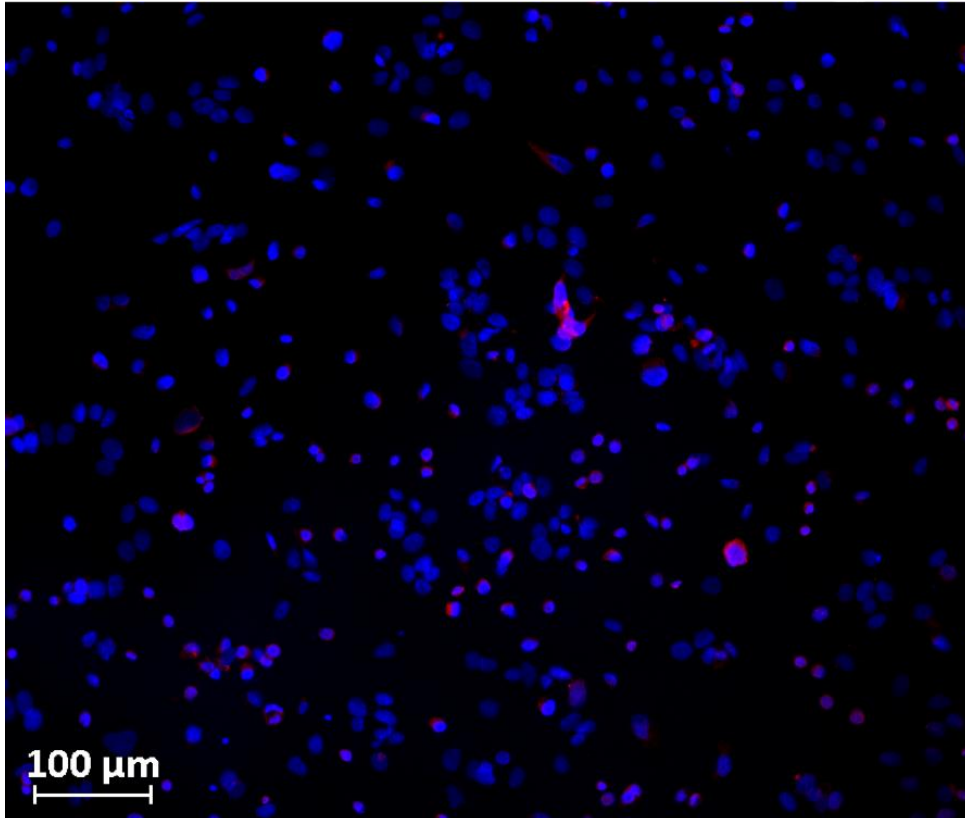


Figure A 16: Immunofluorescence image of all the cell lines (MCF-7, MDA-MB-435 and SKBR3) and PBMCs, incubated with anti-CD45 antibody and DAPI. CD45 expression was expected in PBMCs, however, a weaker staining was observed in MCF-7 and MDA-MB-435 cells, which is not expected and can be due to the use of an antibody concentration higher than needed.

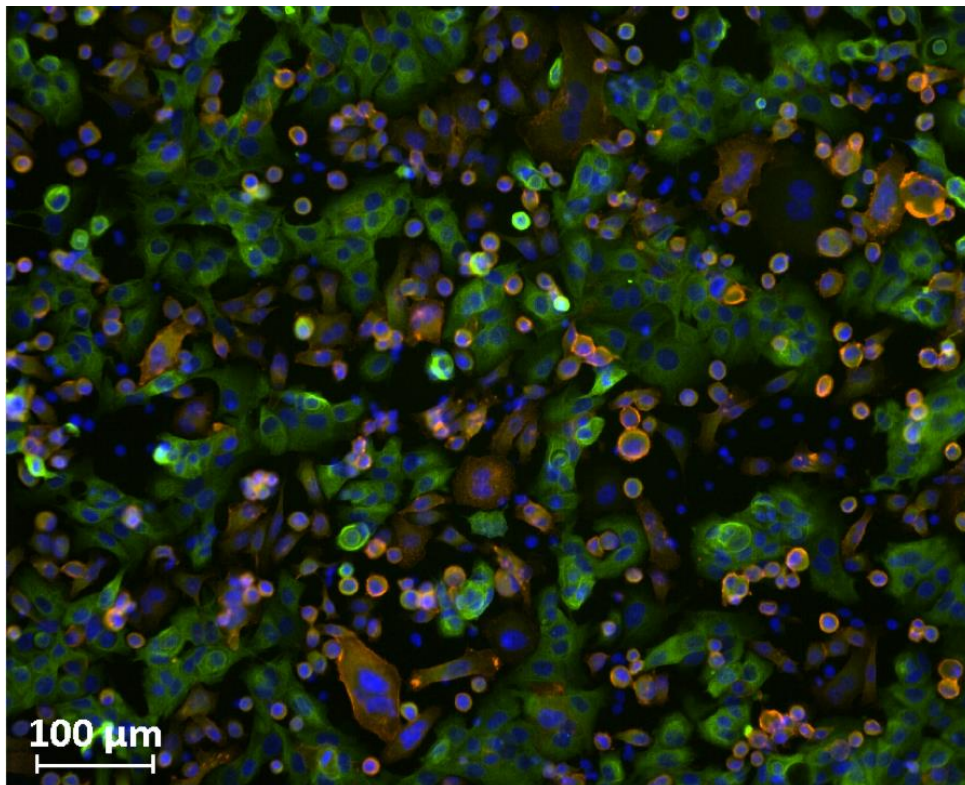


Figure A 17: Immunofluorescence image of all the cell lines (MCF-7, MDA-MB-435 and SKBR3) and PBMCs, incubated with an antibody cocktail containing all the antibodies used in this study. MCF-7 and SKBR3 cells are stained with CK, HER2 is present in SKBR3 cells, PBMCs exhibit CD45, also CD45 unspecific staining can be found in MCF-7 and MDA-MB-435.